

CMOS phase-locked loops:  
74HC(T)4046A/7046A & 74HCT9046A

HCMOS Designer's Guide - advance information

Revised edition: June 1995



Remember to Visit  
**Philips Logic**  
on the Web!  
<http://www.philipslogic.com>



**PHILIPS**

## CONTENTS

	Page
<b>PLL BASICS</b> .....	1
<b>TYPES OF PLL</b> .....	2
<b>PLL TERMINOLOGY</b> .....	2
<b>HCMOS PLL CIRCUITS: 4046A, 7046A &amp; 9046A</b>	
Voltage-controlled oscillator of the 4046A and the 7046A .....	5
Voltage-controlled oscillator of the 9046A .....	12
Phase comparators .....	16
Lock detection indication .....	29
Effect of temperature .....	32
Supply voltage .....	32
Part-to-part spread .....	33
<b>PLL ANALYSIS</b>	
Basic feedback system .....	35
Loop filters .....	35
Second-order loop .....	37
Bode plot .....	37
Root locus plot .....	38
Phase and gain margin .....	38
Transient behaviour .....	41
Sinusoidally modulated input signal .....	42
Ripple suppression .....	43
Phase noise .....	44
Overview of the PLL parameters .....	45
<b>PLL DESIGN PROGRAM</b>	
About the program .....	46
Initial PLL default settings .....	47
Optimizing a loop .....	48
Evaluating existing designs .....	49
<b>APPLICATION EXAMPLES</b>	
Filter output clamping .....	50
Frequency synthesizer .....	51
Video horizontal line synchronizer .....	61
FM demodulator .....	63
FSK decoder .....	65
Crystal oscillator .....	66
<b>APPENDIX A</b>	
Variable gain of PC2 (type a: 74HC(T)4046A/7046A only) .....	67
<b>APPENDIX B</b>	
Transient response calculations .....	69
<b>APPENDIX C</b>	
Bode plot measuring circuit .....	72
<b>APPENDIX D</b>	
Symbols .....	73
<b>REFERENCES</b> .....	73

Development of single-chip Phase-Locked Loops (PLLs) has brought about an enormous growth in the use of PLL techniques throughout electronic engineering. Formerly, uneconomic or impractical in many applications, PLL techniques are now in widespread use, bringing excellent noise immunity and tracking ability to ever more designs. In the field of communication, the applications for PLLs include frequency synthesizers, data modems, clock regeneration and FM and AM demodulators, to name but a few examples. In other fields too, PLLs are widely used, for example, in motor speed-control systems, tracking voltmeters and spectrum analyzers.

The aim of this publication is to assist those designing with Philips high-speed CMOS (HCMOS) integrated PLL circuits. With this in mind, there is a design program<sup>1</sup> which can be used to put many of the principles described here into practice. The program which runs on an IBM PC, or compatible, enables PLLs to be designed and optimized fast. The effect of altering loop parameters can be readily observed. For many, the design program alone will suffice; for those requiring more insight into the theory behind the workings of the program, the chapter 'PLL Analysis' is included in this publication.

The PLL circuits described (the 74HC/HCT4046A, the 74HC/HCT7046A and the 74HCT9046A) are high-speed silicon-gate CMOS ICs and are specified in compliance with JEDEC standard No. 7. All of these circuits are available in a 16-pin DIL or a 16-pin SO package. The 4046A is pin-compatible with the '4046' of Philips' HE4000B series (except for pin 15, the ZENER input of the HE4000B circuit, which is now used as the output of an additional phase comparator). The HC/HCT7046 includes an extra lock detect circuit instead of the third phase comparator of the 4046A, PC3. The last circuit described is the HCT9046. This is a new PLL IC with an improved VCO section with a band-gap controlled reference voltage and an optimized phase comparator PC2 with a current-source tri-state output switch.

## PLL BASICS

A PLL is basically a feedback system which synchronizes an oscillator in phase and frequency to an incoming signal. A PLL has three main parts: a phase comparator, a low-pass filter and a voltage controlled oscillator (VCO), see Fig.1. The phase

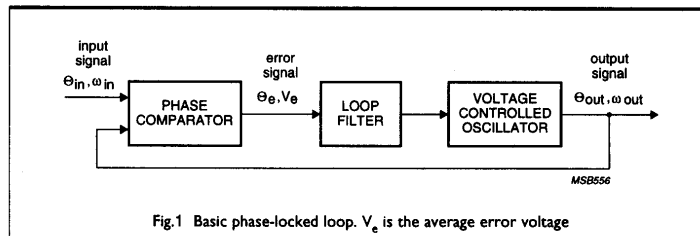


Fig.1 Basic phase-locked loop.  $V_e$  is the average error voltage

comparator measures the phase difference between the input and output signals and produces an error signal proportional to the measured phase difference. If the low-pass filter is disregarded for the moment, the error signal will drive the VCO, changing its frequency so as to minimize the phase difference between the input and output signals. Ultimately, the frequency of the output signal will be identical to that of the input signal and will follow every change of the latter. However, if the error signal is low-pass filtered, the VCO will not react to high-frequency changes or noise in the input signal and will run at only the average frequency of the input signal. This electronic flywheel characteristic of a PLL is the one that is most used. To enable a PLL to acquire lock in the first place, it should of course be designed so that the difference between the input and output frequencies is not so large that, after filtering, there is no control signal for the VCO.

<sup>1</sup>Available from Philips Semiconductors, ordering code 9398 706 74011.

## TYPES OF PLL

There are analog PLLs and digital PLLs, the main difference being the phase comparator used. In an analog PLL, the phase comparator is often a four-quadrant multiplier or mixer using high-performance analog amplifiers to produce a pure sinusoidal output from a sinusoidal input. This type of linear PLL is often used to detect and retrieve very weak signals from a noisy communication channel.

The 4046A, the 7046A and the 9046A PLL circuits have digital phase comparators, chosen because they can be used in virtually every PLL application. A self-biasing input stage enables them to operate with AC input signals as low as 20 mV (peak-to-peak) at  $V_{CC} = 4.5$  V, as well as with signals between the HCMOS family input logic levels. Although these circuits have digital phase comparators, the VCO is controlled by an analog signal – the average output voltage of the phase comparator. A wholly-digital HCMOS PLL circuit is available – the HC/HCT297. In this circuit, the VCO is replaced by a 'pulse swallower'. Further details are available in the publication "All-digital PLLs using the 74HC/HCT297", ordering code 9398 065 90011, Philips Semiconductors.

## PLL TERMINOLOGY

There is a multiplicity of terminology in common use for PLLs. Therefore, it is useful to list the terminology used throughout this publication before the circuits are described. Only the main PLL terms are listed here; a complete glossary of symbols and terms appears in Appendix D.

### Hold range: $\pm\Delta\omega_H$

The range of frequencies over which a loop will remain locked. A loop is considered to be out of lock when the maximum permissible phase error is exceeded.

For the 4046A and 7046A HCMOS circuits, the hold range is only valid when phase comparator PC1, or PC3, and a passive low-pass filter are used, see 'Phase comparators'. When comparator PC2 or an active filter, or both, are used, the hold range is equal to half the output frequency range of the VCO.

### Pull-in range: $\pm\Delta\omega_{PI}$

The frequency range over which the PLL can acquire lock. This range which is usually less than the hold range is proportional to the natural frequency of the loop ( $\omega_n$ ). The time to acquire lock is called the pull-in time ( $T_p$ ).

When phase comparator PC2 is used, the pull-in range is equal to the VCO output frequency range, because PC2 is both phase-sensitive and frequency-sensitive.

### Pull-out range: $\pm\Delta\omega_{PO}$

The frequency step at the input, referenced to the VCO centre frequency ( $\omega_0$ ), which causes a locked loop to lose lock.

Since the pull-out range is normally within the pull-in range, the loop will reacquire lock (in the pull-in time).

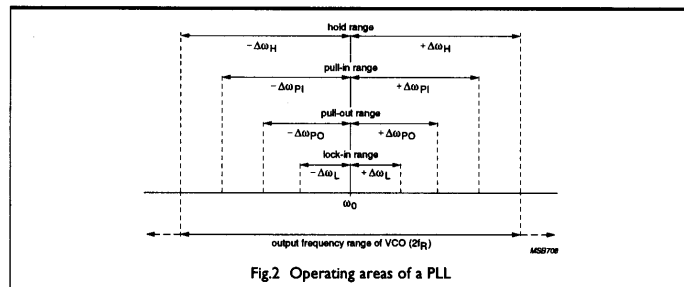


Fig.2. Operating areas of a PLL

**Lock-in range:  $\pm\Delta\omega_L$** 

The frequency range over which the loop can acquire lock without cycle slip.

The time to acquire lock within the lock-in range is called the lock-in time or settling time ( $T_S$ ).  $T_S$  is inversely proportional to the natural frequency of the loop ( $\omega_n$ ). Note that the term settling time is also used in frequency synthesizer applications, where it is the time for the loop's output to settle to within 5% of the applied step, after switching between two channels. This settling time is identified by the symbol  $T_{S(5\%)}$ .

**Centre frequency (free-running frequency):  $\omega_0$** 

This is the output frequency of the VCO when the VCO input control voltage is half of the supply voltage. At this frequency, the VCO is at the centre of all its operating ranges.

**Natural frequency:  $\omega_n$** 

The frequency at which the loop would oscillate if it was not damped (that is, if the damping factor  $\zeta = 0$ ). In the Bode plot of the (underdamped) closed second-order loop, the natural frequency is that frequency which gives the largest positive deviation from the DC gain.

Components of the input signal higher than the natural frequency will be damped by an amount depending on the damping factor.

**Phase comparator conversion gain:  $K_d$** 

The conversion constant relating the phase comparator's average output voltage to the phase difference between the signal input and the VCO output signal.  $K_d$  has units of volts per radian.

**VCO conversion gain:  $K_o$** 

The conversion gain constant relating the linear frequency range of the VCO ( $2f_R$ ) to the VCO control voltage range.  $K_o$  has units of radians per second per volt.

**VCO output frequency range:  $2f_R$** 

Although not a system parameter, the VCO frequency range is included here for completeness. It is the maximum output frequency range of the VCO in a particular application.

## HCMOS PLL CIRCUITS: 4046A, 7046A & 9046A

The 74HC/HCT4046A and 74HC/HCT7046A are very similar. Each circuit has a linear VCO and two phase comparators (PC1: EX-OR, and PC2: edge-triggered) with a common comparator input amplifier and a common signal input amplifier. The 4046A has a third phase comparator (PC3: edge-triggered), while the 7046A has improved lock-detection circuitry. As can be seen in Fig.3(a), only a low-pass filter and a few external components are needed to form a complete PLL.

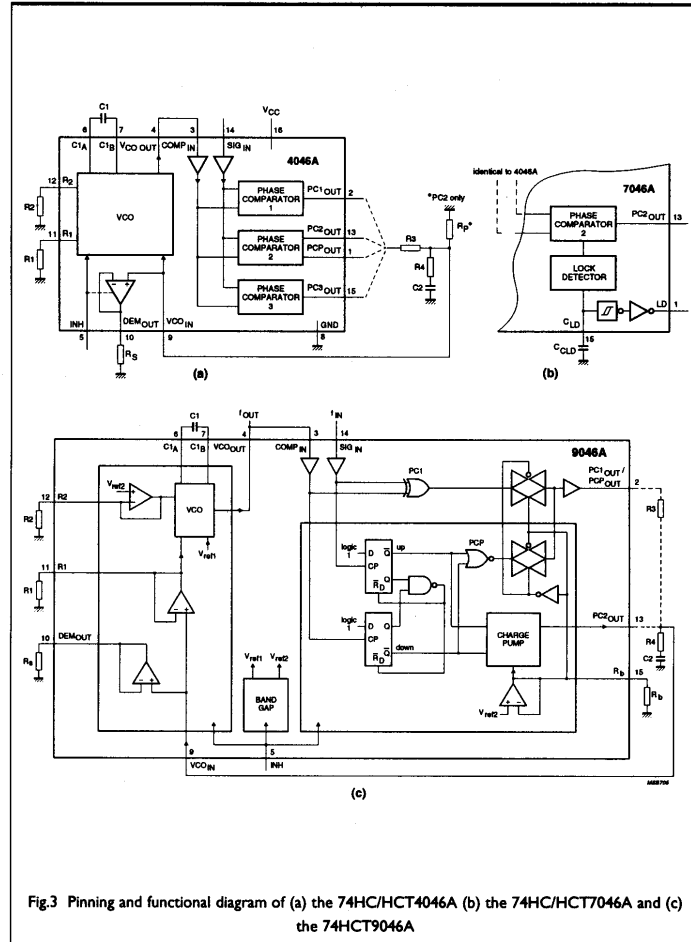


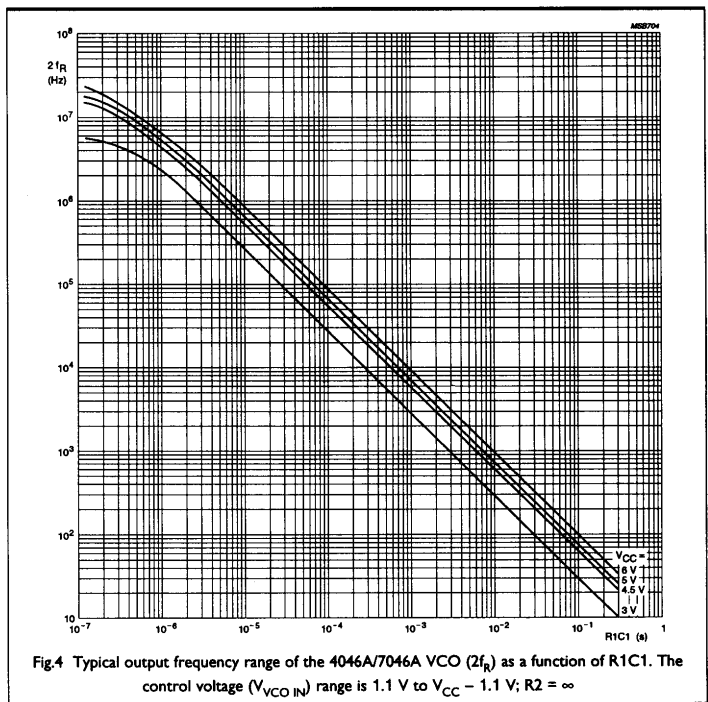
Fig.3 Pinning and functional diagram of (a) the 74HC/HCT4046A (b) the 74HC/HCT7046A and (c) the 74HCT9046A

The HCT9046A, as shown in Fig.3(c), is a revised and adapted version of the 4046 basic circuit. The VCO circuit has a similar configuration but uses a comparator with a band-gap reference voltage instead of the ST levels of the 4046 to improve the frequency stability. Furthermore the HCT9046 has a phase comparator PC2 with an adapted output section. The original 4046 has a voltage-source output for PC2 which involves a small dead zone around zero phase of the transfer function of output charge as a function of the phase difference. Therefore, the PC2 phase comparator of the HCT9046A has been provided with current charge outputs to achieve a linear transfer

function, even with very low phase errors. Connecting resistor  $R_b$  between pin 15 and ground will set the amplitude of the output charge current of the PC2 output and enable PCP at pin 2. Without  $R_b$ , and pin 2 connected to  $V_{CC}$ , the PC2 output is disabled and phase comparator PC1 is enabled at the pin 2 output.

**Voltage-controlled oscillator of the 4046A and the 7046A**

The VCO is completed by one external capacitor, C1, and one or two external resistors, R1 and R2 (Fig.3a). R1 and C1 determine the centre frequency ( $f_0$ ) and the operating range ( $2f_R$ ) of the VCO (see Figs 4, and 5). R2 enables the VCO to have a frequency offset ( $f_{off}$ ) if required; the offset depending on R2 and C1 (see Fig.6). The linearity of the VCO is excellent, owing to the use of linear op-amp techniques. An extremely high input resistance (pin 9;  $V_{COIN}$ ) enables a wide variety of loop filters to be used.



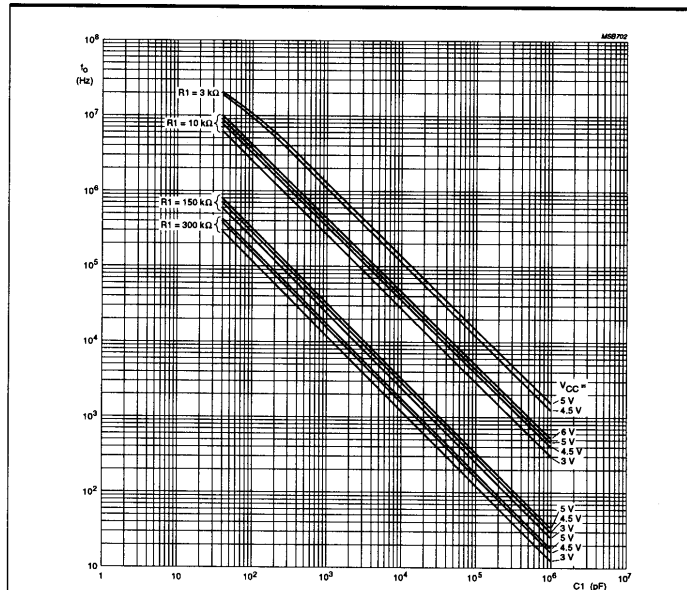


Fig.5 Typical VCO centre frequency for the 4046A/7046A ( $f_0$ ) as a function of  $C_1$ .  $R_2 = \infty$ ;  $V_{VCO IN} = 0.5 V_{CC}$ ;  $INH = GND$ ;  $T_{amb} = 25^\circ C$ . For optimum VCO performance,  $C_1$  should be as small as possible but larger than 100 pF. The curves can be interpolated for other values of  $R_1$ , because a constant  $R_1 C_1$  product produces almost the same VCO output frequency

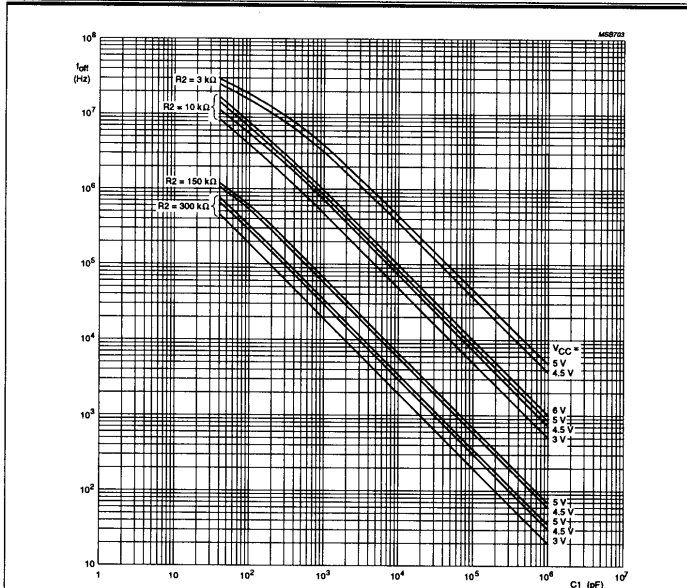


Fig.6 Typical frequency offset for the 4046A/7046A ( $f_{off}$ ) as a function of  $C_1$ .  $R_1 = \infty$ ;  $V_{VCO IN} = 0.5 V_{CC}$ ;  $INH = GND$ ;  $T_{amb} = 25^\circ C$ ;  $f_{off} = f_0 - 1.6f_R$ . For optimum VCO performance,  $C_1$  should be as small as possible but larger than 100 pF. The curves can be interpolated for other values of  $R_2$ , because a constant  $R_2 C_1$  product produces almost the same VCO offset frequency



Figure 7 is a circuit schematic of the VCO. The current  $I'$  is mirrored via transistors N1 and N3, the latter providing the bias current for an emitter-coupled input stage whose non-inverting and inverting inputs are the gates of N4 and N5 respectively.

Assume that the gates of N4 and N5 are at the same DC level; both transistors conduct equally and their drains are at the same potential. If the VCO input voltage (on pin 9) is raised, N4 conducts more and its drain voltage falls, increasing the gate-to-source drive of P4 and P5. This in turn raises the potential at pin 11 and hence that on the gate of N5, making the DC levels on the gates of N4 and N5 equal again.

From the above, it can be concluded that:

- Pin 11 follows the positive input ( $V_{CO\_IN}$ ) exactly
- Increasing the VCO input voltage produces a linear increase of the current through R1;
- The current through R1 is mirrored via P5 to the current-controlled oscillator, which generates the charging current for C1 which sets the VCO output frequency.

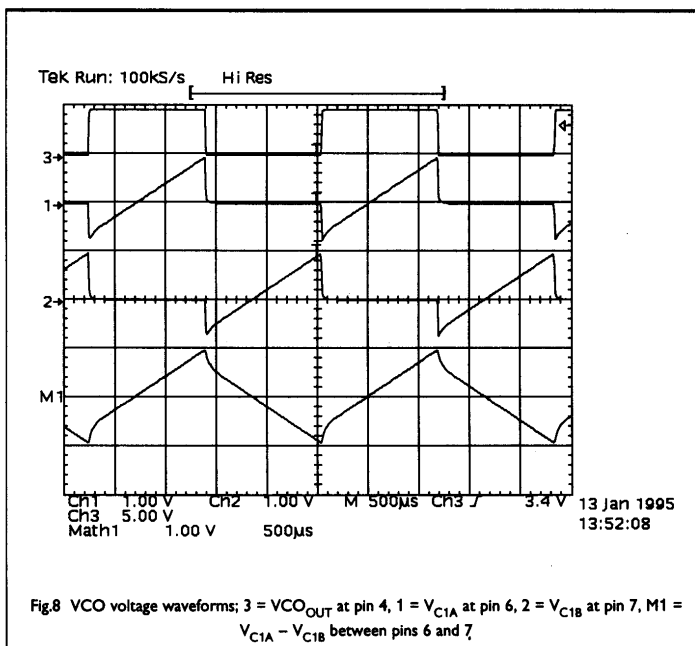
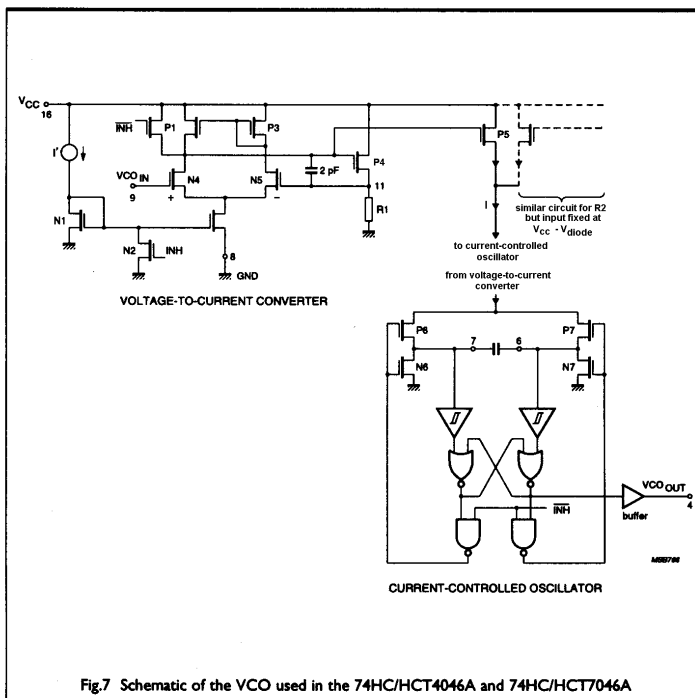
When C1 is charged via P6 (or P7) and one of its terminals with the current  $I$ , the other terminal of C1 is held low by N7 (or N6). When the positive threshold voltage,  $V_{T+}$ , of one of the Schmitt-triggers is reached, P6 (or P7) is turned off and the other terminal of C1 is charged via P7 (or P6), see Fig.8.  $V_{CO\_OUT}$  (pin 4) is HIGH during the charge period at pin 6.

An identical circuit in parallel with P5 gives the current contribution of R2, for a frequency offset, but here the non-inverting input of the op-amp is fixed at  $V_{CC} - V_{diode}$ .

#### **Jitter and interference considerations**

At low frequencies, the slope of the sawtooth across C1 will become very flat. Practical experience has shown that external switching edges, like those from the phase comparator outputs, may cause interference transients on this sawtooth. If such transients coincide with the actual switching point at the sawtooth maximum level, they may affect the VCO switching behaviour and cause extra phase jitter at the VCO output. Correct circuit layout with an extra ground-plane will minimize these effects. In some cases such interference may cause the positive VCO output edge to show instability with a short glitch of about 10 ns preceding it. Such a glitch would cause counting errors, and cycle slip of the PLL loop, if the VCO is used together with the edge-triggered phase comparator PC2, or if a divider section is used. Smoothing the positive VCO output edge with a 100 ns RC series filter (e.g.  $R_s = 1\text{ k}\Omega$  and  $C_f = 33\text{ pF}$  to 100 pF connected to ground) will avoid such loop errors.

If phase comparator PC2 is used, it will be very likely that some of the phase comparator output edges will be close to the top of the sawtooth because this type of comparator operates typical with zero phase error. For such applications, interference with jitter at the VCO output can be avoided by connecting a relatively high value resistor ( $R_p$ ) between the PC2 output and positive supply voltage  $V_{CC}$ . This will force the loop to feed a compensating discharge current to the loop filter capacitor by phase shifting the  $SIG_{IN}$  signal just after the VCO output and  $COMP_{IN}$  signals. The disturbing phase comparator outputs will then occur behind the VCO switching point and will not interfere. More information on the use of resistor  $R_p$  is given in the Section "Phase and frequency jitter considerations" of PC2 of the HC/HCT4046A/7046A.

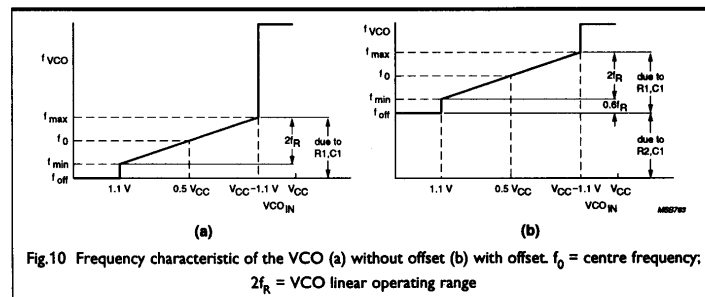
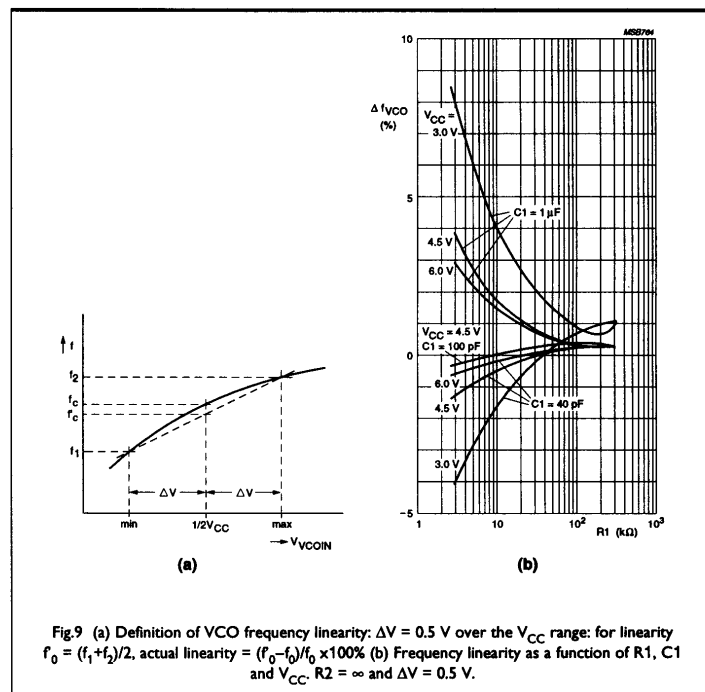


## Linearity

The op-amp technique used in the voltage-to-current converter of the VCO provides excellent linearity (see Fig.9) over the allowed control voltage range of the VCO ( $1.1\text{ V}$  to  $V_{CC} - 1.1\text{ V}$ ). Control voltages outside this range produce a step in the VCO output frequency, see Fig.10. When the VCO input voltage exceeds  $V_{CC} - 1.1\text{ V}$ , the VCO oscillates at its highest frequency ( $>20\text{ MHz}$ ). When the VCO input voltage is below  $1.1\text{ V}$ , the VCO oscillates at:

- A few Hertz when R2 is not used (see Fig. 10(a)), because the VCO is biased only by internal leakage currents
- $f_{\text{off}}$  (i.e.  $f_0 - 1.6f_R$ ) when R2 is used (see Fig.10(b)).

A properly-designed PLL will never generate signals outside the allowed control voltage range of the VCO, so a control voltage clamp is generally superfluous. A clamp may however be useful in applications where the input signal is outside the VCO frequency operating range for a long time relative to the filter time-constant. A suitable clamp is described in the section 'Application Examples'.



### Demodulator output

For demodulation applications, a buffered  $V_{COIN}$  signal is available at pin 10 ( $DEM_{OUT}$ ) of both the 4046A and the 7046A. An op-amp similar to that used in the VCO buffers the signal, so as not to affect the characteristics of the low-pass filter. The offset voltage is typically only about 20 mV at  $V_{CC} = 4.5$  V.

To bias the output stage correctly, a load resistor ( $R_S$ ) of between 50 k $\Omega$  and 300 k $\Omega$  should be connected between pin 10 and ground.

### Duty factor

The duty factor of the VCO output signal depends on the symmetry of both branches of the current-controlled oscillator, (i.e. on the symmetry of the Schmitt triggers, NOR and NAND gates and N6/P6 and N7/P7 in Fig.7) and on the on-chip spread of the  $V_{T+}$  of the Schmitt triggers. Well-balanced transistor sizes and loads limit the deviation from a 50% duty factor to typically  $\pm 1\%$  over the full temperature and supply voltage range.

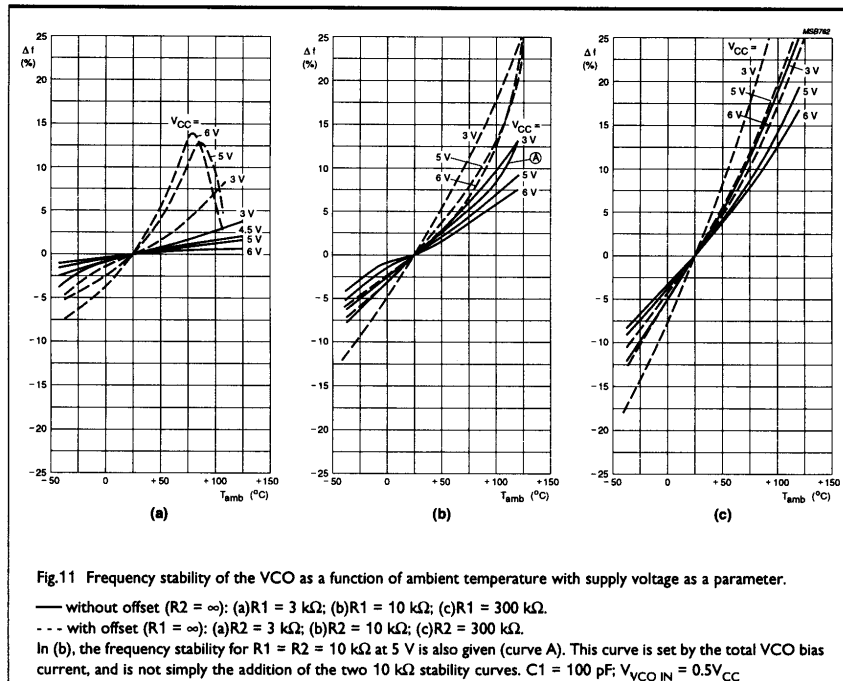
### Conversion gain

The conversion gain of the VCO ( $K_o$ ) depends on the VCO output frequency range ( $2f_R$ ), and varies slightly with supply voltage. Note that the VCO range in Fig.4 is in Hz whereas rad/s should be used when calculating  $K_o$ . For example, with a frequency range of  $10^4$  Hz and  $V_{CC} = 5$  V:

$$K_o = \frac{\text{VCO frequency range}}{\text{VCO input voltage range}} = \frac{2\pi 10^4}{(5 - 2.2)} = 22\,440 \text{ rad/s/V.} \quad (1)$$

### Effect of temperature

Figure 11 shows the frequency stability of the VCO as a function of ambient temperature. In a PLL, these frequency deviations of the VCO are, of course,



compensated automatically by the loop, only the absolute value of the phase difference between the input signal (pin 14) and the VCO output signal will vary slightly when comparators PC1 and PC3 are used. This is discussed in more detail in the next section. The best stability is at high bias currents together with low values of C1. At high ambient temperatures, the current-to-frequency converter decreases the output frequency, owing to the increased propagation delay of the logic, but not sufficiently to compensate an increasing charge current. This results in a lower temperature coefficient with low values for R1 and R2 as shown in Fig.11(a). Within the range 0 °C to 75 °C the typical temperature coefficient is from 0%/K to 0.2%/K.

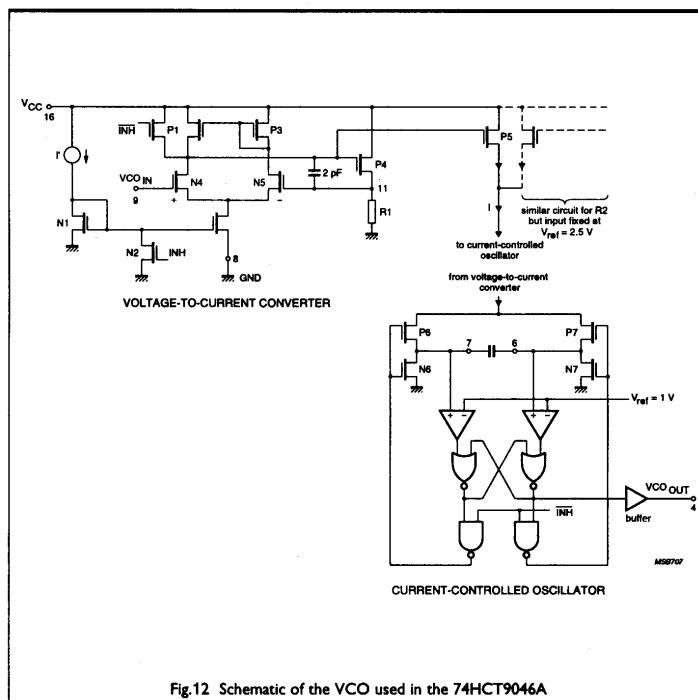
When there is a frequency offset, the temperature coefficient is larger, because R2 is biased via a diode whose forward voltage is also temperature dependent.

Note that the measurements of frequency stability were taken with R1 and R2 held at a constant 25 °C, which is unlikely in practice. If R1 and R2 are normal metal-film resistors, their positive temperature coefficient will partly compensate the frequency changes due to variations of ambient temperature. In addition, C1 should have a negligible temperature coefficient, e.g. an NP0 capacitor. If both R1 and R2 are used, the total frequency change is not the sum of a pair of curves shown in Fig.11, but is set by the total VCO bias current (curve A).

### Voltage-controlled oscillator of the HCT9046A

The circuit of the VCO section of the HCT9046 has a similar configuration to the 4046 VCO as shown in Fig.7. However, two measures have been taken to improve the frequency stability and to reduce the part-to-part spread to  $\pm 10\%$ .

The first measure is the use of a comparator with a band-gap reference voltage  $V_{ref1} = 1V$  to detect the switching levels of the VCO sawtooth, see Fig.12. This improves the frequency stability as a function of variation of  $V_{CC}$  and temperature. The VCO of the 4046 uses level detection by the threshold levels of Schmitt trigger circuits, which is much more temperature and voltage dependent. Furthermore, the reference voltage for the current source for the offset frequency set by R2 is not taken from  $V_{CC}$  minus one diode voltage, but from a band-gap controlled reference voltage  $V_{ref2} = 2.5V$ . Therefore,  $I_{offset} = V_{ref2}/R2$ , and the stabilized band-gap reference largely eliminates the effect of temperature, voltage supply or part to part variations on the offset frequency.



Similarly to the 4046, the values of R1 and C1 determine the centre frequency ( $F_0$ ) and the operating frequency range  $2f_R$  of the HCT9046 VCO, see Figs.13(a) and 13(b). Over the entire range of values for R1, R2 and C1, the working frequency operating range is quite linear and very wide (from 10 Hz to about 20 MHz). A minimum value for the frequency offset with zero VCO input voltage can be selected with R2, see Fig.13(c).

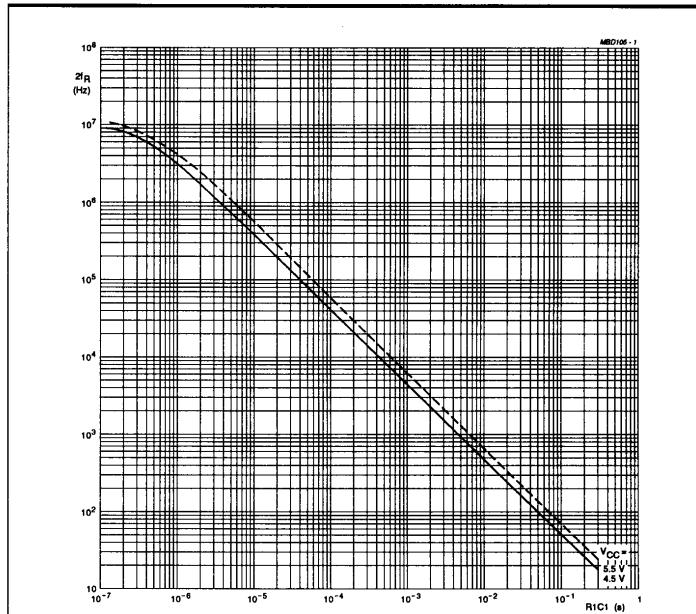


Fig.13(a) Typical 74HCT9046A VCO frequency range ( $2f_R$ ) as a function of  $R1C1$ .  
 $K_V = (2f_R/V_{VCO IN range}) \times 2\pi(r/s/V)$ ;  $V_{VCO IN} = 1.1V$  to  $V_{CC} - 1.1V$

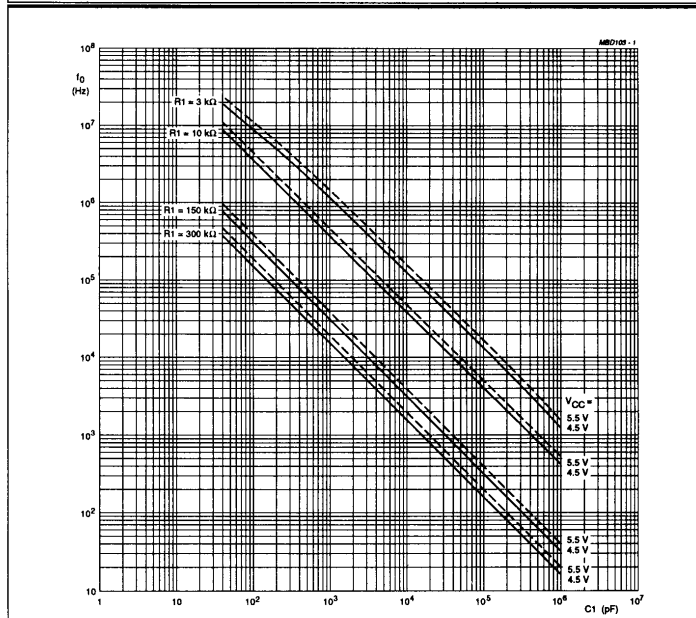
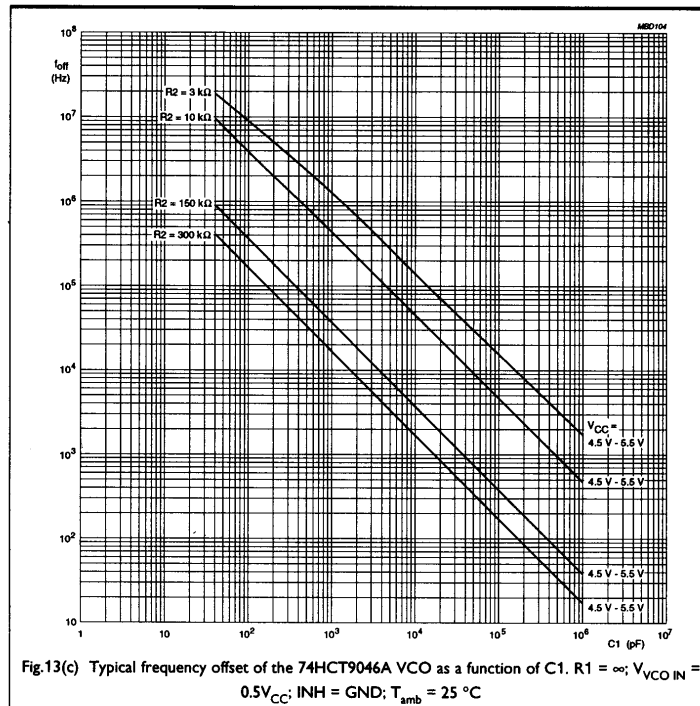


Fig.13(b) Typical value of the 74HCT9046A centre frequency ( $f_0$ ) as a function of  $C1$ .  $R2 = \infty$ ;  
 $V_{VCO IN} = 0.5 V_{CC}$ ;  $INH = GND$ ;  $T_{amb} = 25^\circ C$



#### Jitter and frequency considerations

As explained earlier for the VCO of the HC/HCT4046A, external transients or pulse edges may effect the switching point of the sawtooth oscillator at low frequencies and cause additional phase jitter. In rare cases, and within limited operating ranges, these interference spikes may also effect the positive edge of the VCO output signal and cause glitches. As with the 4046A, PLL loop errors due to such glitches can be avoided by using a glitch filter between VCO<sub>OUT</sub> and COMP<sub>IN</sub>, or by connecting a relatively high value resistor (R<sub>p</sub>) between PC2<sub>OUT</sub> and V<sub>CC</sub>, which will delay the SIG<sub>IN</sub> edge after the VCO switching point.

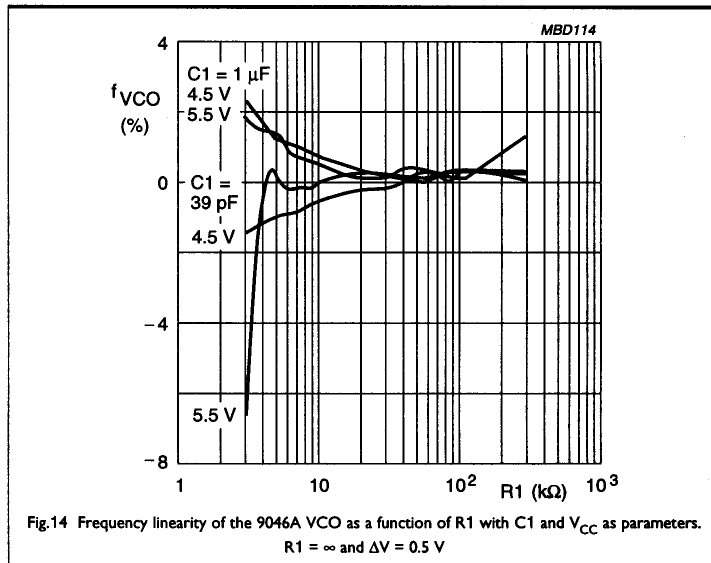
Correct ground connections and good PCB layout with short connections for critical components such as the VCO capacitor will reduce phase jitter due to transient interference. When using PC2 with a typical phase error of zero, interference from the phase comparator output edges to the sawtooth can be shifted to an inactive position after the switching point by connecting a resistor (R<sub>p</sub>) between the PC2 output and V<sub>CC</sub>. This will be explained in the next Section about phase comparators.

#### Linearity

The VCO of the HCT9046A uses op-amp techniques in the voltage-to-current converter as well as in the VCO oscillator. High performance current mirrors are used to control the charge current to achieve even better linearity than that of the 4046A/7046A VCO. The graph in Fig.14 shows that, with R1 between 5 kΩ and 300 kΩ, and V<sub>VCO IN</sub> between 1.1 V and V<sub>CC</sub> - 1.1 V, the linearity is better than ±1%.

As with the VCO of the 4046A, the input voltage of the 9046A VCO should stay within the range 1.1 V to V<sub>CC</sub> - 1.1 V for optimum linearity. Outside this range, the frequency characteristic will be as shown in Fig.10.



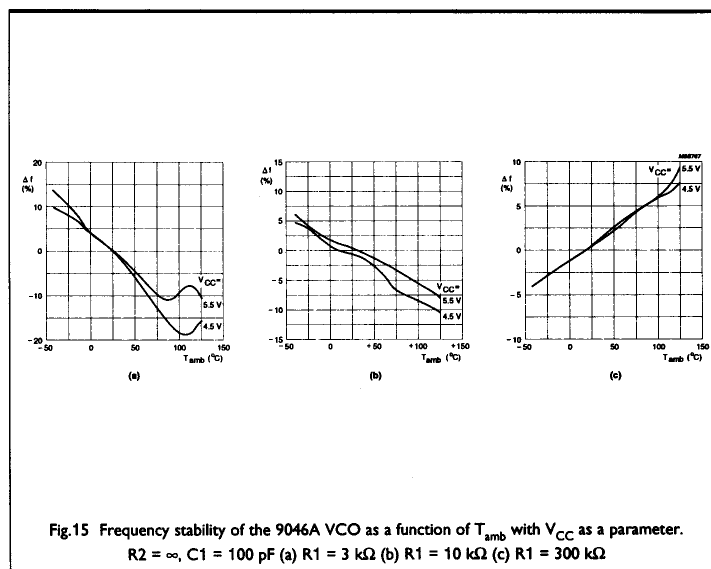


**Duty factor, demodulator output and conversion gain of the HCT9046A VCO**

Due to the similar circuit configuration, these characteristics are the same as those for the HC/HCT4046A. Please refer to the description of the VCO of the HC/HCT4046A.

**Effect of temperature**

The frequency stability of the VCO of the HCT9046A is shown in Fig. 15(a), 15(b) and 15(c) for R1 = 3 kΩ, 10 kΩ and 300 kΩ respectively. The typical stability over the temperature range will be less than 0.1%/K. Depending on the value of R1 and the consequent charging current of the VCO capacitor, the stability deviation can be positive or negative. A value of about 20 kΩ for R1 will result in even better frequency stability.



## Phase comparators

The 4046A, 7046A and 9046A circuits have two different phase comparators:

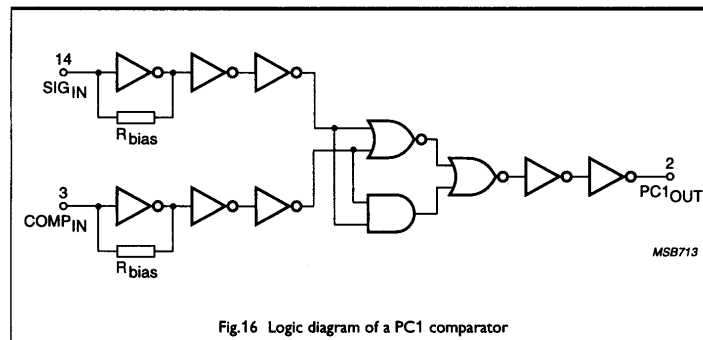
- PC1: an exclusive-OR circuit
- PC2: an edge-triggered circuit with either a 3-state voltage-controlled or current-controlled output switch:
  - PC2a: used in the 4046A/7046A. It has a voltage-controlled output source
  - PC2b: used in the HCT9046A. It has a current-sourced 3-state output. Such a switch has a linear phase error transfer function, even around zero phase. Its operation will be described in a separate Section.

The 4046A has an additional edge-triggered comparator (PC3) with a set/reset type of flip-flop.

The signal input,  $SIG_{IN}$ , and comparator input (usually connected to the VCO output),  $COMP_{IN}$ , can be directly coupled to the self-biasing amplifiers provided the signal swing is between the standard HCMOS input logic levels. Capacitive coupling can be used for smaller AC signals with an amplitude down to as low as 20 mV peak-to-peak.

### Phase comparator 1 (PC1)

This comparator is solely phase-sensitive (i.e. the average output voltage bears no relation to the frequency difference between the input signals). PLLs using it can retain lock with noisy input signals, because the full input signal (not only the rising edges) is used to determine the comparator's average output voltage. The pull-in range depends on the low-pass filter characteristics, and can be made as wide as the hold range. Note that PC1 can lock onto input frequencies close to harmonics of the input frequency.



### Function

When  $SIG_{IN}$  and  $COMP_{IN}$  have the same polarity, the output of the comparator,  $PC1_{OUT}$ , is LOW; when they have opposite polarity, the output is forced HIGH. Figure 17 shows the output signal due to a phase difference between  $SIG_{IN}$  and  $COMP_{IN}$  when the input frequencies are the same.

A phase difference of  $90^\circ$ , see Fig.17(a) (corresponding to an input signal equal to the VCO centre frequency,  $f_0$ , or no signal at all) gives an average output of  $0.5V_{CC}$  (see Fig.17(d)), causing the VCO to oscillate at  $f_0$ .

When the  $SIG_{IN}$  input frequency isn't  $f_0$ , the VCO input is raised or lowered, depending on the frequency difference, to adjust the VCO output frequency towards the input frequency. The VCO input voltage is altered by changing the duty factor of the output signal of the comparator. If PC1 adjusts the phase difference between  $SIG_{IN}$  and  $COMP_{IN}$  away from  $90^\circ$ , the duty factor of the comparator's output signal changes accordingly, see Fig.17(b) and (c). Therefore, if the input frequency isn't  $f_0$ , the phase difference isn't  $90^\circ$ , but some other value between  $0^\circ$  and  $180^\circ$ .

With the PC1 comparator, only the input frequencies are made equal – the absolute

phase difference in a locked loop can be any value between  $0^\circ$  and  $180^\circ$  (unless an active loop filter is used, in which case the phase difference remains at  $90^\circ$ , because the VCO input voltage is generated via an integrator).

For the widest hold range, the signal and comparator input frequencies should have a duty factor of 50%. The effect of a smaller duty factor is illustrated in Fig.18.

In Fig.18(a), the duty factor of  $COMP_{IN}$  is only one third that of Fig.17. Now the minimum average output voltage of the comparator is already reached for a minimum phase difference of  $+60^\circ$ , while in Fig.14(b) the maximum average voltage is reached with a maximum phase difference of  $+120^\circ$ . Outside these values, the average voltage won't change, so the range over which PC1 can adjust has shrunk by the same amount as the duty factor (two-thirds). This means that the lock-in range, hold range, pull-out and pull-in ranges are also lowered by the same amount. And the transfer characteristic (input phase error to average output voltage) has changed from that of Fig.17(d) to that of Fig.18(c).

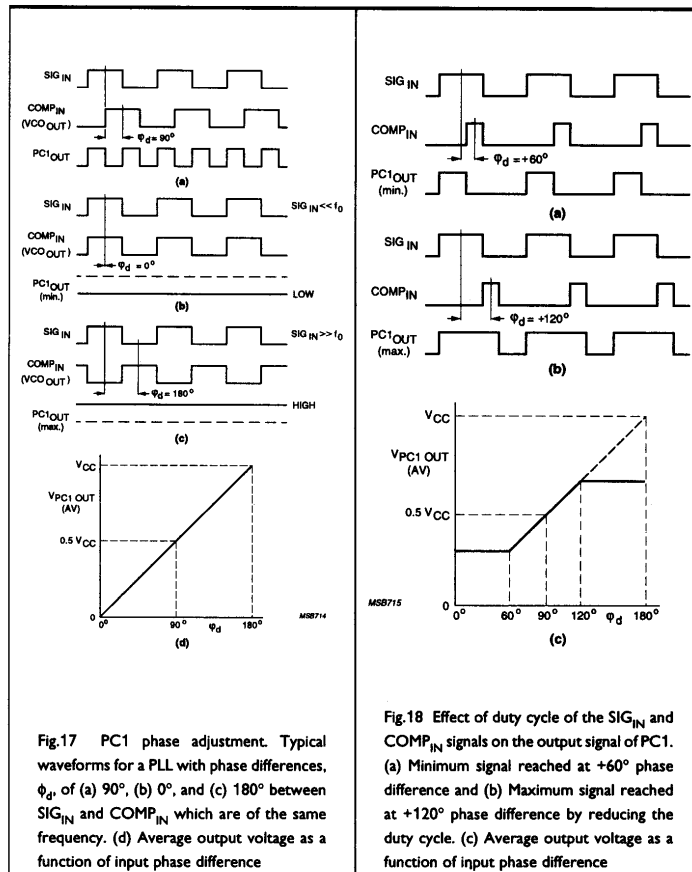
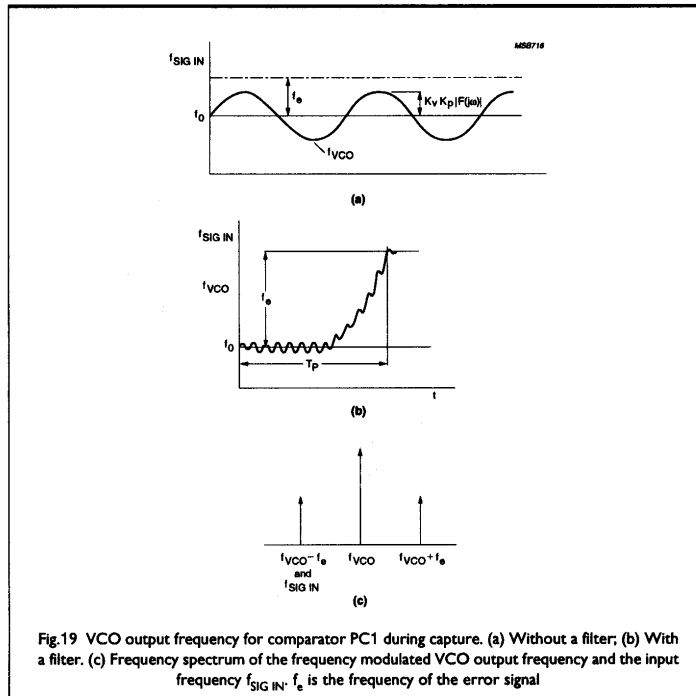


Fig.17 PC1 phase adjustment. Typical waveforms for a PLL with phase differences,  $\phi_d$ , of (a)  $90^\circ$ , (b)  $0^\circ$ , and (c)  $180^\circ$  between  $SIG_{IN}$  and  $COMP_{IN}$  which are of the same frequency. (d) Average output voltage as a function of input phase difference

Fig.18 Effect of duty cycle of the  $SIG_{IN}$  and  $COMP_{IN}$  signals on the output signal of PC1. (a) Minimum signal reached at  $+60^\circ$  phase difference and (b) Maximum signal reached at  $+120^\circ$  phase difference by reducing the duty cycle. (c) Average output voltage as a function of input phase difference

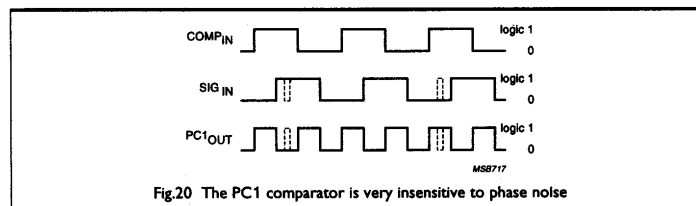


Since the  $SIG_{IN}$  and  $COMP_{IN}$  inputs are fully interchangeable, the average output voltage of the comparator is the same irrespective of whether the  $SIG_{IN}$  frequency is higher or lower than  $COMP_{IN}$  (only the sign of the phase error will change). Thus, the exclusive-OR is not frequency-sensitive, but solely phase-sensitive.

With no loop filter, the output of the PC1 comparator will either raise or lower the VCO frequency arbitrarily, and the loop is likely to stay unlocked, see Fig.19(a). However, with a loop filter, the VCO output will be frequency-modulated. Since the  $SIG_{IN}$  frequency ( $f_{SIG IN}$ ) equals  $f_{VCO} - f_e$ , the multiplication of both signals in PC1 produces a DC voltage which is accumulated by the integrating low-pass filter. If  $f_{SIG IN}$  is lower than  $f_{VCO}$ , this voltage is negative, decreasing  $f_{VCO}$  towards  $f_{SIG IN}$ . Conversely, if  $f_{SIG IN}$  frequency is higher than  $f_{VCO}$ ,  $f_{VCO}$  is increasing towards  $f_{SIG IN}$ . As the VCO frequency approaches the  $SIG_{IN}$  frequency, the DC level increases until lock is achieved as shown in Fig.19(b).

#### Noise sensitivity

The PC1 comparator is very insensitive to noise as can be seen in Fig.20. The average output voltage is hardly altered by the spike which will usually be removed by the filter.



### Ripple frequency

Owing to the EX-OR operation of PC1, there is a ripple on its output of twice the input frequency and of 50% duty factor (typ.). Since the ripple frequency is rather high, it is easily suppressed by the low-pass filter.

### Backlash

Backlash can only arise in sequential phase detectors, so not in PC1. Backlash is discussed in the Section on PC2a.

### Free running frequency

With no input signal, the output frequency of PC1 is the same as that of the comparator input,  $COMP_{IN}$ . And because its duty factor is 50%, the average output voltage is  $0.5V_{CC}$  which sets the VCO to its centre frequency  $f_0$ . So, even with no input signal, the VCO input is kept within the VCO's operating area without any clamping circuitry.

### Conversion gain

The output transfer function of PC1, as shown in Fig.17, is given by:

$$V_{PC1out} = V_{CC}/\pi \times (\phi SIG_{IN} - \phi COMP_{IN}), \text{ with } \phi \text{ in radians.}$$

The operating range of PC1 ( $0^\circ$  to  $180^\circ$ ) and the corresponding output voltage swing from 0 V to  $V_{CC}$  results in a conversion gain,  $K_d$ , for input signals with a duty factor of 50% (and of other values) of:

$$K_d = V_{CC}/\pi \quad \text{V/rad.} \quad (2)$$

Although  $K_d$  is independent of duty factor, as already explained, the lock-in range, hold range, pull-out and pull-in ranges are reduced for duty factors other than 50%.

### Phase comparator 2 (PC2a of the 4046A/7046A)

This is the most commonly-used phase comparator. It is a positive edge-triggered phase and frequency detector, comprising two D-type flip-flops, control gating and a 3-state output stage, see Fig.21. Since it is edge-triggered, the duty factor of the input signals is (unlike the PC1) unimportant.

### Function

The circuit functions as a 3-state up-down counter where  $SIG_{IN}$  causes an up-count and  $COMP_{IN}$  a down-count.

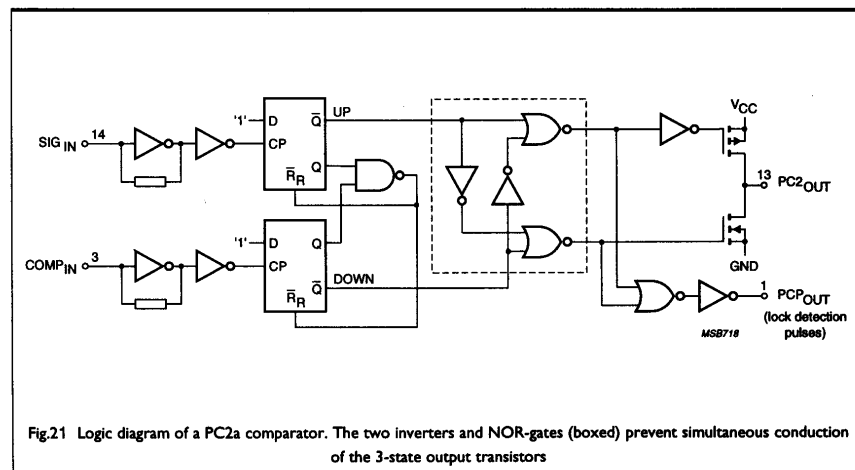
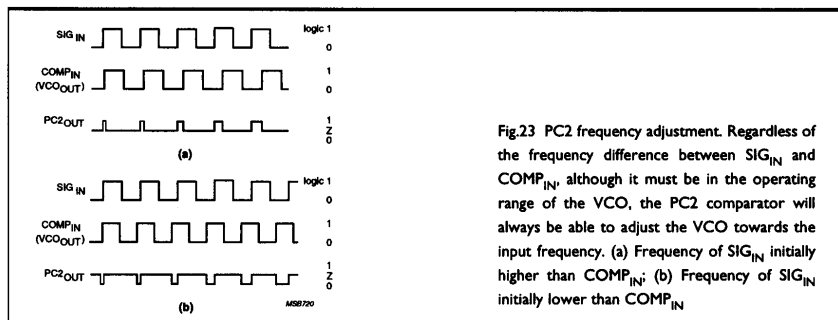
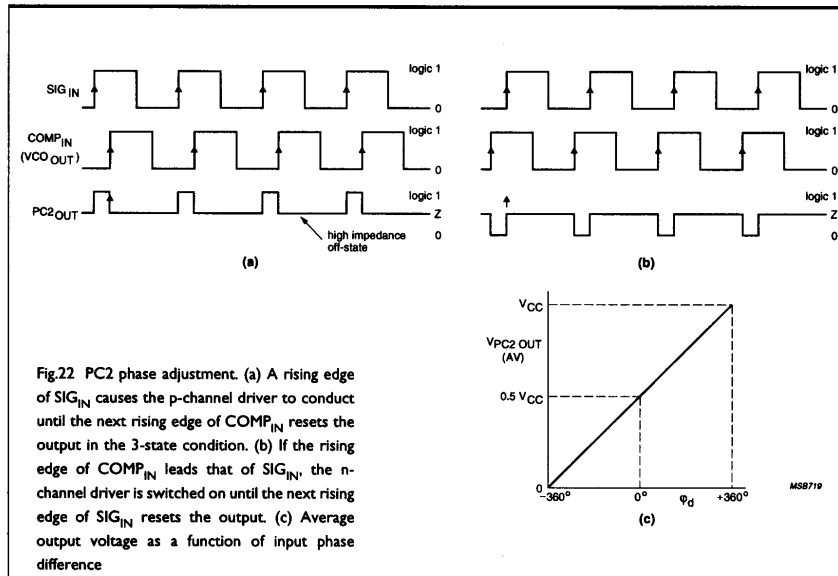


Fig.21 Logic diagram of a PC2a comparator. The two inverters and NOR-gates (boxed) prevent simultaneous conduction of the 3-state output transistors

If the frequencies of  $SIG_{IN}$  and  $COMP_{IN}$  are equal, but the phase of  $SIG_{IN}$  leads that of  $COMP_{IN}$ , the p-channel output driver is held on for a time corresponding to the phase difference. When the phase of  $SIG_{IN}$  lags that of  $COMP_{IN}$ , the n-channel driver is held on, see Fig.22. In Fig.22(a), the positive output pulses increase the VCO frequency until the phase error,  $\phi_e$ , is zero, while in Fig.22(b), the negative pulses reduce the VCO frequency.

If the frequency of  $SIG_{IN}$  is higher than that of  $COMP_{IN}$ , the p-channel output driver is held on for most of the input signal cycle, and for the remainder of the cycle both n- and p-channel drivers are off (3-state). Conversely, if the frequency of  $SIG_{IN}$  is lower than that of  $COMP_{IN}$ , the n-channel driver is held on for most of the cycle. Therefore, the voltage on the filter capacitor C2, connected to PC2<sub>OUT</sub>, varies until the signal and comparator inputs are equal in phase and frequency, see Fig.23. To obtain this characteristic with the PC1 or PC3 comparator, an active loop filter is required. Therefore, even with a passive filter, PC2 can be regarded as a phase comparator with an ideal integrator resulting in a high-gain loop without phase error. This is discussed further in Appendix A.

When locked, the PC2 output is in its high-impedance 3-state. In a locked loop, there is no phase difference between  $SIG_{IN}$  and  $COMP_{IN}$  over the full frequency range of the VCO.



### Noise sensitivity

Unlike the PC1 comparator, PC2 is sensitive to phase noise because it uses a D-type flip-flop at the output, see Fig.20, and requires signals with a signal-to-noise ratio of

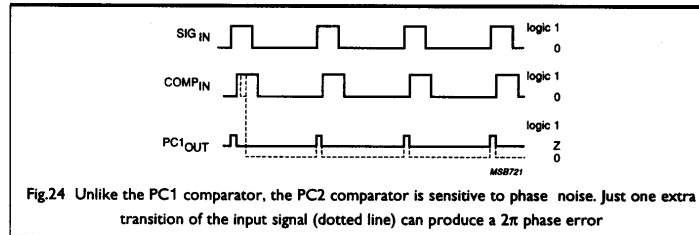


Fig.24 Unlike the PC1 comparator, the PC2 comparator is sensitive to phase noise. Just one extra transition of the input signal (dotted line) can produce a  $2\pi$  phase error

typically  $>30$  dB to operate correctly.

Slow rising or falling edges of the SIG<sub>IN</sub> or COMP<sub>IN</sub> signals may have small transients around the input switching level of the self-biasing input amplifiers. To avoid  $2\pi$  phase errors due to these transients, it is recommended that the edges of the comparator input signals have a slope of at least  $0.5$  V/ $\mu$ s and are monotonically rising or falling. This point requires particular attention, if small AC signals are capacitively coupled via SIG<sub>IN</sub> to the self-biasing input amplifiers.

### Ripple frequency

Ideally, when the PLL is locked, the comparator output remains in the 3-state condition and the filter capacitor voltage is constant. However, because filter capacitor C2, the 3-state output and the VCO input are not ideal, they sink or source a small leakage current, altering the capacitor voltage, and hence the VCO frequency, a little. This causes the comparator output to generate small correction pulses intermittently, however, the PLL is still considered to be locked. The frequency of these pulses (ripple frequency) is never higher than the input frequency. The amplitude of the sidebands produced is typically much lower than for PC1, because of the smaller duty factor of the ripple frequency.

### Backlash

Owing to internal delays, phase comparator PC2a needs a minimum phase difference between SIG<sub>IN</sub> and COMP<sub>IN</sub> to generate an output pulse. This minimum phase difference is called the backlash time or dead zone, and is specified in seconds. The advanced design of the HCMOS comparator restricts the total backlash time to 2 ns (typ.), 4 ns (max.).

### Phase and frequency jitter considerations

The intrinsic parasitic capacitances of the PC2 type-a output ( $C_{par}$ , about 10 pF) widen the output correction pulses by an amount dependent on the RC time-constant, see Fig.25. With a 5 k $\Omega$  loop filter resistor R3, the pulse width is already about 50 ns longer than it should be, adjusting the phase error more than needed. At the next sample point, the same effect occurs, but in reverse, introducing phase jitter which, for video monitor applications in particular, is unacceptable. In addition, if the discharge time is long relative to the period of the input frequency, the actual output pulse width bears no relationship to the phase error any more. This situation can be avoided by selecting the lowest allowable value for the series resistor of the filter section,  $R3 = 470\Omega$ , which reduces the discharge time to about 4.5 ns and allows correct operation over the whole VCO frequency range. To reduce the value and size of the filter capacitors at lower frequencies (below about  $f_0 = 100$  kHz), a higher value may be chosen for R3.

If C2 is much larger than C<sub>par</sub>, although there will be no jitter, another effect due to the parasitic capacitance, and the backlash, is to low-frequency-modulate the VCO output. When the VCO frequency moves slowly away from the input frequency, at least the backlash time (2 ns) is required before PC2 generates an output pulse. Then, the parasitic capacitance is also charged, altering the voltage on the filter capacitor (C2) by:  $\Delta V_{C2} \approx \Delta V_{PC2OUT} C_{par} / C2$ , with a charge:  $\Delta Q = C_p (V_{CC} - V_{C2})$ .

This in turn alters the VCO frequency by:

$$\Delta f \approx \Delta V_{C2} \text{ VCO gain} / 2\pi.$$

The number of input cycles (n) needed before the delay between the rising edges of SIG<sub>IN</sub> and COMP<sub>IN</sub> is again 2 ns (backlash time), but with opposite polarity, is:

$$n = \frac{\text{twice the total backlash time (4 ns)}}{1/f_{in} - 1/(f_{in} + \Delta f)}$$

The modulation frequency is  $f_{in}/2n$ , and depends solely on C2, the backlash time, the VCO gain, and the input frequency, so it cannot be filtered out. Increasing C2 will only decrease the modulation frequency. The way to avoid modulation is to add a leakage resistor as described below.

#### Applying parallel resistance R<sub>p</sub> to eliminate backlash operation

The phase jitter and backlash can be eliminated by connecting a resistor (R<sub>p</sub>) between the output of PC2 (pin 13) and ground (or V<sub>CC</sub>), such that the leakage current through R<sub>p</sub> compensates, within one period, for the surplus charge injected by the parasitic output capacitance. See Fig.25(b). For equal charge, the required value for R<sub>p</sub> is given by:

$$(V_{CC} - V_{C2}) \times C_p \leq V_{C2} / (R_p \times f_{in}) \quad \text{or,}$$

$$R_p \leq \frac{V_{C2init}}{1 \text{ to } 3 \times C_p \times (V_{CC} - V_{C2init}) f_{in}} \quad \Omega. \quad (3)$$

with V<sub>CC</sub> = 5 V, f<sub>in</sub> in Hz, C<sub>p</sub> = 10 × 10<sup>-12</sup> Farads and V<sub>C2 init</sub> = 1 to 4 V.

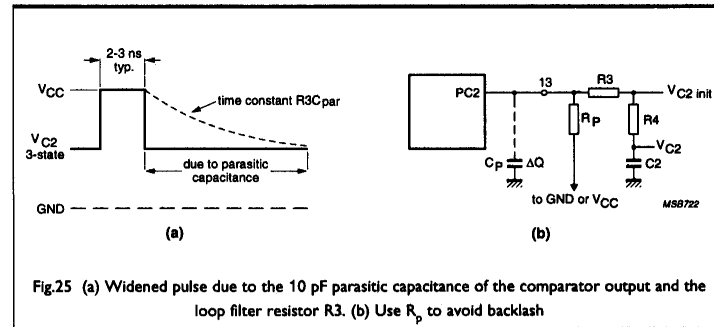


Fig.25 (a) Widened pulse due to the 10 pF parasitic capacitance of the comparator output and the loop filter resistor R3. (b) Use R<sub>p</sub> to avoid backlash

The safety factor 3 in the denominator ensures that only positive correction pulses are generated, even for the largest parasitic capacitances and with R<sub>p</sub> connected between PC2<sub>OUT</sub> and ground. With R<sub>p</sub> connected between PC2<sub>OUT</sub> and V<sub>CC</sub> in the in-lock condition, only negative pulses are generated to discharge the extra charge from R<sub>p</sub>.

As mentioned in the VCO section, it is preferable to connect R<sub>p</sub> to V<sub>CC</sub>. In that case, the pulse edges of the input signal SIG<sub>IN</sub>, and also the related edges of the phase comparator outputs, will be shifted behind the switching point of COMP<sub>IN</sub> and VCO<sub>OUT</sub>, see Fig.22. Otherwise, with R<sub>p</sub> connected to ground, the edges of the SIG<sub>IN</sub> input appear just in front of the VCO<sub>OUT</sub> switching pulse. This will cause some interference or transients near to the top of the VCO sawtooth voltage, causing extra jitter on the VCO output frequency or disturbing the VCO output edge. With R<sub>p</sub> connected to V<sub>CC</sub>, jitter due to this interference will be avoided.



**Note:** Using  $R_p$  forces the loop to operate outside the dead zone of PC2a. A disadvantage of this is that input signal  $SIG_{IN}$  and the VCO output signal  $COMP_{IN}$  will show a very small, constant, phase difference with a shift of up to 50 ns. In many applications, this difference is not important. In applications which need to operate around zero phase-shift without dead zone, or in applications with a phase-modulated input signal, it is recommended to use the HCT9046A to take advantage of the backlash-free operation of PC2b. The actual phase shift, due to  $R_p$ , is given by:

$$\frac{0.5V_{CC}}{R_p} \times T(SIG_{IN}) = \frac{\Delta T \times 0.5V_{CC}}{R3}, \text{ or}$$

$$\Delta T = \frac{R3}{R_p} \times \frac{1}{f(SIG_{IN})}, \text{ at } V_{C2 \text{ init}} = 0.5V_{CC}$$

**Free running frequency**

With no input signal, the positive transitions of the VCO set the comparator output LOW and discharge the filter capacitor. However, the time-constant of the loop filter is normally large enough to keep the VCO input voltage within the linear operating range. When it isn't, the VCO output frequency will either be  $f_{off}$ , or a few Hz as described in 'VCO linearity'. If this is not acceptable in the application, control voltage clamping must be used, see 'Application examples'.

**Conversion gain**

Since the comparator has an operating range of  $\pm 360^\circ$  ( $\pm 2\pi$ ) and an output voltage swing of  $V_{CC}$ , the conversion gain if an active filter is used is:

$$K_d = V_{CC}/4\pi \text{ V/rad.} \tag{4}$$

A filter with a resistor voltage clamp will reduce the effective output swing of the comparator, reducing the conversion gain, see 'Application examples'.

When a passive filter is used with PC2, the phase comparator gain will vary with the average output voltage (VCO input voltage) and:

$$K_d = \text{average output voltage}/2\pi \text{ V/rad.} \tag{5}$$

For a  $V_{CC}$  of 5 V, the gain will vary from  $1.1/2\pi$  to  $3.9/2\pi$ , thus by about 3.5:1 over the VCO's operating range. Equation 5 is derived in Appendix A which also discusses the effect of the varying gain in more detail.

**Phase comparator 2 (PC2b of the 9046A)**

This is a positive edge-triggered phase and frequency detector. When the PLL is using this comparator, the loop is controlled by positive signal transitions, and the duty factors of  $SIG_{IN}$  and  $COMP_{IN}$  are insignificant.

**Function**

PC2b comprises two D-type flip-flops, control gating, and a 3-state output stage with

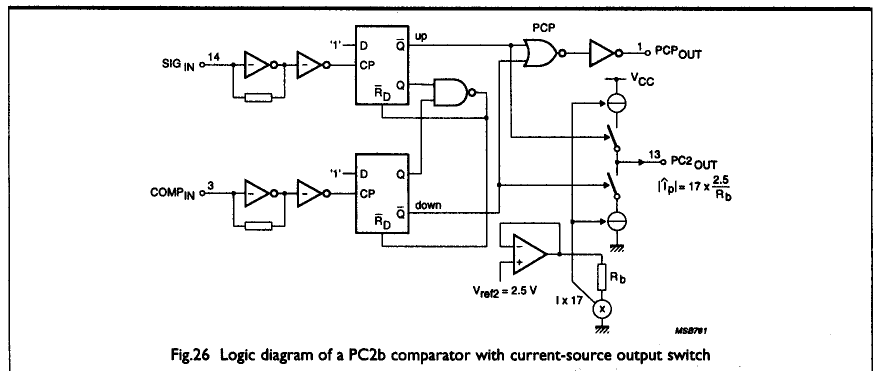
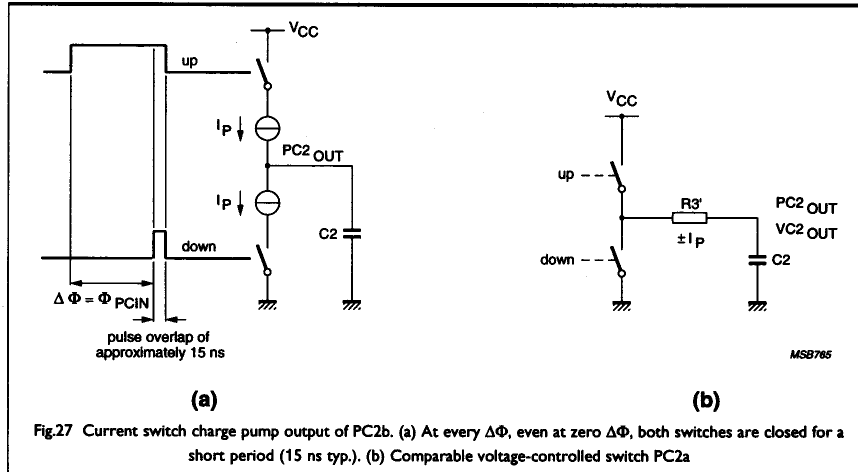


Fig.26 Logic diagram of a PC2b comparator with current-source output switch



sink and source transistors acting as current sources, henceforth called the charge pump output of PC2b.

The circuit functions as an up-down counter where  $SIG_{IN}$  causes an up-count, and  $COMP_{IN}$  causes a down-count. The current switch charge pump output allows virtually ideal performance of PC2b because some pulse overlap is applied to the up and down signals, see Fig.27(a). In contrast to the voltage-controlled switch of PC2a, see Fig.21, the current-source output of PC2b has no cross-link between the outputs which would prevent such overlapping.

The pump current is independent of the supply voltage and is set by the internal band-gap reference of 2.5 V:

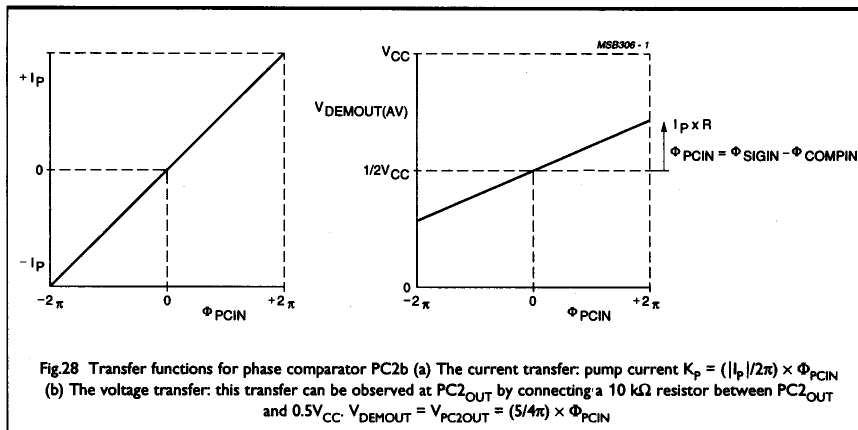
$$I_p = 17 \times \frac{2.5}{R_b} \text{ (A)}$$

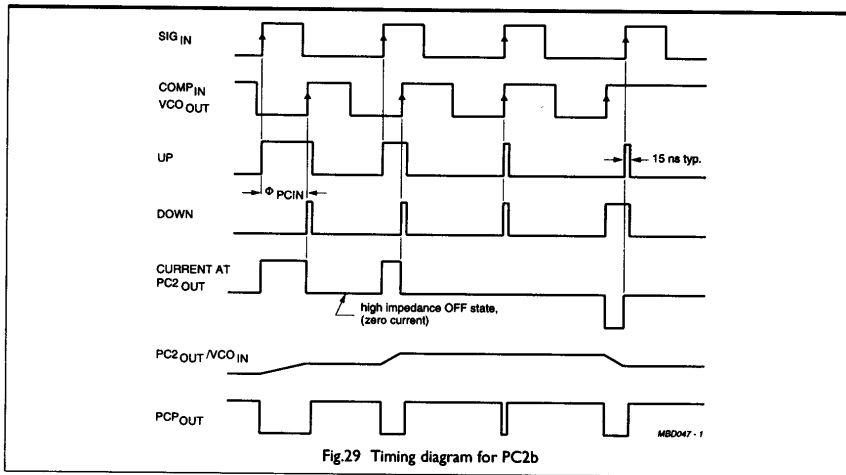
where 17 is the gain factor for the current mirror and  $R_b$  is the external bias resistor between pin 15 and ground. The current and voltage transfer functions of PC2b are shown in Fig.28.

The phase comparator gain is:

$$K_p = \frac{|I_p|}{2\pi} \text{ (A/r)}$$

Typical waveforms for the PC2b loop are shown in Fig.29.

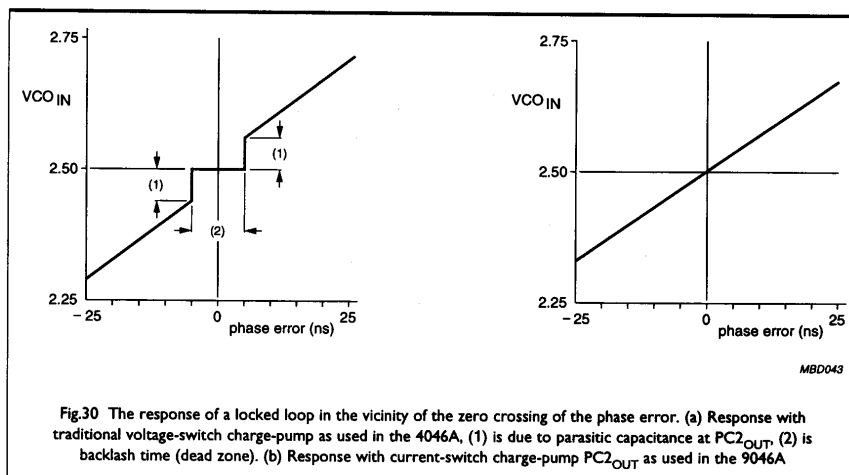




When the frequencies of  $SIG_{IN}$  and  $COMP_{IN}$  are equal but the phase of  $SIG_{IN}$  leads that of  $COMP_{IN}$ , the up output driver at  $PC2_{OUT}$  is held 'ON' for a time corresponding to the phase difference ( $\Phi_{PCIN}$ ). When the phase of  $SIG_{IN}$  lags that of  $COMP_{IN}$ , the down or sink driver is held 'ON'.

When the frequency of  $SIG_{IN}$  is higher than that of  $COMP_{IN}$ , the source output driver is held 'ON' for most of the input signal cycle time, and for the remainder of the cycle time both drivers are 'OFF' (3-state). If the frequency of  $SIG_{IN}$  is lower than that of  $COMP_{IN}$ , the sink driver is held 'ON' for most of the cycle. Subsequently, the voltage at the capacitor (C2) of the low-pass filter connected to  $PC2_{OUT}$  varies until the signal and comparator inputs are equal in both phase and frequency. At this stable point, the voltage on C2 remains constant as the PC2 output is in 3-state and the VCO input at pin 9 is high impedance. Also in this condition, the signal at the phase comparator pulse output ( $PCP_{OUT}$ ) has a minimum output pulse width equal to the overlap time, so it can be used for indicating a locked condition.

Thus, for PC2b, there is no phase difference between  $SIG_{IN}$  and  $COMP_{IN}$  over the full frequency range of the VCO. Moreover, the power dissipation due to the low-pass filter is reduced because both output drivers are OFF for most of the signal input cycle. It should be noted that the PLL lock range for this type of phase comparator is equal



to the capture range and is independent of the low-pass filter. With no signal present at SIG<sub>IN</sub>, the VCO adjusts, via PC2b, to its lowest frequency.

By using current sources as charge pump outputs on PC2b, the dead zone or backlash time could be reduced to zero. Also, the pulse widening due to the parasitic output capacitance plays no role here. This allows a linear transfer function, even in the vicinity of the zero crossing. The differences between a voltage switch charge pump and are current switch charge pump are shown in Fig.30.

#### Phase and frequency jitter considerations

As previously mentioned, the 9046A has no backlash. However, as with the 4046A, parasitic coupling of pulse edges of the PC2 output may result in spikes on the VCO ramp and cause extra phase jitter. In some applications, working around zero phase shift between SIG<sub>IN</sub> and COMP<sub>IN</sub>, it is advisable to connect a resistor R<sub>p</sub> between PC2<sub>OUT</sub> and V<sub>CC</sub>. For a description about the use of R<sub>p</sub>, see page 22.

#### Conversion gain

The design of the low-pass filter is somewhat different when using current sources. External resistor R3 is no longer present when using PC2b as a phase comparator. The current-source is set by R<sub>b</sub>. A simple capacitor now behaves as an ideal integrator because it is charged by a constant current. The transfer function of the voltage-switch charge-pump may be used. In fact, it is even more valid because the transfer function is no longer restricted to only small changes. Furthermore, the current is independent of both the supply voltage and the voltage across the filter. For those familiar with the low-pass filter design for the 4046A, a relationship can show how R<sub>b</sub> relates to a fictive series resistance called R3'.

This relationship can be derived by first assuming that a voltage-controlled switch PC2a of the 4046A is connected to filter capacitor C2 via this fictive R3', see Fig.27(b). During the PC2 output pulse, the charge current equals:

$$|I_P| = \frac{V_{CC} - V_{C2(0)}}{R3'}$$

With the initial voltage V<sub>C2(0)</sub> at 0.5V<sub>CC</sub> = 2.5 V:

$$|I_P| = \frac{2.5}{R3'}$$

As previously shown, the charge current of the current-switch of the 9046A is:

$$|I_P| = 17 \times \frac{2.5}{R_b}$$

Hence:

$$R3' = \frac{R_b}{17} \text{ (}\Omega\text{)}$$

Using this equivalent resistance R3' for the filter design, the voltage can now be expressed as a transfer function of PC2, assuming ripple (f<sub>r</sub> - f<sub>i</sub>) is suppressed, as:

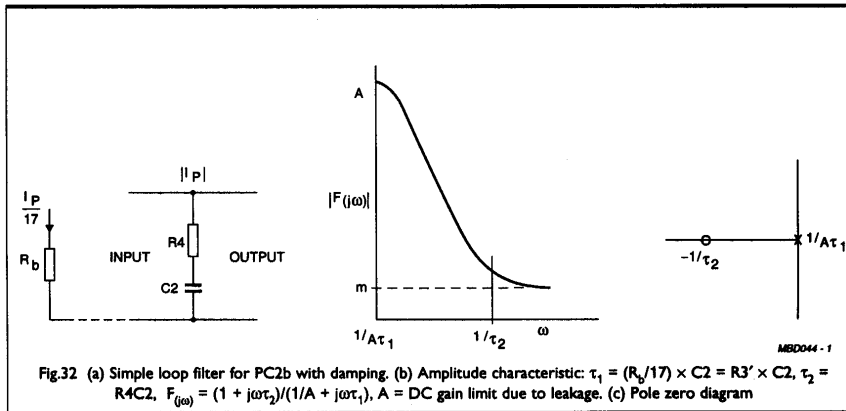
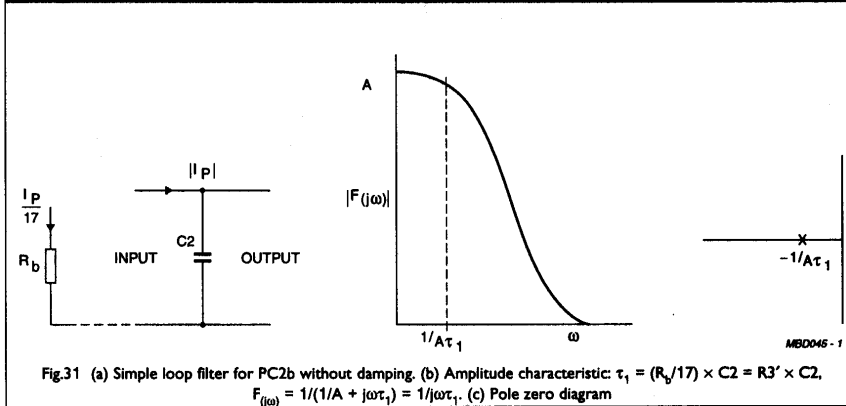
$$K_{PC2} = \frac{5}{4\pi} \text{ (V/r)}$$

Again, this illustrates the supply-voltage-independent behaviour of PC2b.

#### Filter design

Examples of PC2b combined with a passive filter are shown in Figs. 31 and 32. Figure 31 shows that PC2b with only a C2 filter behaves as a high-gain filter. For stability, the damped version with series resistor R4 shown in Fig.32 is preferred.

Practical design values for R<sub>b</sub> are between 25 kΩ and 250 kΩ with R3' = 1.5 kΩ to 15 kΩ for the filter design. Higher values for R3' require lower values for the filter capacitor which is very advantageous at low values of the loop natural frequency ω<sub>n</sub>.

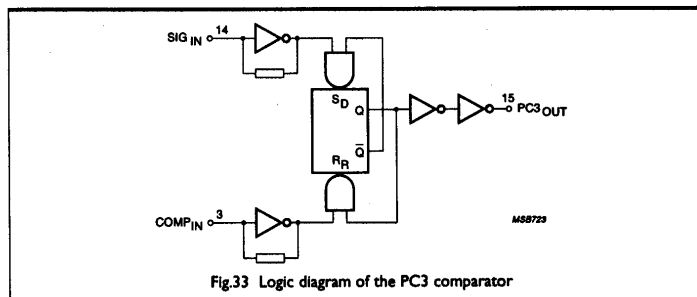


#### Noise sensitivity

Because the logic comparator part of PC2b of the 9046A is equal to that of the voltage-controlled output switch of PC2a, except for the output section, its noise sensitivity, ripple frequency and free-running frequency are the same as previously described in the Section dealing with PC2a.

#### Phase comparator 3 (PC3)

Only the HC/HCT4046A has this phase comparator which is a positive edge-triggered



SR flip-flop as shown in Fig.33. This comparator is less sensitive to phase noise than PC2, but still requires input signals with a signal-to-noise ratio larger than about 20 dB.

**Function**

Since PC3 is an edge-triggered comparator, the duty factors of SIG<sub>IN</sub> and COMP<sub>IN</sub> are unimportant. A positive transition of SIG<sub>IN</sub> sets the flip-flop and the push-pull output is HIGH. The next rising edge of COMP<sub>IN</sub> resets the flip-flop and the output is set LOW again. The average voltage on the low-pass filter capacitor (which depends on the duty factor of the comparator output) adjusts the VCO accordingly.

Figure 34 shows phase adjustment using PC3 when both input frequencies are equal.

Figure 35 shows the situation when there is a frequency difference between SIG<sub>IN</sub> and COMP<sub>IN</sub>, along with the output signal which will adjust the VCO until both signals are equal in frequency. Figure 35(c) shows that when the difference is large, PC3 adjusts quickly, but takes longer to make the final adjustments as the VCO frequency approaches the input frequency.

A phase difference of 180° gives an average output of 0.5V<sub>CC</sub> which sets the VCO at its centre frequency, f<sub>0</sub> (see Fig.34(b)). If the frequency of SIG<sub>IN</sub> is not equal to f<sub>0</sub>, the VCO needs to be adjusted, the phase difference between SIG<sub>IN</sub> and COMP<sub>IN</sub> being increased or reduced depending on the frequency difference, until the average output voltage sets the VCO frequency to the SIG<sub>IN</sub> frequency. The phase difference may vary between 0° and 360° but circuits are usually designed for a difference of about 180°, to

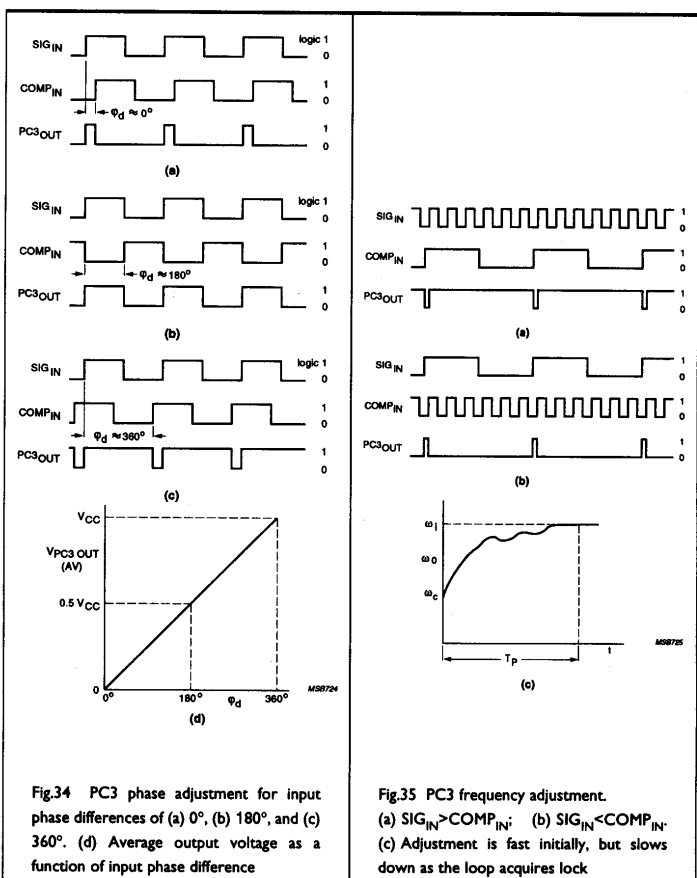


Fig.34 PC3 phase adjustment for input phase differences of (a) 0°, (b) 180°, and (c) 360°. (d) Average output voltage as a function of input phase difference

Fig.35 PC3 frequency adjustment. (a) SIG<sub>IN</sub> > COMP<sub>IN</sub>; (b) SIG<sub>IN</sub> < COMP<sub>IN</sub>; (c) Adjustment is fast initially, but slows down as the loop acquires lock

give a symmetrical capture range. With PC3 and a passive filter, only the input frequencies are adjusted to be equal, no absolute phase relationship exists between the two input signals.

If an active filter is used, the phase difference remains at 180°, because the VCO input voltage is then generated by an integrator.

#### Noise sensitivity

The PC3 comparator is less sensitive to phase noise than PC2, see Fig.36, because its set/reset flip-flop is not sensitive to extra transitions.

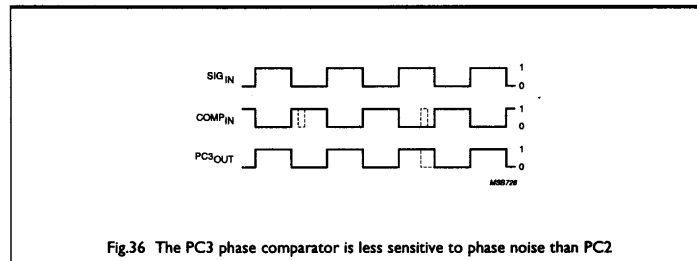


Fig.36 The PC3 phase comparator is less sensitive to phase noise than PC2

#### Ripple frequency

The ripple frequency on the output of PC3 is the same as the input frequency, but with a duty factor of typically 50%. Since the output of PC3 swings by a greater amount than PC2 for input phase differences, and the duty factor is typically 50%, the ripple content of the output signal is higher than for PC2, requiring more filtering.

#### Backlash

Since a typical loop using PC3 is designed to have a phase difference of 180° between SIG<sub>IN</sub> and COMP<sub>IN</sub>, the dead zone is usually on the edge of the operating area of the comparator (0° or 360°). Therefore, the effect on the performance of the comparator is unnoticeable.

#### Free-running frequency

The behaviour of PC3 is very similar to that of PC2. With no input signal, the output is set LOW, which discharges the filter capacitor.

Depending on the application, a voltage clamp may be needed to keep the VCO input voltage within range.

#### Conversion gain

The operating range of PC3 is from 0° to 360° and the output voltage swing is V<sub>CC</sub>, which results in a conversion gain of:

$$K_d = V_{CC}/2\pi \quad \text{V/rad.} \quad (6)$$

If a filter with a clamp is used, the effective output swing, and hence the conversion gain, will be smaller.

#### Lock detection indication

It is sometimes convenient to have an indication of whether a PLL is locked. A lock detection indicator can be built for all HCMOS PLL circuits – the 4046A and 9046A requiring some extra circuitry, the 7046A having this already built-in.

The lock indication is derived from the phase difference between SIG<sub>IN</sub> and COMP<sub>IN</sub>. Since the PC2 phase comparator has a phase difference of 0° over the entire VCO operating range, it is the easiest comparator for which to build a lock indicator. Of course, even when the PLL is locked, the VCO needs some small adjustments to stay

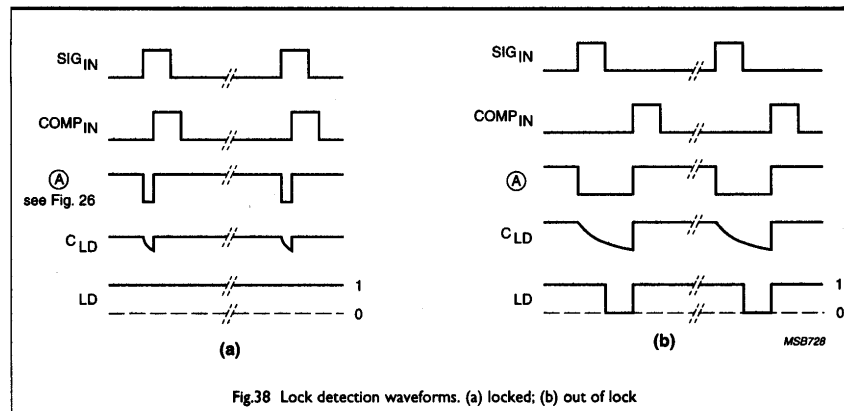
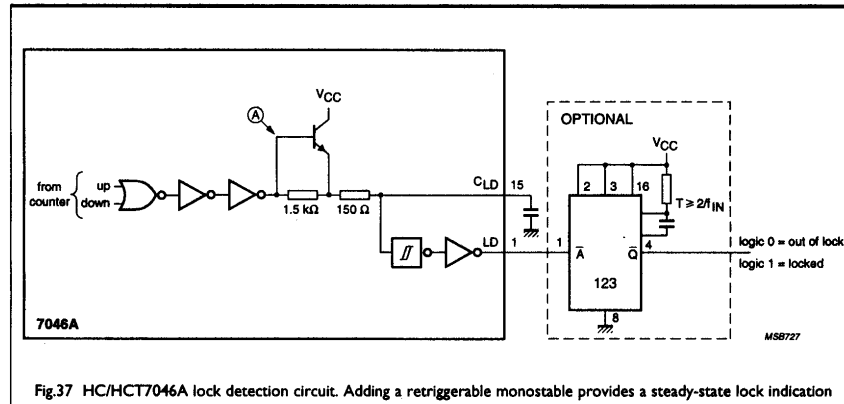
locked, so the phase difference is not exactly  $0^\circ$ , but varies slightly depending on the loop parameters and the backlash time. The phase difference that is considered to represent 'out-of-lock' will depend on the application.

When the PC1 or PC3 comparator is used, together with a passive filter, lock-indication cannot be derived from the phase difference, because it can vary from  $0^\circ$  to  $180^\circ$  for PC1 and from  $0^\circ$  to  $360^\circ$  for PC3 (depending on the difference between  $f_0$  and  $SIG_{IN}$ ), while the loop is still considered to be locked. For these applications, lock detection can be achieved by using cycle slip detection as shown in Fig.41.

**Lock detector for the 74HC/HCT7046A**

Figure 37 shows the circuit of the 7046A lock detection circuit.

When the PLL is locked, no pulses, or only very short pulses come from the up/down 'counter' of PC2. Any short pulses are removed by an RC filter and a Schmitt trigger produces a steady HIGH level at pin 1 (LD: lock detect) which indicates that the loop is locked, see Fig.38(a). If the up/down pulses are too long to be filtered out, the LD output will be pulsed LOW, indicating that the loop is out of lock (Fig.38(b)).



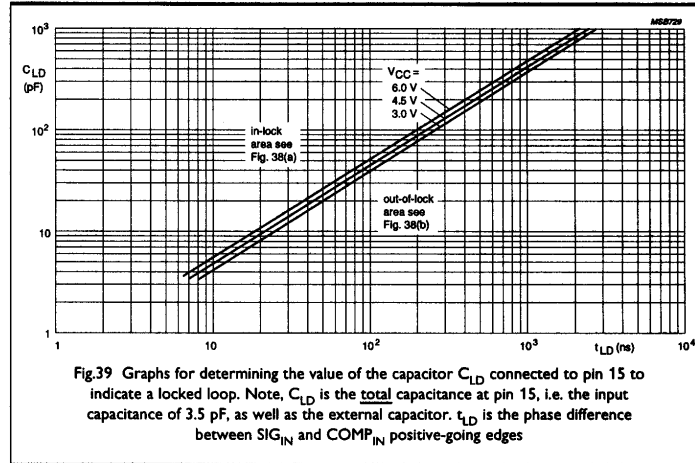


The value of the external capacitor  $C_{LD}$  can be determined using Fig.28. First, define the maximum permissible phase error,  $\phi_{max}$ , between  $SIG_{IN}$  and  $COMP_{IN}$  for your application, then convert this into seconds using:

$$t_{LD} = \frac{\phi_{max}}{360} \times \frac{1}{f_{SIG\ IN}} \quad (7)$$

Read off the value of  $C_{LD}$  from Fig.39.

With the addition of one retriggerable monostable (e.g. a '123', '423' or '4538'), a steady-state LOW and HIGH indication can be obtained, see dotted part of Fig.37. The pulse duration of the monostable must be longer than twice the period of the input signal ( $SIG_{IN}$ ).

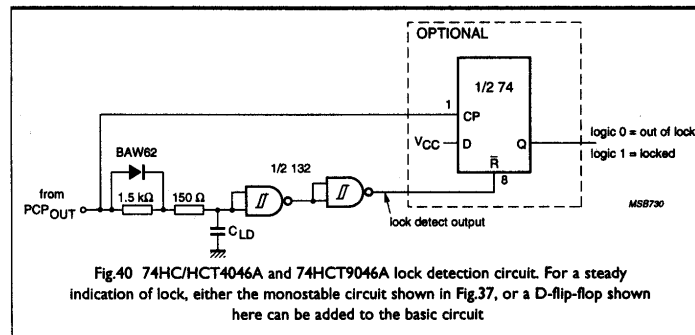


#### Lock detector for the 74HC/HCT4046A and the 74HCT9046A

A very similar lock detection circuit can be built with PC2 of the 4046A and 9046A and using the  $PCP_{OUT}$  pin, see Fig.40.

The waveforms shown in Fig.38 apply here too, only for signal A, read  $PCP_{OUT}$ . The same optional circuitry can also be used to obtain steady-state levels. In addition, since the  $PCP_{OUT}$  signal (the unfiltered output pulses from the phase comparator) is available with the 4046A, another circuit can be built using a D-flip-flop (74HC/HCT74) instead of the 74HC/HCT123 for better correlation with the maximum allowed phase error ( $\phi_{e\ max}$ ) at higher frequencies (>5 MHz), see Fig.40.

To trigger a worst-case D-flip-flop, the pulse duration of each  $PCP_{OUT}$  pulse must be at least 16 ns ( $V_{CC} = 4.5\ V$ ) which sets the minimum  $t_{LD}$  at 16 ns too.



### Cycle slip detection

A signal can also be generated when the phase error exceeds  $360^\circ$  (cycle slip detection). Figure 41 shows a detection circuit suitable for all three phase comparators.

If two positive transitions occur on an input ( $SIG_{IN}$  or  $COMP_{IN}$ ), while no positive transitions occur on the other, an output pulse is generated. This pulse can be used to trigger a monostable, for example. **Note:** When using this circuit with PC2 of the 4046A or 9046A, avoid phase errors around zero and use  $R_p$  as explained on page 22.

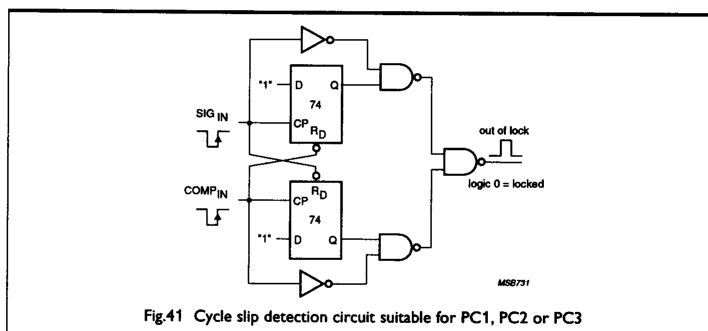


Fig.41 Cycle slip detection circuit suitable for PC1, PC2 or PC3

### Effect of temperature

The effect of ambient temperature on the frequency stability of the VCO has already been described. In this section, the effect of temperature on a complete, locked PLL is examined. The effect of temperature on the propagation delay of the phase comparators is the same as for standard HCMOS digital gates.

To recap for the VCO, if the output frequency increases at higher ambient temperature, the VCO input voltage must be decreased to maintain a constant output frequency (Fig.11). In a closed loop, all three phase comparators will adjust the VCO in the desired manner to make the output frequency independent of temperature. However, with phase comparators PC1 and PC3, with a passive filter, to reduce the VCO input voltage, for example, the duty factor of the PC1 or PC3 output signal must be reduced to lower the average voltage on the loop-filter capacitor. Therefore, the absolute phase difference between  $SIG_{IN}$  and  $COMP_{IN}$  will decrease too. This effect is absent when the PC2 comparator is used; its 3-state output goes LOW and stays LOW until the capacitor voltage is lowered sufficiently and the phase difference is zero again. To summarize, the absolute phase difference between  $SIG_{IN}$  and  $COMP_{IN}$  is temperature-dependent when PC1 or PC3 are used with a passive filter, and independent of temperature when PC2 is used. In addition, note that the VCO output frequency range is temperature-dependent. The phase difference variations when using PC1 or PC3 can be minimized by making the output frequency range of the VCO as wide as possible by raising the VCO conversion gain. They can be made completely independent of ambient temperature by using an active filter which has the same effect as using PC2.

### Supply voltage

#### HC versions

Although the phase comparators of an HCMOS PLL can be regarded as standard digital circuitry requiring a supply voltage between 2 V and 6 V, the VCO section consists of several op-amps which need a supply voltage of at least 3 V. Therefore, the supply voltage range for the 74HC4046A/7046A is from 3 V to 6 V.

#### HCT versions

The 74HCT4046A, 74HCT7046A and 74HCT9046A are specified from 4.5 V up to 5.5 V supply voltage. The only other difference between the HC and HCT versions is the input level specification of the VCO inhibit input (pin 5).

### HC and HCT versions

Slow variations of the supply voltage have no influence on the PLL output frequency when the loop is locked and stays within the operating range of the VCO. However, with PC1 and PC3, any changes in the VCO input voltage to keep the loop locked for a varying supply voltage will alter the phase difference between  $SIG_{IN}$  and  $COMP_{IN}$ , in a manner as described under 'Effect of temperature'.

Fast changes of voltage, or spikes on the VCO supply due to other logic circuits can influence the spectral purity of the VCO output frequency. Therefore, it is good practice to place decoupling capacitors as close as possible to the HCMOS PLL IC. For improved suppression of supply noise, connect a series inductor of say 100  $\mu$ H between the normal digital supply and the  $V_{CC}$  of the IC. In addition, connect two capacitors (10  $\mu$ F and 100 nF) between the  $V_{CC}$  of the IC and the GND pin for filtering.

### Part-to-part spread

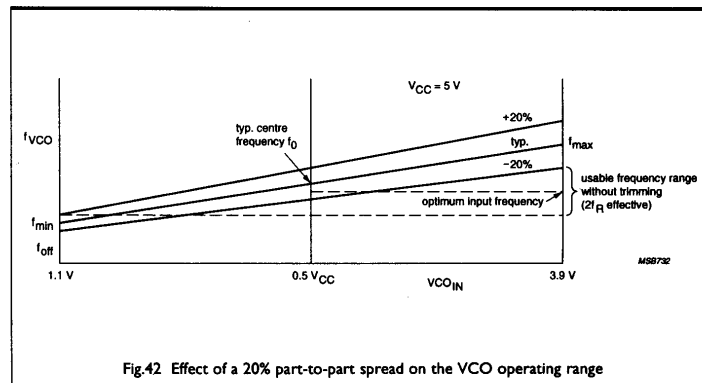
All the PLL circuits are manufactured using an advanced CMOS process with tight control of all process parameters to minimize part-to-part spreads. However, owing to the small spreads that remain, the output frequency of the VCO (set by R1, R2 and C1) can vary slightly from circuit to circuit. Although this variation can be eliminated by trimming R1 and R2, this is sometimes not desirable - for example, it's difficult with hybrid circuits. Some alternative methods are suggested below.

The part-to-part spread of a 74HC4046A VCO is  $\pm 20\%$  for both the output frequency range ( $2f_R$ ) and for the centre frequency ( $f_0$ ). However, the spread in the maximum and minimum operating frequency ( $f_{max}$  and  $f_{min}$ ) from circuit to circuit is limited, because circuits with maximum  $f_0$  have a maximum  $2f_R$ . Similarly, those with minimum  $f_0$  have a minimum  $2f_R$ . The part-to-part spread of a 74HCT9046A VCO is  $\pm 10\%$ .

There are three ways of determining suitable values for the external components (R1, R2 and C1) while guaranteeing that the input frequency is within the minimum  $2f_R$  range:

- Make the  $2f_R$  range 20% larger than needed and trim the centre frequency to the desired value with R2
- Trim C1, which has the advantage that both the centre frequency and the  $2f_R$  range can be adjusted to near their typical values
- Make the gain of the VCO, and hence  $2f_R$ , much larger than required for the application. Although the sidebands of the VCO output frequency will be increased when a divider is used in the loop, this can be compensated by lowering the natural frequency of the loop,  $\omega_n$ , which will increase the settling time.

Figure 42 shows the effect of a  $\pm 20\%$  part-to-part spread on the VCO operating range. In this example,  $f_0$  equals  $2f_R$ .



**Example**

In the following example, the part-to-part spread (on VCO operating frequency) is assumed to be  $\pm 20\%$  to which the tolerance of R1, R2 and C1 must be added. So, for 1% resistors and a 2% capacitor, the total spread is  $\pm(20 + 1 + 1 + 2) = \pm 24\%$ .

First, calculate the  $2f_R$  required by the application, i.e. the effective  $2f_R$  ( $2f_{R_e}$ ):

$$\begin{aligned} 2f_{R_e} &= f_{\max(\text{typ})}(1-d) - f_{\min(\text{typ})}(1+d), \\ &= 2f_{R(\text{typ})} - 2df_0(\text{typ}). \end{aligned} \quad (8)$$

where  $d = \frac{\text{spread in \%}}{100}$

Therefore, the typical  $2f_R$  must be:

$$2f_{R(\text{typ})} = 2f_{R_e} + 2df_0(\text{typ}). \quad (9)$$

The input frequency ( $f_{\text{SIG IN}}$ ) is:

$$\begin{aligned} f_{\text{in}} &= 2f_{R_e}/2 + f_{\min(\text{typ})}(1+d) \\ &= f_0(\text{typ}) - df_{R(\text{typ})} \end{aligned} \quad (10)$$

Therefore, the typical centre frequency must be at:

$$f_0(\text{typ}) = f_{\text{in}} + df_{R(\text{typ})} \quad (11)$$

Because this value of centre frequency is slightly different to the original one, this new value should be inserted in Eq.(9), yielding:

$$2f_{R(\text{typ})} = \frac{(2f_{R_e} + 2df_{\text{in}})}{1-d^2} \quad (12)$$

These values of  $f_0$  and  $2f_R$  ensure that the input frequency is always within the operating range of the VCO. In the PLL design program, they are calculated automatically from the specified input frequency and part-to-part spread.

The  $2f_{R(\text{typ})}$  just calculated can be so large that a negative offset is required. Since this is not possible, one has to trim one of the external components as mentioned earlier. For no offset, or positive offset:

$$f_0(\text{typ}) \geq 1.6f_{R(\text{typ})}. \quad (13)$$

## PLL ANALYSIS

The capture process for a PLL is highly complex and does not lend itself to simple mathematical analysis. A locked PLL, however, can be approximated as a linear control system and analyzed using Laplace transform techniques. In fact, most PLLs are designed using these techniques. In this section, the basic equations that describe a PLL are derived together with several graphical methods of evaluating the loop performance. The equations are basically those used in the PLL design program, and can be used to design a PLL manually, but are presented here to assist those using the program. In addition, the transient response and stability of a PLL are discussed.

### Basic feedback system

Figure 43 shows a basic feedback system. From this figure, the closed-loop transfer function,  $H(s)$  is:

$$H(s) = \frac{A(s)}{1 + A(s)B(s)} \quad (14)$$

where:

$s$  is the Laplace operator;

$A(s)$  is the product of the feed-forward (i.e. open-loop) transfer functions;

$B(s)$  is the product of the feedback transfer functions.

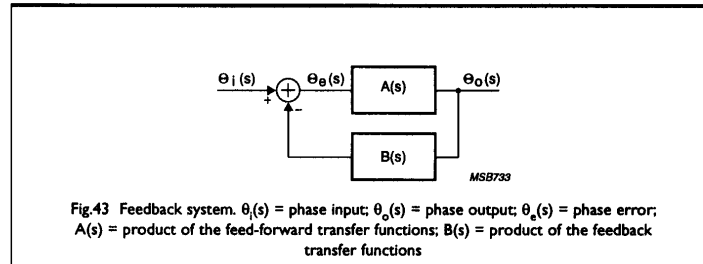


Fig.43 Feedback system.  $\theta_i(s)$  = phase input;  $\theta_o(s)$  = phase output;  $\theta_e(s)$  = phase error;  $A(s)$  = product of the feed-forward transfer functions;  $B(s)$  = product of the feedback transfer functions

The error response is:

$$H_e(s) = \frac{\theta_e(s)}{\theta_i(s)} = \frac{1}{1 + A(s)B(s)} \quad (15)$$

For a PLL,

$$A(s) = \frac{K_o K_d F(s)}{s} \quad (16)$$

where:

$K_o$  is the VCO gain;

$K_d$  is the phase comparator gain;

$F(s)$  represents the low-pass filter.

In Eq.(16),  $K_o$  is divided by  $s$ , because the frequency of the VCO output is converted to phase at the input of the phase comparator.

In many applications,  $B(s) = 1$ , which represents a unity-gain feedback. In some applications, e.g. in frequency synthesizers, see 'Application Examples', a divider (divide-by-N counter) is put in the feedback path between the VCO and phase comparator, and  $B(s) = 1/N$ . In these cases, the VCO operates at N-times the input frequency.

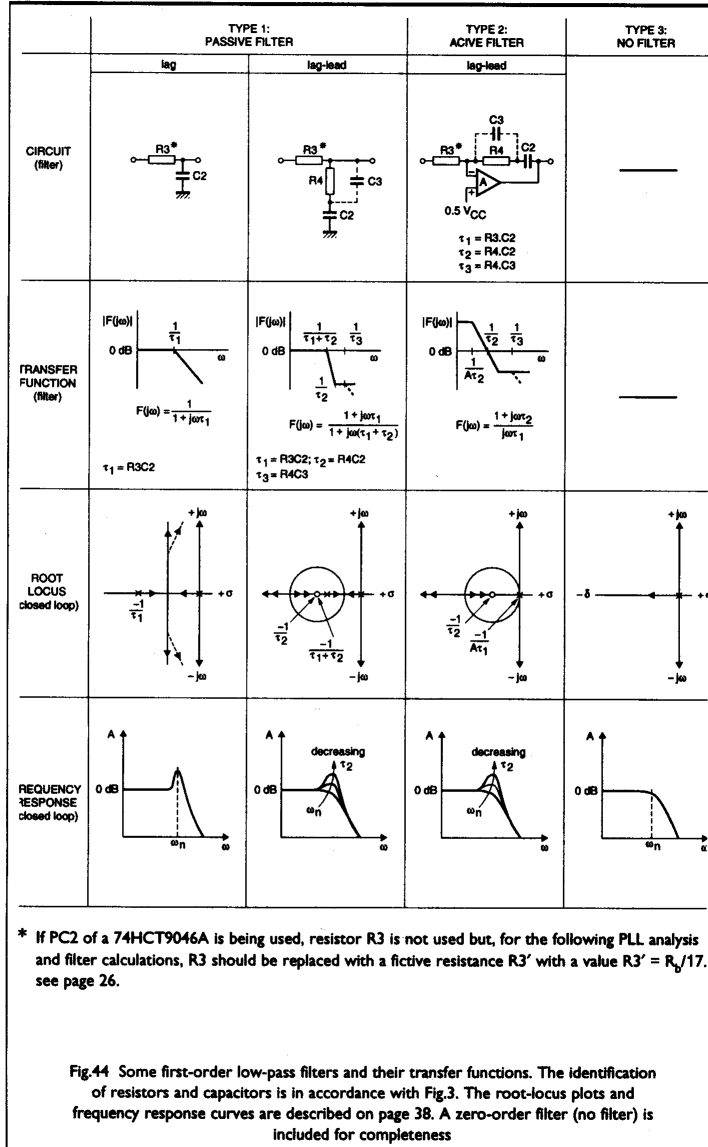
### Loop filters

If the dynamic response of a system can be described by an  $n$ -th-order differential equation, the order of the system is said to be  $n$ . If the transfer function of a (first-order) filter,  $F(s)$ , is inserted in Eq.(16) and  $A(s)$  inserted in Eq.(14), the order of the transfer function  $H(s)$  of the complete PLL, and that of the error function, is two. In other words, the order of the PLL is the order of the loop filter plus one. If  $F(s) = 1$  (no

filter), the PLL is first order.

Because second-order PLLs are by far the most commonly used, only these are dealt with here. Second-order PLLs behave in a similar way to an RLC resonant circuit.

Of the many loop filters that can be used, only those shown in Fig.44 will be examined in the following Section.



## Second-order loop

As previously mentioned, to obtain the closed-loop transfer function,  $H(s)$ , of a second-order PLL, the transfer function of the loop filter must be inserted in Eq.(14). Because the lag filter is a special case of a lead-lag filter with  $\tau_2 = 0$ , only the transfer functions of loops with lead-lag filters are calculated below.

For a PLL with an active loop filter, or when using PC2 with a passive filter:

$$H(s) = \frac{K_o K_d (s\tau_2 + 1)/\tau_1}{s^2 + \frac{s(K_o K_d \tau_2)}{\tau_1} + \frac{K_o K_d}{\tau_1}} \quad (17)$$

For a PLL with a passive loop filter with PC1 or PC3:

$$H(s) = \frac{K_o K_d (s\tau_2 + 1)/(\tau_1 + \tau_2)}{s^2 + \frac{s(1 + K_o K_d \tau_2)}{\tau_1 + \tau_2} + \frac{K_o K_d}{\tau_1 + \tau_2}} \quad (18)$$

To simplify the calculation,  $N$  was taken to be one, i.e. no divider in the feedback.

By making suitable substitutions, the denominators of Eqs.(17) and (18) can be written in the normalized form:

$$s^2 + 2\zeta\omega_n s + \omega_n^2$$

where:

$\omega_n$  is the natural frequency

$\zeta$  is the damping factor.

For the active loop, the substitutions are:

$$\omega_n = (K_o K_d / \tau_1)^{1/2} \quad (19)$$

and

$$\zeta = 0.5\tau_2 (K_o K_d / \tau_1)^{1/2} \quad (20)$$

For the passive loop, they are:

$$\omega_n = \frac{(K_o K_d)^{1/2}}{(\tau_1 + \tau_2)^{1/2}} \quad (21)$$

and

$$\zeta = \frac{0.5(K_o K_d)^{1/2}(\tau_2 + 1/K_o K_d)}{(\tau_1 + \tau_2)^{1/2}} \quad (22)$$

These substitutions result in the following transfer functions:

**for the PLL with active loop filter and for PC2 with a passive filter:**

$$H(s) = \frac{2\zeta\omega_n s + \omega_n^2}{s^2 + 2\zeta\omega_n s + \omega_n^2} \quad (23)$$

**for the PLL with passive loop filter and with PC1 or PC3:**

$$H(s) = \frac{s\omega_n(2\zeta - \omega_n/K_o K_d) + \omega_n^2}{s^2 + 2\zeta\omega_n s + \omega_n^2} \quad (24)$$

If  $\omega_n/K_o K_d \ll 2\zeta$ , Eqs.(23) and (24) are the same and the loop with the passive filter is called a high-gain loop.

When a lag filter (Fig.44) is used,  $\omega_n/K_o K_d = 2\zeta$ , so the loop is always low-gain. In addition, for lag filters, good tracking (large  $K_V$ ) cannot be combined with a narrow loop bandwidth ( $\omega_n$ ) which is sometimes required for noise suppression.

When an active filter is used, the PLL is always considered to be a high-gain loop. In practice, most PLLs are high-gain loops, and all equations in the remainder of this publication are for high-gain loops, unless stated otherwise.

## Bode plot

Figure 45 is a Bode plot of the closed-loop transfer function of a high-gain second-order PLL. The frequency scale is normalized to the natural frequency  $\omega_n$ , so the plot can be used with any second-order PLL system. The plot illustrates the low-pass characteristic of such a PLL - slow variations of the input frequency are followed by the output, but frequency changes beyond the -3 dB point of the filter are damped.

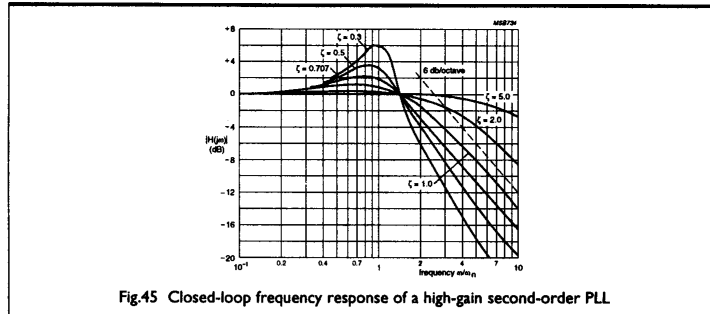


Fig.45 Closed-loop frequency response of a high-gain second-order PLL

The Bode plot also illustrates that the damping factor,  $\zeta$ , has a significant effect on the dynamic performance of the PLL:

when  $\zeta = 1$ , the system is critically damped;

when  $\zeta < 1$ , the transient response is oscillatory;

when  $\zeta = 1/\sqrt{2}$ , the transfer function is optimally flat and corresponds to that of a second-order Butterworth low-pass filter.

The -3 dB bandwidth (closed loop) is:

$$\text{for a high-gain loop: } \omega_n [1 + 2\zeta^2 + (2 + 4\zeta^2 + 4\zeta^4)^{1/2}]^{1/2} \quad (25)$$

$$\text{for a low-gain loop: } \omega_n [1 - 2\zeta^2 + (2 - 4\zeta^2 + 4\zeta^4)^{1/2}]^{1/2} \quad (26)$$

### Root-locus plot

The roots of the denominator of Eqs.(23) and (24) are the closed-loop poles of the overall loop transfer function. The root-locus technique of determining the position of the system poles and zeros in the s-plane is often used to graphically visualize the stability of a system (Ref.1). The root-locus plot illustrates how the locus of the closed-loop poles varies with loop gain. For stability, all poles must lie in the left half of the s-plane. In general, the locus is drawn for the full range of gain variation - from zero to infinity. The plot starts (zero gain) on the open-loop poles and terminates (infinite gain) on the open-loop zeros.

The open-loop transfer function of any PLL is:

$$K_V F(s)/s, \text{ where } K_V = K_o \times K_d/N \quad (27)$$

Thus, the open-loop poles always include one pole at the origin (due to the integrating action of the VCO) besides the poles of  $F(s)$  which represent the filter. The open-loop zeros are the zeros of  $F(s)$  and a zero at infinity due to the  $1/s$  term.

The root-locus plots and the corresponding Bode plots for the passive filters are shown in Fig.44. For the simple lag filter, as the gain increases, the root loci bends as indicated by the dashed line owing to parasitic effects, and the poles move very close to the right half of the s-plane, indicating very little damping and that the loop is underdamped. This can happen if either the loop gain or the filter time constant is too large. Potential loop instability can be eliminated by using a lag-lead filter. When a leading term is introduced, ( $R4$  in the filter), the poles also become complex when they meet, however, the complex portion of the locus is now a circle centred at  $-1/\tau_2$  and which stays away from the right-half plane.

Another tool that provides information about the stability of a feedback system is the Bode plot of the open loop, which is described in the next section.

### Phase and gain margin

A feedback loop can oscillate if its open-loop gain is unity and, simultaneously, its open-loop phase shift is  $180^\circ$ . A simple method of judging the stability of a PLL is the Bode plot of the open loop.

The easiest way to construct a Bode plot for a PLL is to plot the filter,  $F(j\omega)$ , separately from the VCO, phase comparator and feedback. Superposition of the individual plots yields the Bode plot of the complete (open) loop.



### Passive filter

Figure 36 shows an example for a loop with a passive filter. The phase margin is measured at the frequency where the amplitude curve intersects the x-axis (0 dB value) and is the difference between the actual phase shift and  $-180^\circ$ . The gain margin is measured at the frequency where the phase shift is  $-180^\circ$  and is the difference between the actual gain and 0 dB. For second-order systems, the phase margin is of interest, because in virtually every application, it is the worst-case parameter to design. If the phase margin is small, say less than  $20^\circ$ , the loop will oscillate in response to a step input. To prevent this, a loop is normally designed to have a phase margin of  $45^\circ$  to  $55^\circ$ . As can be seen in Fig.46(a), a simple RC filter can result in very small phase margins if a large bandwidth is required.

If a zero is introduced in  $F(j\omega)$  by using a lag-lead filter, the phase margin can be increased to the desired value by varying  $\tau_2$ , see Fig.46(b). Because of this zero, the PLL will act as a first-order loop at high frequencies, decreasing the noise and ripple suppression due to the phase comparator. Adding C3 will improve the suppression, but so as not to affect the phase margin, the additional pole introduced by C3 should typically be at  $\tau_2/10$ .

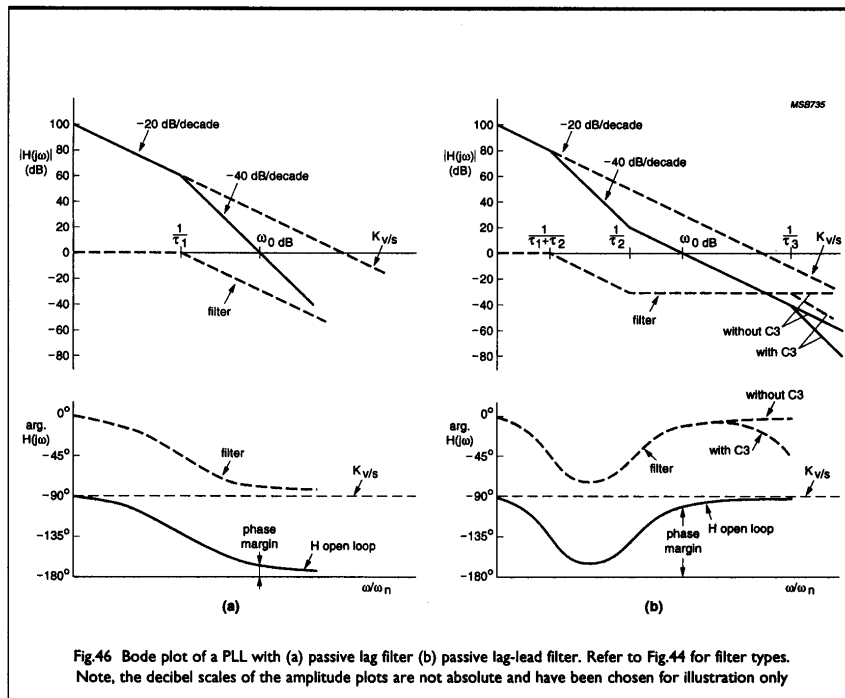


Fig.46 Bode plot of a PLL with (a) passive lag filter (b) passive lag-lead filter. Refer to Fig.44 for filter types. Note, the decibel scales of the amplitude plots are not absolute and have been chosen for illustration only

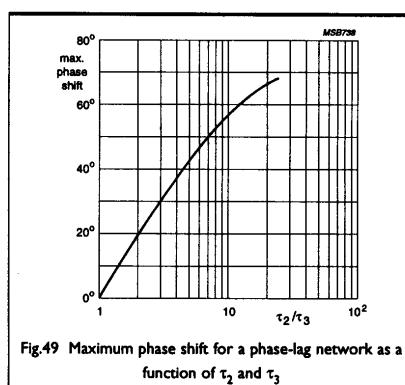
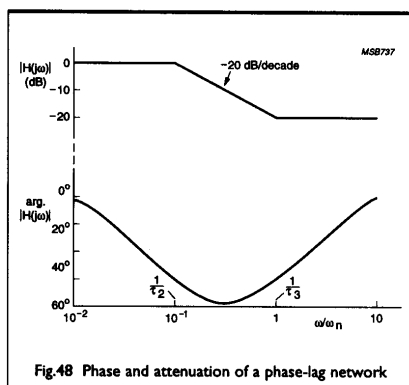
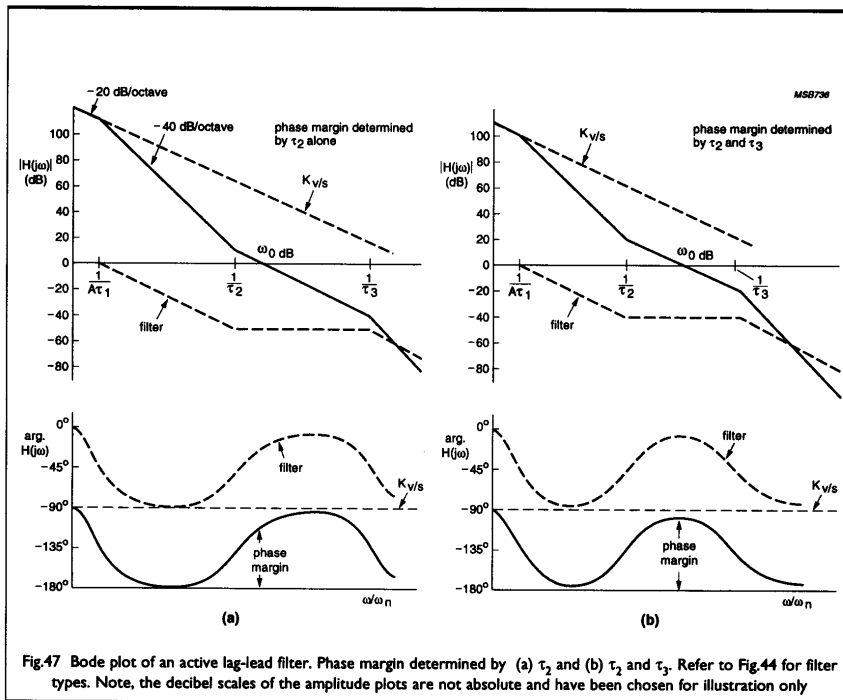
### Active filter

For an active filter, the approach of positioning the additional pole is slightly different, see Fig.47. Only an active lag-lead filter is discussed, because an active RC filter will give an unacceptable phase margin of approximately  $0^\circ$ .

The first pole is at  $1/A\tau_1$ , where A is the open-loop gain of the filter's op-amp. Since A is very large ( $>10^3$ ), this pole is nearly on the y-axis and the phase plot actually starts near  $-180^\circ$  instead of  $-90^\circ$ . The phase margin is now totally defined by  $\tau_2$ , or by  $\tau_2$  and  $\tau_3$ .

In Fig.47(a), the phase margin is determined by  $\tau_2$  alone, and  $\tau_3$  is located at  $\tau_2/10$  as for the passive filter. If  $\tau_3$  is located closer to  $\tau_2$ , the phase margin will be reduced, but the noise and ripple suppression will be increased, because the  $-40$  dB/decade slope starts at a lower frequency. If  $\tau_2$  is moved to the left, the phase margin will be increased again. To simplify the positioning of  $\tau_2$  and  $\tau_3$ , a special phase-lag network is used, see Fig.47(b) and Fig.48.

If  $\tau_2$  and  $\tau_3$  are positioned equidistant from  $\omega_0$  dB, the phase margin equals the difference between the maximum phase shift of this network and  $-180^\circ$ . Figure 49 shows the maximum phase shift for this network as a function of  $\tau_3/\tau_2$ .



By using this method of defining the phase margin and positioning  $\tau_2$  and  $\tau_3$ , both  $\tau_2$  and  $\tau_3$  are shifted to the left on the Bode plot and the amplitude roll-off starts earlier with the  $-40$  dB/decade slope giving improved ripple and noise suppression.

As already discussed in the section on the PC2 comparator, the combination of PC2 with a passive filter results in a transfer function similar to that for when an active filter is used. The reason is that PC2 operates as a 'charge pump' (it's actually a voltage pump in the 4046A). The only disadvantage with the passive filter is the varying gain of PC2 when using the 4046A or 7046A, see Appendix A. The first pole is now unlikely to be located at  $1/A\tau_1$ , since A was the open-loop gain of the filter op-amp. However, the open-loop gain of the op-amp can also be seen as the ratio of  $R_0/R_3$ , where  $R_0$  is a resistor connected between the output of the op-amp and the inverting input. A value of  $A \times R_3$  for  $R_0$  gives the maximum possible gain, or open-loop gain A. An equivalent situation occurs for PC2 with a passive filter. Now, 'A' equals the ratio between the leakage current of the capacitor C2 to that of R3, because the first pole is at  $1/j\omega R_{leak}C = 1/\tau_1(R_{leak}/R_3)$  (that is, at  $1/A\tau_1$ ).

The resulting value of 'A' can be of the same order of magnitude as for an op-amp, resulting in a similar Bode plot.

### Transient behaviour

An important characteristic of a PLL is its transient response to a frequency step or a phase step. This step can be a normal operating condition (for example, a FSK or PSK modulated input, frequency synthesizer) or an anticipated error condition. In both cases, it is necessary to know the overshoot as a percentage of the step, and the time when the output frequency or phase has resettled, say to within 5% of its end value.

A background to the validity of the graphs in this section is given in Appendix B.

Figure 50 shows the response of a low-gain second-order loop. The curves indicate both the phase response to a step in phase and the frequency response to a step in frequency. The curves are only valid for low-gain loops (passive filter), that is, where  $\omega_n/K_oK_d > 2\zeta$ , or  $\tau_2 = 0$  (from Eq.(24)). The response of high-gain loops is shown in Fig.51. When  $\omega_n/K_oK_d \approx 2\zeta$ , or  $\tau_2 \approx 0$ , there is a gradual change from the curves of Fig.50 to those of Fig.51.

Figure 52 shows the phase response of a high-gain loop to a step in frequency. The phase error  $\theta_e(t)$  approaches zero for large t. For low-gain loops using phase comparator PC1 or PC3, the curves are similar but the phase error does not decay to zero, but remains finite:

$$\theta_e(\infty) = \Delta\omega/K_oK_d \quad (28)$$

where  $\Delta\omega$  is the frequency step measured from the VCO centre frequency.

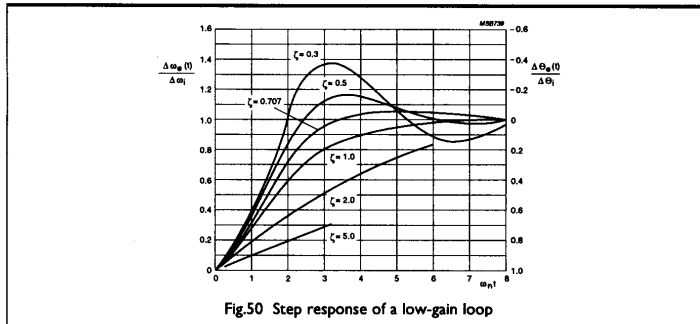


Fig.50 Step response of a low-gain loop

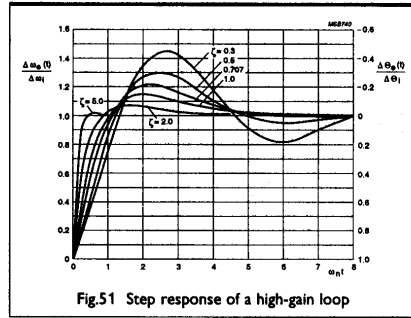


Fig.51 Step response of a high-gain loop

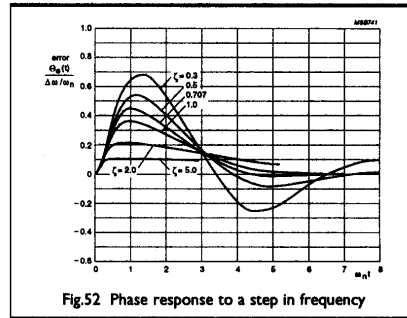


Fig.52 Phase response to a step in frequency

### Sinusoidally modulated input signal

The input signal can be sinusoidally modulated in frequency or in phase.

For phase modulation:

$$\theta_i(t) = \Delta\theta \sin \omega_m t \quad (29)$$

and for frequency modulation:

$$\theta_i(t) = \Delta\omega / \omega_m \cos \omega_m t \quad (30)$$

where  $\Delta\theta$  is the peak phase deviation,  $\Delta\omega$  the peak frequency deviation, and  $\omega_m$  the modulating frequency.

The maximum amplitude of the phase error is obtained by multiplying  $\theta_i$  by the magnitude of the error transfer function,  $|H_e(j\omega_m)|$ , see Eq.(15), yielding a peak phase error for phase modulation of:

$$\theta_e(\max) = \Delta\theta \frac{\omega_m^2}{\{(\omega_n^2 - \omega_m^2)^2 + (2\zeta\omega_n\omega_m)^2\}^{1/2}} \quad (31)$$

and for frequency modulation, of:

$$\theta_e(\max) = \Delta\omega \frac{\omega_m}{\{(\omega_n^2 - \omega_m^2)^2 + (2\zeta\omega_n\omega_m)^2\}^{1/2}} \quad (32)$$

For phase modulation with a fixed phase deviation,  $\Delta\theta$ , the phase error is small at low modulating frequencies, rises at 40 dB/decade and levels out at high frequencies to the value of the phase deviation, see Fig.53.

For frequency modulation with a fixed frequency deviation,  $\Delta\omega$ , the phase error is small at low modulating frequencies, rises to a maximum at  $\omega_m = \omega_n$  and falls off at higher frequencies, see Fig.54. The asymptotes at low and high frequencies are 20 dB/decade.

For sinusoidal frequency-modulated input signals, it can be concluded that when  $\omega_n \gg \omega_m$ , the peak phase error is extremely small. And for sinusoidal phase-modulated input signals, make  $\omega_n \ll \omega_m$  to demodulate the input signal with minimum distortion.

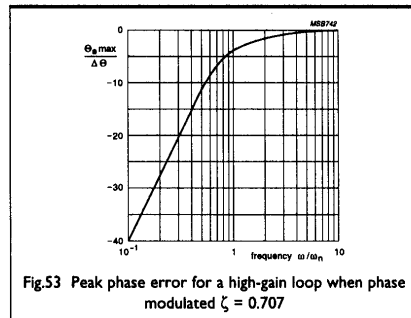


Fig.53 Peak phase error for a high-gain loop when phase modulated  $\zeta = 0.707$

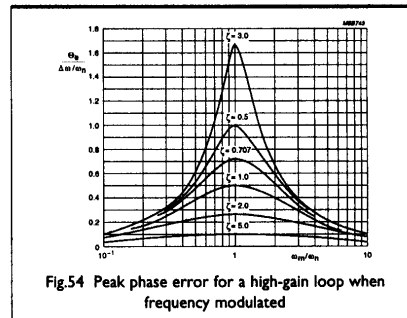


Fig.54 Peak phase error for a high-gain loop when frequency modulated

## Ripple suppression

An ideal phase comparator produces a DC signal which only varies when the phase difference between the inputs varies. Therefore, in a PLL with an ideal comparator, the low-pass filter would only be needed to suppress noise and to limit the maximum rate of phase changes seen by the loop. However, the HCMOS comparators PC1 and PC3 produce a pulsed output signal whose average DC value is related to the phase differences between the inputs. So, in an HCMOS PLL, the filter also has to average the signal from the phase comparator, and ideally fully suppresses the pulsed signal. The output of comparator PC2 is near ideal, but again the relatively short correction pulses won't be completely suppressed by the low-pass filter. Figure 55 shows the effect of the remaining ripple on the VCO output frequency for several values of division ratio N.

As already mentioned in 'HCMOS PLL circuits', the ripple frequency of PC1 is twice the input frequency, whereas the output frequency of PC3 and PC2 is equal to the input frequency.

When PC1 is used, the VCO output frequency will be modulated by the ripple of the phase comparator only if  $N \geq 3$ , generating sidebands in the spectrum of the VCO output spaced at multiples of the reference input frequency.

When PC3 is used, the duty factor of the VCO output frequency is affected by the ripple if  $N = 1$ . If  $N > 1$ , the output frequency is modulated by the ripple and sidebands are produced. In addition, since the Common Mode rejection Ratio of the op-amp used in the VCO is not infinite, sidebands will always be generated via the on-chip supply ripple, even if  $N = 1$ .

When PC2 is used, the output is modulated if  $N \geq 1$ . However, the sidebands produced will be much smaller than with PC1 & PC3 owing to the relatively small correction pulses. Since these pulses are both positive and negative, the sidebands will be spaced at half the input frequency. If a bias resistor,  $R_p$ , is used on the output of PC2 to compensate for the RC time constant of the parasitic output capacitance as described in 'Phase and frequency jitter considerations', the sidebands spaced at the reference input frequency will be dominant, because only the positive correction pulses appear on the output of PC2.

If it is assumed that the modulation index is low (i.e. ripple suppressed to a relatively low level), the level of the first sidebands (the only significant ones) can be calculated as follows.

The main component of the pulsed output of PC1 and PC3 is:

$$V_{\text{ripple}} \approx (2V_{CC}/\pi)\sin\omega_m t \quad (33)$$

where  $\omega_m$  is the modulation frequency.

This signal is damped by the filter, resulting in a ripple on the VCO input signal of:

$$V_{\text{ripple(VCO)}} \approx (2V_{CC}/\pi)\sin\omega_m t \times |F(j\omega)| \quad (34)$$

where  $|F(j\omega)|$  is the modulus of the filter (response) at  $\omega = \omega_{\text{ripple}}$ .

The VCO output frequency is:

$$VCO(t) = 0.5V_{CC}\cos(\omega_0 t + \beta \sin \omega_m t) \quad (35)$$

where:

$$\beta = (K_o 2V_{CC}/\pi f_m) \times |F(j\omega_{\text{ripple}})|.$$

Since only the first sideband is assumed to be significant:

$$\text{sideband/carrier} \approx 20 \log[(K_o V_{CC}/2\pi^2 f_m) \times |F(j\omega_{\text{ripple}})|] \text{ dB} \quad (36)$$

Equation (36) is valid for rectangular output signals having a 50% duty factor. When the other sidebands cannot be neglected, it is only a very rough approximation of performance.

For PC2, the calculations are similar, yielding:

$$\text{sideband/carrier} \approx 20 \log [K_o V_{CC} \tau \times |F(j\omega_{\text{ripple}})|] \quad (37)$$

where  $\tau$  is the width of the correction pulse. Note that Eq.(37) is also only an indication of performance, owing to the assumptions that have been made.

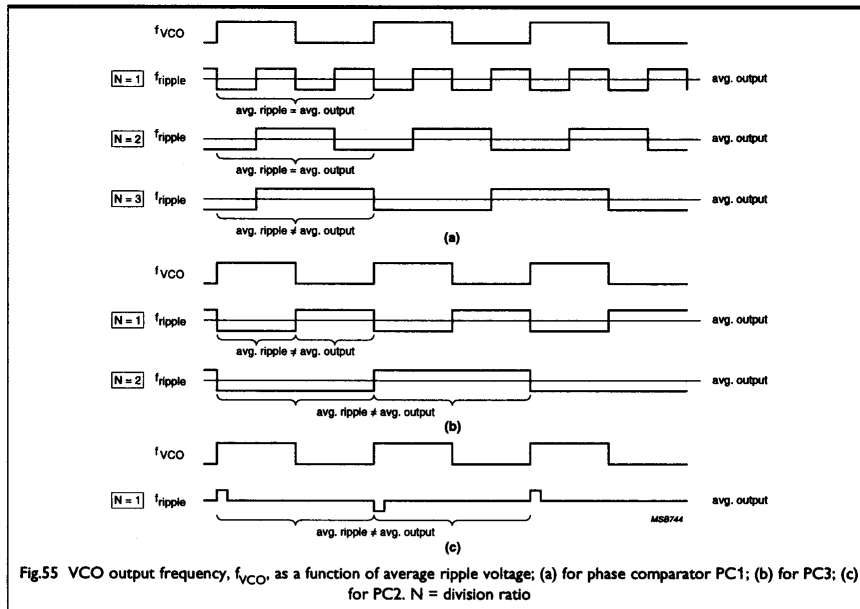


Fig.55 VCO output frequency,  $f_{VCO}$ , as a function of average ripple voltage; (a) for phase comparator PC1; (b) for PC3; (c) for PC2. N = division ratio

### Phase noise

If the signal-to-noise ratio of the input signal ( $SNR_i$ ) is less than about 20 dB to 30 dB, only the PC1 comparator should be used, and then,  $SNR_i$  should still be >6 dB for correct operation. With PC2 and PC3, missing edges or transients (due to noisy input signals) can cause incorrect operation, although if the missing or extra transitions only occur occasionally, a fast settling time can be a remedy. It is therefore recommended that sufficient  $dV/dt$  is used for the rising edges of the  $SIG_{IN}$  signal, particularly if  $SIG_{IN}$  is a small, capacitively coupled, AC signal. The minimum recommended  $dV/dt$  is 0.5 V/ $\mu$ s. PC3 is less sensitive than PC2 to extra transitions as described earlier. The remainder of this section applies to PC1 only.

Phase noise (jitter) on the VCO output signal is caused in part by noise on the input signal even though this is normally strongly attenuated by the PLL.

To calculate the signal-to-noise ratio of the VCO output frequency ( $SNR_o$ ), it is necessary to know the  $SNR_i$  and the input noise bandwidth ( $B_i$ ).

The actual phase jitter is:

$$(\Delta\phi)_{RMS} = 1/2SNR_i \text{ rad.} \quad (38)$$

where  $SNR_i$  is expressed as a factor, and not in dB ( $10\log SNR$ ), as usually measured. And the  $SNR_o$  is:

$$SNR_o = SNR_i \times B_i/2B_L \quad (39)$$

where  $B_L$  is the noise bandwidth of the loop.

Thus, the PLL improves the  $SNR_i$  by  $B_i/2B_L$ , and:

$$B_L = 0.5\omega_n(\zeta + 1/4\zeta) \text{ Hz} \quad (40)$$

where  $\omega_n$  is in rad/s.

Clearly, low values of  $\omega_n$  will improve  $SNR_o$ , and the noise bandwidth is lowest for values of  $\zeta$  between 0.5 and 1.

The phase jitter of the VCO output caused by the input noise equals:

$$(\Delta\phi_o)_{RMS} = 1/2SNR_o \text{ rad.} \quad (41)$$

For PC1, the average time before the loop loses lock due to the input noise, and for  $\zeta = 0.7$ , is:

$$T_{AV} \approx (2/\omega_n)\exp(\pi SNR_o) \text{ sec.} \quad (42)$$

### Overview of PLL parameters

Table 1 gives a summary of the most important design equations for a second-order PLL.

**Table 1 The main design equations for a second-order PLL using a 4046A, a 7046A or a 9046A**

	PC1	PC3	PC2
Hold range $\pm\Delta\omega_H$	$2f_R$ (active filter) $\pi K_V/2$ (passive filter)	$2f_R$ (active filter) $\pi K_V$ (passive filter)	$2f_R$
Lock-in range $\pm\Delta\omega_L$	$\approx \pi\zeta\omega_n$	$\approx 2\pi\zeta\omega_n$	$\approx 4\pi\zeta\omega_n$
Settling time $T_S$	$\approx 1/\omega_n$	$\approx 1/\omega_n$	$\approx 1/\omega_n$
Pull-in range $\pm\Delta\omega_{PI}$	$\approx (\pi\sqrt{(2\zeta\omega_n K_d)})/2$	$\approx \pi\sqrt{(2\zeta\omega_n K_d)}$	$2f_R$
Pull-in time $T_P$	$\approx (4\Delta\omega^2_o)/(\pi^2\zeta\omega_n^3)$	$\approx (\Delta\omega^2_o)/(\pi^2\zeta\omega_n^3)$	$\approx (N\tau_1 + \tau_2)/(K_d K_d^*)$
Pull-out range $\pm\Delta\omega_{PO}$	$\approx 1.8\omega_n(\zeta + 1)$	$\zeta < 1:$ $\pi\omega_n \exp \left[ \frac{\zeta}{\sqrt{1-\zeta^2}} \frac{\tan^{-1}\sqrt{1-\zeta^2}}{\zeta} \right]$ $\zeta = 1:$ $\pi\omega_n \exp 1$ $\zeta > 1:$ $\pi\omega_n \exp \left[ \frac{\zeta}{\sqrt{\zeta^2-1}} \frac{\tanh^{-1}\sqrt{\zeta^2-1}}{\zeta} \right]$	$\zeta < 1:$ $2\pi\omega_n \exp \left[ \frac{\zeta}{\sqrt{1-\zeta^2}} \frac{\tan^{-1}\sqrt{1-\zeta^2}}{\zeta} \right]$ $\zeta = 1:$ $2\pi\omega_n \exp 1$ $\zeta > 1:$ $2\pi\omega_n \exp \left[ \frac{\zeta}{\sqrt{\zeta^2-1}} \frac{\tanh^{-1}\sqrt{\zeta^2-1}}{\zeta} \right]$

All parameters are related to the input of the PLL, and are valid for high-gain loops only.

N is the division ratio.

\*  $K_d = V_{CC}/\omega_n$  (out-of-lock gain).

## PLL DESIGN PROGRAM

All the main parameters of a PLL can be calculated from the information in the previous sections, but it is clearly a time-consuming task when done manually. In addition, because most parameters are interdependent, all the calculations should be repeated every time a parameter is altered. Short-cuts taken to simplify the recalculation often result in non-optimum loop performance. To solve this problem, we have developed a computer program which as well as making all the necessary calculations fast, allows the designer to make modifications and to see their effect in a few seconds. The program runs on an IBM PC or compatible with MSDOS. A graphics card such as an EGA or Hercules card is helpful, but not essential. The program is suitable for use with three types of loop filter, see Fig.44:

- Type 1 (passive) with or without C3
- Type 2 (active) with or without C3
- Type 3 (no filter) for FSK and PSK applications.

### About the program

After some introductory text when you start the program, you'll come to a block diagram of a PLL showing the basic components. The next screens show the pin configurations of the 4046A and the 9046A. Then the PLL type (4046A or 9046A) must be selected from this screen. The main program starts by asking for system information such as input frequency, division ratio, supply voltage, and the type of phase comparator you wish to use. One of three application areas is then chosen depending on the division ratio and input frequency (see the following pages for more details):

- Fixed division ratio, fixed input frequency (ratio N from 1 up to a maximum of 5E5. Examples: tracking filter, multiplier)
- Fixed division ratio, modulated input frequency. Examples: FM, PM, FSK, PSK
- Variable division ratio, fixed input frequency. Example: frequency synthesizer.

With a maximum value for  $N_{max} = 500000$ , the permitted ratio for  $N_{max}/N_{min}$  depends on the VCO frequency range, the part-to-part spread of the VCO components, and the input frequency drift. With no spread,  $N_{max}/N_{min}$  can be selected up to a maximum value of 4.3. With a total spread of 30%,  $N_{max}/N_{min}$  must be less than 2.5. Values for spreads of 10% and 20% are 3.6 and 3.0.

Help is available for most questions by pressing the [?] key. For example, when selecting the filter type, a drawing of the possible filter configurations for the 9046A (Fig.56) will be shown on the screen.

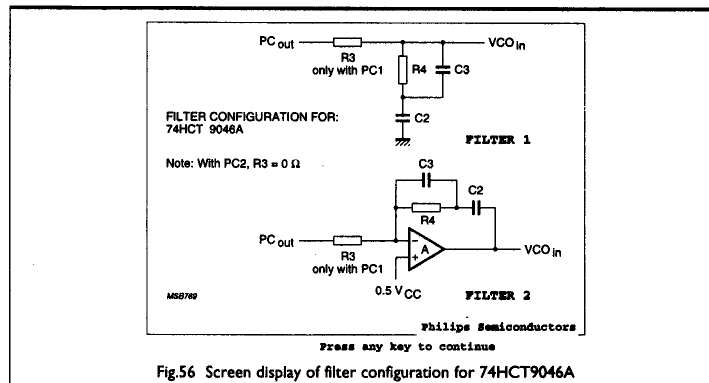


Fig.56 Screen display of filter configuration for 74HCT9046A

After selecting all the input values, the calculations start using default settings which will always produce a stable loop design. The results are presented in three groups, see Fig.57:

- The system parameters you specified



- The calculated values of the external bias components for the VCO, and the values of the loop filter components and constants
- The calculated dynamic loop parameters.

INPUT PARAMETERS			
PC	: 1	f <sub>in</sub> (Hz)	: 1.000E+05 Spread input freq. (%) : 0.0
N <sub>max</sub>	: 30	2f <sub>R</sub> (Hz)	: 2.897E+06 Part-to-part spread (%) : 32.0
Filter	: 1	f <sub>0</sub> (Hz)	: 2.963E+06 Vcc (Volt) : 5.0
N <sub>used</sub>	: 30		
VCO and FILTER PARAMETERS 74HC/HCT 4046A/7046A			
T1 (sec)	: 1.2E-03	T2 (sec)	: 8.2E-05
T3 (sec)	: 7.2E-06		
f1 (Hz)	: 1.2E+02	f2 (Hz)	: 1.9E+03
f3 (Hz)	: 2.2E+04		
R1 (Ohm)	: 1.5E+04	R3 (Ohm)	: 1.0E-04
R4 (Ohm)	: 6.9E+02		
R2 (Ohm)	: 1.3E+05	C2 (Far)	: 1.2E-07
C3 (Far)	: 1.1E-08		
C1 (Far)	: 1.0E-10		
DYNAMIC PARAMETERS			
W <sub>n</sub> /2π (Hz)	: 2.6E+03	pull-in time (sec)	: 2.6E-03
W <sub>0dB</sub> /2π (Hz)	: 4.4E+03	pull-in range (Hz)	: 2.2E+04
zeta	: 0.70	pull-out range (Hz)	: 8.0E+03
overshoot (%)	: 21.03	hold range (Hz)	: 8.6E+04
R <sub>v</sub>	: 3.4E+05	settling time (<5%) (sec)	: 2.8E-04
W <sub>input</sub> /W <sub>0dB</sub>	: 22.7	lock-in range (Hz)	: 5.7E+03
phasemargin with C3 (deg)	: 55	ripple suppr. with C3 (dB)	: -23
without C3 (deg)	: 64	without C3 (dB)	: -6
zetamin	: 0.70	W <sub>min</sub> /2π (Hz)	: 2.6E+03
zetamax	: 0.86	W <sub>max</sub> /2π (Hz)	: 3.2E+03

Optimize ? (Y/N) : Y

Fig.57 Example of a 'result window'. The window lists all parameters which define the dynamic performance of the loop, and the filter components R3, R4, C2 and C3. External components R1, R2 and C1 which set the free-running frequency of the VCO are also calculated

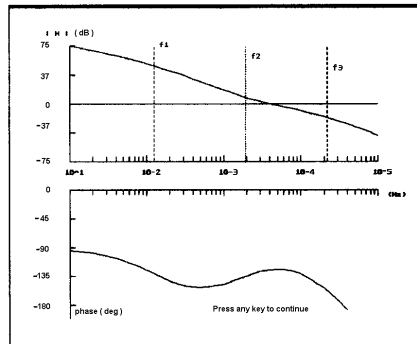


Fig.58 Example of an open-loop Bode plot generated by the design software. The corner frequencies  $f_1$ ,  $f_2$  and  $f_3$  are indicated by the vertical lines on the amplitude curve

An extremely useful feature of the program is the already-mentioned ability to tailor the loop parameters to specification quickly. After optimization, you can print the results. And if your PC has a suitable graphics card, you can generate a Bode plot of the open loop to examine the loop stability, see Fig.58, returning to the optimization menu to make further alterations to the design as required. One option in the optimization menu can be used to evaluate existing designs.

Hard copies of the results and the Bode plot can be made on an Epson or IBM printer, or compatible.

#### Initial PLL default settings

To ensure that the loop is stable, the program starts with a set of default values for parameters such as the damping factor and the phase margin. Other default values depend on the application area as follows.

#### Fixed division ratio and fixed input frequency

To obtain an acceptable ripple and noise suppression and a fast settling time, the natural frequency of the loop ( $\omega_n$ ) is set to an arbitrary value of  $0.05\omega_{in}$ .

The corner frequencies of the filter are determined differently depending on whether the filter is passive or active, as described under 'Phase and gain margin'.

For a passive filter (with PC1 or PC3), with the default value of  $\omega_n$  and a default damping factor of 0.7 (Butterworth response),  $\tau_1$  and  $\tau_2$  are determined from Eqs.(21) and (22),  $K_0$  and  $K_d$  already having been determined from the  $2f_R$  range of the VCO and the choice of phase comparator to be used respectively. If  $\tau_1$  or  $\tau_2$  falls below zero,  $\omega_n$  is multiplied by 0.99 and the calculations are repeated. So as not to influence the phase margin,  $\tau_3$  is positioned at  $0.1\tau_2$ .

For an active filter, or when PC2 is used with a passive filter, a default of  $\tau_2/\tau_3 = 10$  is used which gives a phase margin of about  $55^\circ$  (see Fig.49). First,  $\omega_{0dB}$  is calculated with the default  $\omega_n$  and the equation:

$$\omega_{0dB} = (\tau_2/\tau_3)^{0.25}\omega_n \quad (43)$$

Both  $\tau_2$  and  $\tau_3$  are located symmetrically around  $\omega_{0dB}$  by making:

$$\tau_2 = \sqrt{10}/\omega_{0dB} \quad (44)$$

and

$$\tau_3 = 1/(\omega_{0\text{ dB}}\sqrt{10}) \quad (45)$$

$\tau_1$  can be determined from:

$$|H(j\omega)| = 1 \text{ (open loop)} \quad (46)$$

with  $\omega = \omega_{0\text{ dB}}$ , yielding:

$$\tau_1 = \frac{K_v \times \{(1/\omega_{0\text{ dB}}^2) + \tau_2^2 + \tau_3^2 + 2\tau_2\tau_3\}^{1/2}}{\omega_{0\text{ dB}}[\omega_{0\text{ dB}}^2\tau_3^2 + 1]^{1/2}} \quad (47)$$

If  $1/\tau_3 < 5\omega_n$ ,  $\tau_1$  and  $\tau_2$  are determined using Eqs.(19) and (20) and:

$$\omega_{0\text{ dB}} = \omega_n[2\zeta^2 + (4\zeta^4 + 1)^{1/2}]^{1/2} \quad (48)$$

$1/\tau_3$  is now positioned at  $5\omega_n$ .

#### **Fixed division ratio, modulated input frequency**

The default values of  $\omega_n$  and the damping factor,  $\zeta$ , depend on whether the input is sinusoidally modulated (FM, PM) or step modulated (FSK, PSK).

For sinusoidal frequency-modulated input signals, distortion is important, and to keep the maximum phase error small,  $\omega_n$  should be much larger than the modulating frequency,  $\omega_m$ , as Fig.54 shows. An initial default value of  $\omega_n = 100\omega_m$  is used.

For phase-modulated input signals, the initial default is  $\omega_n = .01\omega_m$ .

For FSK or PSK, the graphs of Fig.51 are used. A maximum overshoot or damping factor together with a settling time is used to determine  $\omega_n$ . For example, a maximum overshoot of 21%, or  $\zeta = 0.7$ , results in an  $\omega_n t$  of 1. If the output frequency or phase must settle within 1 ms (settling time),  $\omega_n$  is  $1/0.001 = 1000$  rad/s.

If a passive filter is used, the calculations proceed as described under 'Fixed division ratio and fixed input frequency'.

For an active filter, or if PC2 is used, the factor  $\tau_2/\tau_3$  must be calculated from  $\zeta$  and:

$$\tau_2/\tau_3 = [\tan(\pi/4) - 0.5\text{arctan}(2\zeta)]^{-2}. \quad (49)$$

$\omega_{0\text{ dB}}$  can be calculated from Eq.(43).

The remaining calculations are identical to those described in 'Fixed division ratio and fixed input frequency'.

#### **Varying division ratio, fixed input frequency**

Varying the division ratio or switching between channels introduces a frequency step at the phase comparator input. Therefore, the graphs of Fig.51 are used again to determine  $\omega_n$ . In frequency synthesizer applications, the settling time is defined as 'when the output has settled to within 5% of the applied step. So, the value of  $\omega_n t$  becomes 4.5 for  $\zeta = 0.7$ . Hence, if  $T_{S(5\%)} = 1$  ms,  $\omega_n$  becomes  $4.5/0.001 = 4500$  rad/s. In this case, ( $\zeta = 0.7$ ),  $\omega_n$  is four and a half times that value in the previous example owing to the different definition of settling time. Once  $\omega_n$  has been determined, the calculations are identical to those described under 'Fixed division ratio, modulated input.'

#### **Optimizing a loop**

The program enables sixteen parameters, see Table 2, to be altered individually, the new values of the dependent parameters being calculated automatically. When a parameter is chosen, a 'general information and warnings' window is displayed which gives a description of the parameter and indicates which of the other main parameters will change if the selected parameter is changed. Next, the present value of the parameter is given after which the user can insert the desired value. With the program, a complete loop can be designed quickly to your specification.

In the program, a loop is modified by altering one of the two main loop parameters,  $\omega_n$  or  $\zeta$ . Sometimes, this does not produce the desired result exactly, in which case, re-optimize the value of the parameter to be altered (via the optimize menu), and re-optimize.

With certain loop configurations, e.g. with a particular phase comparator or filter, a warning is displayed when it is impossible to make the modifications requested. In these cases, it is suggested that the following be tried. If the 'General Information and Warnings' window mentions that  $\omega_n$  has been altered to obtain the desired result, it may help to alter the other main loop parameter,  $\zeta$ , using the optimize facility. For example,

although the settling time depends on  $\omega_n$  and  $\zeta$ , in the optimize facility, a requested value of  $T_S$  is obtained by changing  $\omega_n$  alone. If  $\omega_n$  cannot be made large enough,  $T_S$  can be reduced by decreasing  $\zeta$ .

Experimenting with the optimization stage is highly instructive and is recommended to gain insight into the behaviour of a loop and to observe how the different parameters interact.

**Table 2: PLL parameters that can be optimized in the design program**

0	division ratio N, or max. phase error	8	pull-in range
1	VCO output frequency range	9	pull-out range
2	hold range	10	values of the filter components
3	phase margin	11	damping factor $\zeta$
4	ripple suppression	12	natural loop frequency
5	settling time	13	$\omega_0$ dB
6	lock-in range	14	overshoot
7	pull-in time	15	$\omega_{-3dB}$

the numbers correspond to those in the optimization menu.

### Evaluating existing designs

The PLL design program enables existing designs to be evaluated and, if required, redesigned to upgrade system performance.

After the system information has been entered in the usual way, the program calculates the loop parameters using the default settings as previously described. The results and the Bode plot can be compared with those of the existing design. The filter components of the existing design can be entered using option 10 of the optimization menu, and the loop parameters recalculated by the program. These results and the Bode plot give the designer a complete insight into the performance of the loop. Finally, the loop can be optimized and a new set of loop components generated to upgrade the original design. If the existing filter is not one of the three types which the program can handle, see Fig.44, the filter transformations shown in Fig.59 may be helpful.

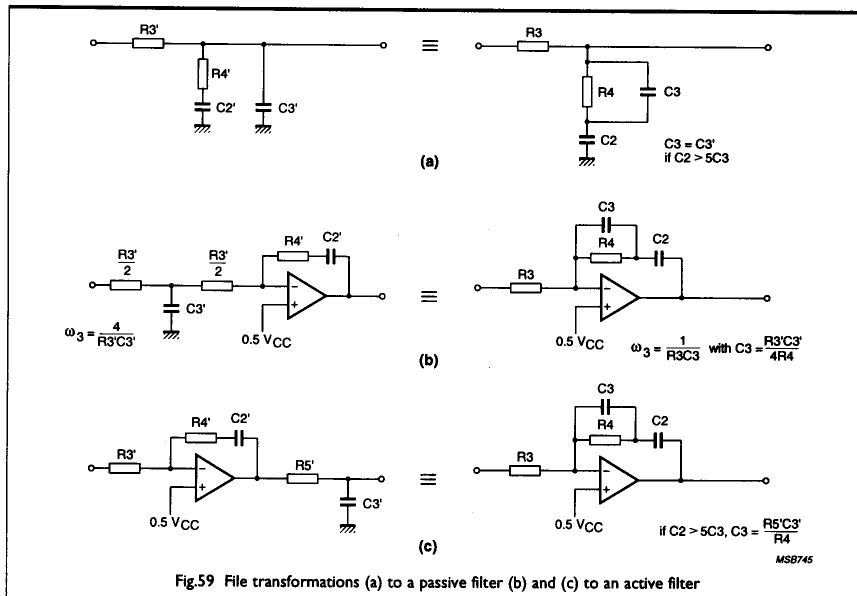


Fig.59 Filter transformations (a) to a passive filter (b) and (c) to an active filter

## APPLICATION EXAMPLES

### Filter output clamping

In some applications, it is useful to clamp the filter output to prevent the VCO running too low or too high. For example, with phase comparators PC2 and PC3, when there is no input signal for a period longer than the filter time constants, the output of the filter can fall below 1.1 V, causing the VCO to stop or to oscillate at its lowest frequency,  $f_{off}$ . And in certain applications, the VCO output frequency must be prevented from exceeding the value corresponding to an input signal of  $V_{CC} - 1.1$  V. In the frequency synthesizer application which follows, the active filter output is clamped, so it's useful to give some more details here, before describing the design of the synthesizer.

### Clamping for a passive filter

To clamp the output of a passive filter, two additional resistors,  $R'$ , are connected as shown in Fig.60. When the clamp is used in conjunction with PC2, it is recommended that the VCO centre frequency,  $f_0$ , be trimmed to near the input frequency with R2 or C1. This is because, when the loop is locked, the output of PC2 is 3-state, so the additional resistances would always bring the  $V_{COIN}$  voltage to  $0.5V_{CC}$ , biasing the VCO output frequency away from the input frequency, introducing a large phase error.

The value of  $R'$  is:

$$R' = \frac{V_{CC}R_3}{1.1} \quad (50)$$

where  $R_3$  is the original resistance in the filter.

At  $V_{CC} = 5$  V,

$$R' = 4.545R_3.$$

This  $R'$  alters the filter constant -  $R_3$  being replaced by the parallel combination of  $R_3$  and  $0.5R'$ . Therefore,  $R_3$  should be increased until the combined parallel combination of  $R_3$  and  $0.5R'$  equals the original  $R_3$ . The required value of  $R_3$  ( $R_3'$ ) is:

$$R_3' = \frac{V_{CC}R_3}{V_{CC} - 2.2} \quad (51)$$

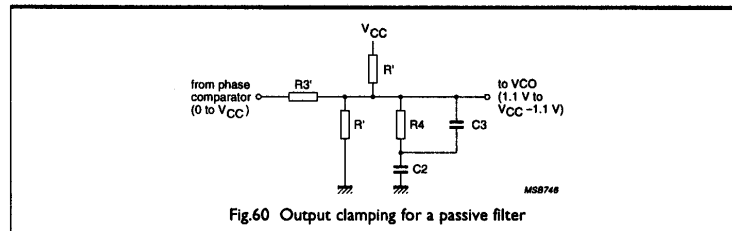


Fig.60 Output clamping for a passive filter

### Clamping for an active filter

To clamp the output of an active filter, three additional resistors,  $R_5$ ,  $R_6$  and  $R_7$ , are connected as shown in Fig.61. This doesn't change the original filter characteristic, and the values of  $R_5$ ,  $R_6$  and  $R_7$  are calculated as follows.

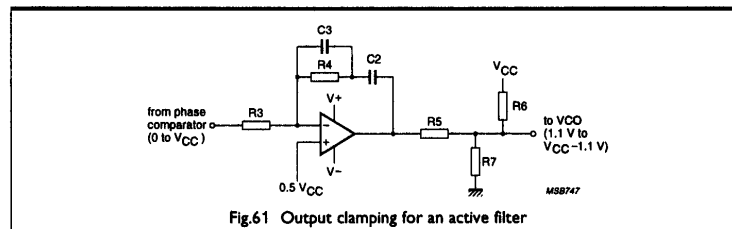


Fig.61 Output clamping for an active filter

First, R5 is set to 10 kΩ which will lead to practical values for R6 and R7 in virtually all cases. Next, the minimum (low) and maximum (high) output voltages of the op-amp are needed ( $V_{high}$  and  $V_{low}$  respectively). These are typically 1 V above the negative supply of the op-amp and 0.5 V below the positive supply of the op-amp respectively. If it is assumed that R6 and the HCMOS PLL circuit are connected to the same supply, then:

$$R6 = \frac{R5\{(V_{CC} - 1.1)^2 - (1.1)^2\}}{1.1\{V_{high} - (V_{CC} - 1.1)\} - (V_{CC} - 1.1)(V_{low} - 1.1)} \quad (52)$$

and

$$R7 = \frac{R6R5(V_{CC} - 1.1)}{1.1R5 + \{(V_{high} - (V_{CC} - 1.1))R6\}} \quad (53)$$

Example: With  $V_{high} = +10$  V and  $V_{low} = -10$  V, the calculated values for the clamp are:  $R5 = 10$  kΩ,  $R6 = 2.8$  kΩ and  $R7 = 3.9$  kΩ. With  $V_{high} = +12.5$  V and  $V_{low} = -12.5$  V,  $R5 = 10$  kΩ,  $R6 = 2.24$  kΩ and  $R7 = 2.88$  kΩ.

### Reduced loop gain

The clamping described reduces the total loop gain. For passive filters:

$$K_{new} = \frac{(V_{CC} - 2.2)}{V_{CC}} K_{old} \quad (54)$$

and for active filters:

$$K_{new} = \frac{(V_{CC} - 2.2)}{V_{high} - V_{low}} K_{old} \quad (55)$$

If the PLL design program is used, the reduced loop gain can be inserted by increasing the VCO input voltage range, which reduces the gain of the VCO, and hence of the total loop. The default VCO input voltage is calculated and displayed on the screen. For  $V_{CC} = 5$  V, this will be  $5 - 2.2 = 2.8$  V. Now, if for example,  $V_{high} - V_{low}$  is 28 V, the default value of 2.8 V should be multiplied by  $28/2.8$ , yielding 28 V. The loop gain will also be altered by the same factor.

### Frequency synthesizer

In this section, the design of a synthesizer using the PLL design program is described for, in turn, PC1, PC2 and PC3 first with a passive filter and then with an active filter, resulting in six designs. In all cases, the designs were first done with the HCT4046A selected as type 1 in the program. For comparison, two designs with the HCT9046A with PC2 and a passive or active filter are shown.

If you have a copy of the PLL design program, it is a good exercise to work through this example for yourself. The general system specifications are:

- Output frequency: 2 MHz to 3 MHz
- Frequency steps: 100 kHz
- Settling time: <1 ms
- Overshoot: <20%
- $V_{CC}$ : 5 V.
- Input frequency spread 0% (crystal controlled)

Figure 62 shows the synthesizer circuit. The external components R1 and R2 have a 1% tolerance and C1 has a 2% tolerance, resulting in a total tolerance of 24% (part-to-part spread of an HCMOS PLL circuit is 20%, see 'Part-to-part spread') to which an estimated 8% maximum temperature variation is added, making 32% in total.

For the three design cases with an active filter type 2, an op-amp with an output swing from  $-12.5$  V to  $+12.5$  V is assumed, together with an input clamp to reduce  $VCO_{in}$  from 1.1 to 3.9 V. For these cases, the VCO gain should be adapted by a factor  $2.8/25$ . This should be done by inserting a value of 25 for the VCO input voltage range. Values for a proper clamp are:  $R5 = 10$  kΩ,  $R6 = 2.24$  kΩ and  $R7 = 2.88$  kΩ as calculated with the equations (52) and (53).

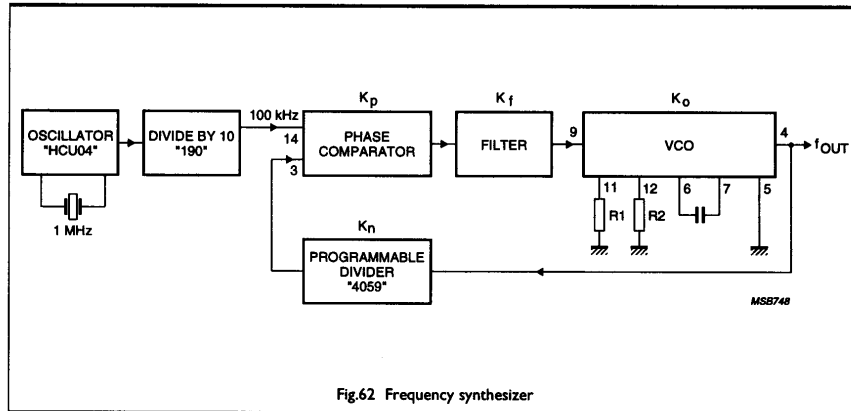


Fig.62 Frequency synthesizer

**Calculating the division ratio**

The minimum and maximum programmable division ratios required are:

$$N_{\min} = \frac{f_{\text{out}(\min)}}{f_{\text{step}}} = \frac{2 \text{ MHz}}{100 \text{ kHz}} = 20 \tag{56}$$

and

$$N_{\max} = \frac{f_{\text{out}(\max)}}{f_{\text{step}}} = \frac{3 \text{ MHz}}{100 \text{ kHz}} = 30. \tag{57}$$

Table 3 lists the states of the control pins for a 74HC4059 programmable divide-by-N counter to step from divide-by-20 to divide-by-30, see also the PC74HC/HCT4059 data in Data Handbook IC06.

**Table 3: Pin status for a 4059 programmable divider for N = 20 to 30.**

N	mode 2*	J <sub>1</sub>	J <sub>2</sub>	J <sub>3</sub>	J <sub>4</sub>	J <sub>5</sub>	J <sub>6</sub>	J <sub>7</sub>	J <sub>8</sub>	J <sub>9</sub> to J <sub>16</sub>
20	10	0	0	0	0	0	1	0	1	0
21	10 remainder 1	1	0	0	0	0	1	0	1	0
22	11	0	0	0	0	1	1	0	1	0
23	11 remainder 1	1	0	0	0	1	1	0	1	0
24	12	0	0	0	0	0	0	1	1	0
25	12 remainder 1	1	0	0	0	0	0	1	1	0
26	13	0	0	0	0	1	0	1	1	0
27	13 remainder 1	1	0	0	0	1	0	1	1	0
28	14	0	0	0	0	0	1	1	1	0
29	14 remainder 1	1	0	0	0	0	1	1	1	0
30	15	0	0	0	0	1	1	1	1	0

\* selected by the mode select inputs: K<sub>a</sub>, K<sub>b</sub> and K<sub>c</sub> = 1 and the latch enable: LE = 0. Mode 2 selects the first counting section of the 4059 to a divide-by-2 counter. The divide-by-N output, Q, is connected to the input of the phase comparator; V<sub>CC</sub> = 5 V; GND = 0 V.

The filter components and VCO bias components are calculated by the program. The VCO centre frequency and operating range are the default values, calculated using the equations of the section 'Part-to-part spread'. This means that the external VCO components don't have to be trimmed to compensate for the VCO part-to-part spread.

The calculated results are compared with measurements on each configuration and are restricted to overshoot, settling time, pull-out range and ripple suppression, and the Bode plot. Figure 63 shows the results, as they are displayed on-screen.

The Bode plot of the open loop was measured with the injection circuit shown in Appendix C together with an HP3577A network analyzer.

```

INPUT PARAMETERS
PC : 1      fIn (Hz) : 1.000E+05  Spread input freq. (%) : 0.0
Mmax : 30  2FR (Hz) : 2.897E+06  Part-to-part spread (%) : 32.0
Filter : 1  f0 (Hz) : 2.963E+06  Vcc (Volt) : 5.0
M_used : 30

VCO and FILTER PARAMETERS 74HC/HCT 4046A/7046A
T1 (sec) : 1.6E-02  T2 (sec) : 3.0E-04  T3 (sec) : 2.5E-05
f1 (Hz) : 9.8E+00  f2 (Hz) : 5.3E+02  f3 (Hz) : 6.3E+03
R1 (Ohm) : 1.5E+04  R3 (Ohm) : 1.0E+04  R4 (Ohm) : 1.9E+02
R2 (Ohm) : 1.3E+05  C2 (Far) : 1.6E-06  C3 (Far) : 1.3E-07
C1 (Far) : 1.0E-10

DYNAMIC PARAMETERS
Wn/2k (Hz) : 7.3E+02  pull-in time (sec) : 3.3E-02
W_0dB/2k (Hz) : 1.3E+03  pull-in range (Hz) : 1.2E+04
zeta : 0.70  pull-out range (Hz) : 2.2E+03
overshoot (%) : 21.03  hold range (Hz) : 8.6E+04
Kv : 3.48E+05  settling time (<5%) (sec) : 1.0E-01
Winput/W_0dB : 79.6  lock-in range (Hz) : 1.6E+03
phasemargin with C3 (deg) : 57  ripple suppr. with C3 (dB) : -46
phasemargin without C3 (deg) : 67  ripple suppr. without C3 (dB) : -16
setamin (Hz) : 0.70  Wmin/2k (Hz) : 7.3E+02
setamax (Hz) : 0.86  Wmax/2k (Hz) : 9.0E+02

```

Optimize ? (Y/N) : Y

(a)

```

INPUT PARAMETERS
PC : 1      fIn (Hz) : 1.000E+05  Spread input freq. (%) : 0.0
Mmax : 30  2FR (Hz) : 2.897E+06  Part-to-part spread (%) : 32.0
Filter : 1  f0 (Hz) : 2.963E+06  Vcc (Volt) : 5.0
M_used : 30

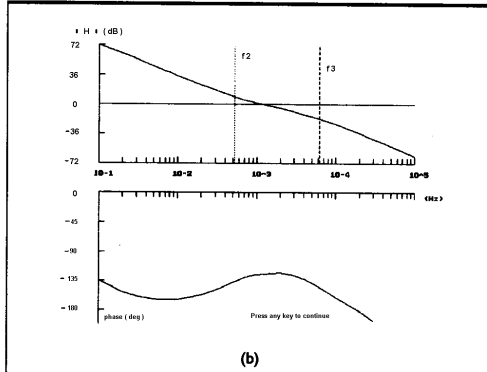
VCO and FILTER PARAMETERS 74HC/HCT 4046A/7046A
T1 (sec) : 1.2E-03  T2 (sec) : 8.2E-05  T3 (sec) : 7.2E-06
f1 (Hz) : 1.2E+02  f2 (Hz) : 1.9E+03  f3 (Hz) : 2.2E+04
R1 (Ohm) : 1.5E+04  R3 (Ohm) : 1.0E+04  R4 (Ohm) : 6.9E+02
R2 (Ohm) : 1.3E+05  C2 (Far) : 1.2E-07  C3 (Far) : 1.1E-08
C1 (Far) : 1.0E-10

DYNAMIC PARAMETERS
Wn/2k (Hz) : 2.6E+03  pull-in time (sec) : 2.6E-03
W_0dB/2k (Hz) : 4.4E+03  pull-in range (Hz) : 2.2E+04
zeta : 0.70  pull-out range (Hz) : 8.0E+03
overshoot (%) : 21.03  hold range (Hz) : 8.6E+04
Kv : 3.48E+05  settling time (<5%) (sec) : 2.8E-04
Winput/W_0dB : 22.7  lock-in range (Hz) : 5.7E+03
phasemargin with C3 (deg) : 55  ripple suppr. with C3 (dB) : -23
phasemargin without C3 (deg) : 64  ripple suppr. without C3 (dB) : -6
setamin (Hz) : 0.70  Wmin/2k (Hz) : 2.6E+03
setamax (Hz) : 0.86  Wmax/2k (Hz) : 3.2E+03

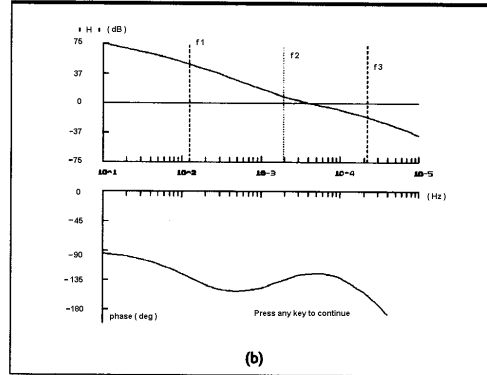
```

Optimize ? (Y/N) : Y

(a)

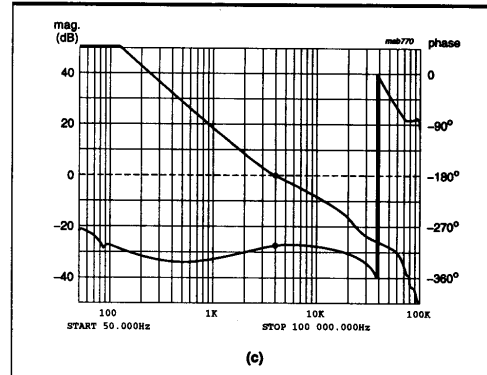


(b)



(b)

Fig.63 (a) Original loop parameters and (b) calculated Bode plot for a PLL using PC1 and a passive filter



(c)

Fig.64 (a) Modified loop parameters and (b) calculated Bode plot for a PLL using PC1 and a passive filter. (c) measured Bode plot; phase margin is 55.9° at 4.120 kHz (0 dB)

### Designing with the program

During the calculation of the PLL parameters, the following error message is displayed: "Error, switching between channels will cause the loop to lose lock. Increase pull-out range to 5.1 kHz."

For example, if the divider in the feedback switches from 21 to 20, the frequency step on the phase comparator input is:

$$\frac{2.1 \text{ MHz}}{20} - 100 \text{ kHz} = 5 \text{ kHz.}$$

Unless the pull-out range exceeds this frequency step, the loop will lose lock when the divider switches, taking the pull-in time to regain lock. In this example, the pull-out range was set to 8 kHz via option 9 of the optimization menu for extra margin. The new results and Bode plot are shown in Fig.64.

In all calculations, the program uses the maximum division ratio,  $N_{\max}$ , because this gives worst-case values for overshoot,  $\zeta$ , and settling time. With 'option 0', all parameters and the Bode plot can be checked by changing  $N$  from  $N_{\max}$  to  $N_{\min}$ .

The results for the remaining five designs are given in Figs 65 to 69. In the case of PC2 used with a passive filter, the gain variation of PC2 is taken into account. In the case of PC3, the same error message was displayed as for the example with PC1 just described, and here too the pull-out range was increased to 8 kHz.

For comparison, also two cases for the 9046A were calculated, one with PC2 plus passive filter and the other for PC2 plus active filter. Because of the higher VCO frequency stability, these designs use a value of 22% for the part-to-part spread, with  $\pm 10\%$  for the circuit spread, 2% for R1, R2 and C1, and 8% for the spread due to temperature variations. The results on screen for both cases are shown in Fig.70 (a) and (b). The Bode plot is the same for both designs and is given in Fig.70(c).

Figure 71 shows the overshoot of a real synthesizer while switching from a division ratio of 28 to 29 and from 20 to 21. The lower-gain loops using PC1 and PC3 with a passive filter have less overshoot than that calculated by the program. This is because the program uses only the step response for a high-gain loop (Fig.51), whereas in practice the loop changes gradually from a high-gain loop to a low-gain loop (Fig.40). In all cases, the measured overshoot was close to that calculated (21%) as was settling time.

To check the need to optimize loops using PC1 owing to the small pull-out range, a synthesizer was built according to the non-optimized parameters. The synthesizer would not work and would not lock at all at division ratios away from the centre ratio of 25.

The ripple suppression ratio is only a rough approximation, so the measured values can be expected to differ from those calculated especially when the calculated value is less than about -10 dB. This is because the modulation index is now large and the first-order approach is no longer accurate. However, the values calculated by the program are useful to see improvements during optimization, and if the ripple suppression rises above -10 dB, exact values are usually not of interest because the instability of the VCO output signal is often unacceptable. Figure 72 shows the ripple suppression (measured on the VCO output signal). The ripple suppression can be improved by using the optimize facility, but this will increase the settling time.

Note, these design examples are only intended to illustrate how the program operates. The values presented are NOT the optimum that can be achieved with the 74HC/HCT4046A and the 74HCT9046A. In practice, the PLLs would be optimized further than shown in the examples to improve performance, for example, the ripple suppression.



```

INPUT PARAMETERS
PC : 1      fin (Hz) : 1.000E+05  Spread input freq. (%) : 0.0
Nmax : 30   2fR (Hz) : 2.897E+06  Part-to-part spread (%) : 32.0
Filter : 2   f0 (Hz) : 2.963E+06  Vcc (Volt) : 5.0
N_used : 30

VCO and FILTER PARAMETERS 74HC/HCT 4046A/7046A
T1 (sec) : 1.6E-04  T2 (sec) : 1.2E-04  T3 (sec) : 8.7E-06
f1 (Hz) : 1.0E-02  f2 (Hz) : 1.3E+03  f3 (Hz) : 1.8E+04
R1 (Ohm) : 1.5E+04  R3 (Ohm) : 9.8E+03  R4 (Ohm) : 7.4E+03
R2 (Ohm) : 1.3E+05  C2 (Far) : 1.6E-08  C3 (Far) : 1.2E-09
C1 (Far) : 1.0E-10

DYNAMIC PARAMETERS
Wn/2π (Hz) : 2.5E+03  pull-in time (sec) : 3.1E-04
W_dB/2π (Hz) : 5.0E+03  pull-in range (Hz) : 7.4E+03
sets (Hz) : 0.73  pull-out range (Hz) : 7.8E+03
overshoot (%) : 20.11  hold range (Hz) : 1.4E+06
Rv : 3.3E+04  settling time (<5%) (sec) : 2.5E-04
Winput/W_dB : 20.2  lock-in range (Hz) : 5.7E+03
phasemargin with C3 (deg) : 56  ripple suppr. with C3 (dB) : -23
without C3 (deg) : 70  without C3 (dB) : -3
zetamin (Hz) : 0.73  Wmin/2π (Hz) : 2.6E+03
zetamax (Hz) : 0.89  Wmax/2π (Hz) : 3.2E+03
    
```

```

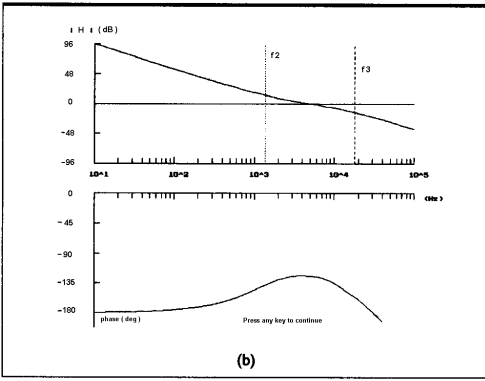
INPUT PARAMETERS
PC : 2      fin (Hz) : 1.000E+05  Spread input freq. (%) : 0.0
Nmax : 30   2fR (Hz) : 2.897E+06  Part-to-part spread (%) : 32.0
Filter : 1   f0 (Hz) : 2.963E+06  Vcc (Volt) : 5.0
N_used : 30

VCO and FILTER PARAMETERS 74HC/HCT 4046A/7046A
T1 (sec) : 6.9E-03  T2 (sec) : 3.4E-04  T3 (sec) : 3.9E-05
f1 (Hz) : 2.3E-04  f2 (Hz) : 4.1E+02  f3 (Hz) : 4.0E+03
R1 (Ohm) : 1.5E+04  R3 (Ohm) : 4.6E+02  R4 (Ohm) : 2.6E+01
R2 (Ohm) : 1.3E+05  C2 (Far) : 1.5E-05  C3 (Far) : 1.5E-06
C1 (Far) : 1.0E-10  Rp (Ohm) : 8.3E+04

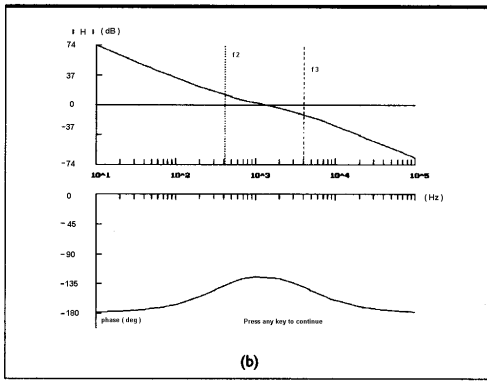
DYNAMIC PARAMETERS
Wn/2π (Hz) : 7.0E+02  pull-in time (sec) : 4.4E-03
W_dB/2π (Hz) : 1.3E+03  pull-in range (Hz) : 1.4E+06
sets (Hz) : 0.71  pull-out range (Hz) : 9.7E+03
overshoot (%) : 20.61  hold range (Hz) : 1.4E+06
Rv : 1.3E+05  settling time (<5%) (sec) : 1.0E-03
Winput/W_dB : 77.3  lock-in range (Hz) : 6.3E+03
phasemargin with C3 (deg) : 56  ripple suppr. with C3 (dB) : -16
without C3 (deg) : 72  without C3 (dB) : -33
zetamin (Hz) : 0.71  Wmin/2π (Hz) : 7.3E+02
zetamax (Hz) : 0.87  Wmax/2π (Hz) : 9.0E+02
    
```

(a)

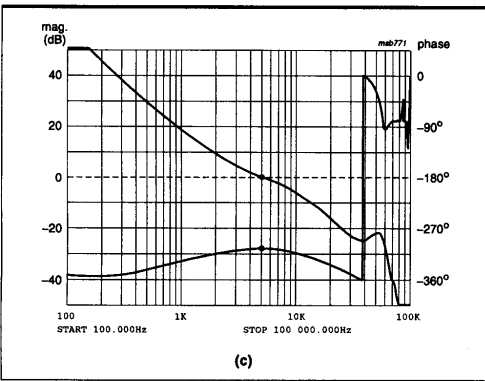
(a)



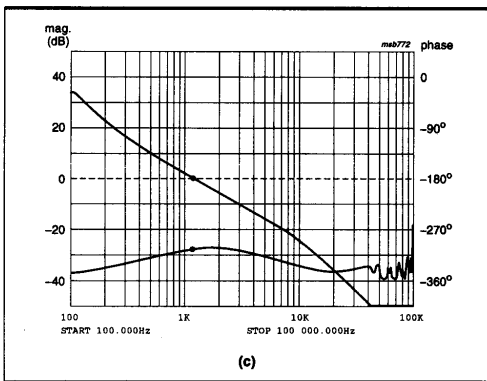
(b)



(b)



(c)



(c)

Fig.65 (a) Loop parameters and (b) calculated Bode plot for a PLL using PC1 with an active filter. (c) measured Bode plot; phase margin is 54.9° at 5.056 kHz (0 dB)

Fig.66 (a) Loop parameters and (b) calculated Bode plot for a PLL using PC2 with a passive filter. (c) measured Bode plot; phase margin is 55.5° at 1.164 kHz (0 dB)

```

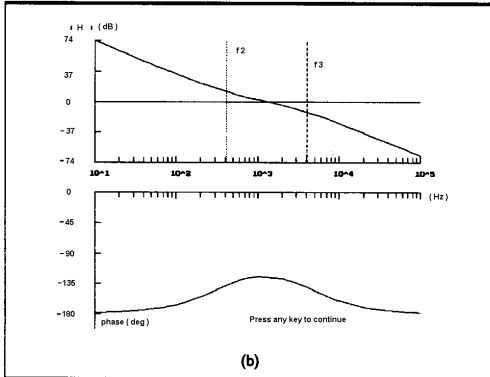
INPUT PARAMETERS
PC : 2      fin (Hz) : 1.000E+05  Spread input freq. (%) : 0.0
Nmax : 30  2fR (Hz) : 2.897E+06  Part-to-part spread (%) : 32.0
Filter : 2  f0 (Hz) : 2.963E+06  Vcc (Volt) : 5.0
N_used : 30

VCO and FILTER PARAMETERS 74HC/HCT 4046A/7046A
T1 (sec) : 5.0E-04  T2 (sec) : 3.8E-04  T3 (sec) : 3.9E-05
f1 (Hz) : 3.2E+03  f2 (Hz) : 4.1E+02  f3 (Hz) : 4.0E+03
R1 (Ohm) : 1.5E+04  R2 (Ohm) : 4.5E+02  R4 (Ohm) : 3.5E+02
R3 (Ohm) : 1.3E+05  C2 (Far) : 1.1E-06  C3 (Far) : 1.1E-07
C1 (Far) : 1.0E-10  Rp (Ohm) : 8.3E+04

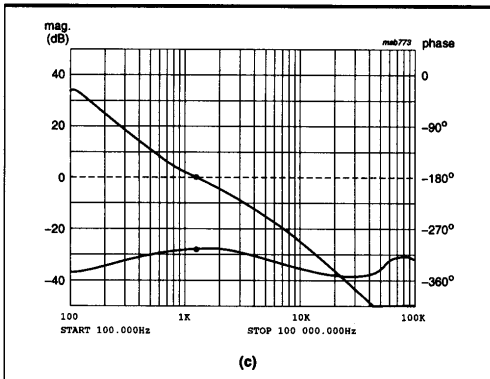
DYNAMIC PARAMETERS
Wn/2K (Hz) : 7.0E+02  pull-in time (sec) : 3.0E-03
W_0dB/2K (Hz) : 1.3E+03  pull-in range (Hz) : 1.4E+06
zeta : 0.71  pull-out range (Hz) : 9.7E+03
overshoot (%) : 20.61  hold range (Hz) : 1.4E+06
Kv : 9.7E+03  settling time (<5%) (sec) : 1.0E-03
Winput/W_0dB (Hz) : 77.3  lock-in range (Hz) : 6.3E+03
phasemargin with C3 (deg) : 56  ripple suppr. with C3 (dB) : -32
zetamin without C3 (deg) : 72  Wmin/2K (Hz) : 7.3E+02
zetamax without C3 (deg) : 87  Wmax/2K (Hz) : 9.0E+02
                                         Philips Semiconductors
Optimize ? (Y/N) : Y

```

(a)



(b)



(c)

Fig.67 (a) Loop parameters and (b) calculated Bode plot for a PLL using PC2 with an active filter. (c) measured Bode plot; phase margin is 56.7° at 1.291 kHz (0 dB)

```

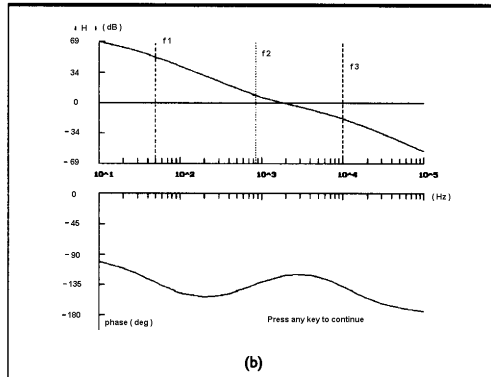
INPUT PARAMETERS
PC : 3      fin (Hz) : 1.000E+05  Spread input freq. (%) : 0.0
Nmax : 30  2fR (Hz) : 2.897E+06  Part-to-part spread (%) : 32.0
Filter : 1  f0 (Hz) : 2.963E+06  Vcc (Volt) : 5.0
N_used : 30

VCO and FILTER PARAMETERS 74HC/HCT 4046A/7046A
T1 (sec) : 3.0E-03  T2 (sec) : 1.9E-04  T3 (sec) : 1.6E-05
f1 (Hz) : 5.0E+01  f2 (Hz) : 8.6E+02  f3 (Hz) : 9.9E+03
R1 (Ohm) : 1.5E+04  R2 (Ohm) : 9.1E+03  R4 (Ohm) : 5.6E+02
R3 (Ohm) : 1.3E+05  C2 (Far) : 3.3E-07  C3 (Far) : 2.9E-08
C1 (Far) : 1.0E-10

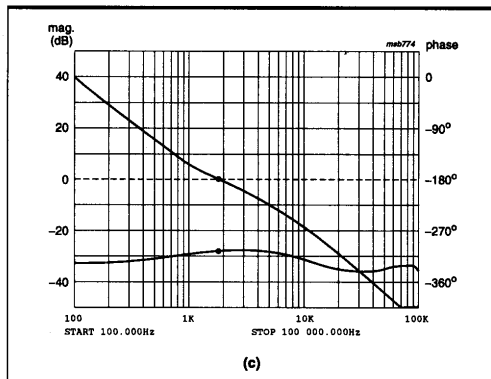
DYNAMIC PARAMETERS
Wn/2K (Hz) : 1.2E+03  pull-in time (sec) : 6.4E-03
W_0dB/2K (Hz) : 2.0E+03  pull-in range (Hz) : 2.3E+04
zeta : 0.70  pull-out range (Hz) : 8.0E+03
overshoot (%) : 21.03  hold range (Hz) : 8.6E+04
Kv : 1.7E+05  settling time (<5%) (sec) : 6.3E-04
Winput/W_0dB (Hz) : 50.6  lock-in range (Hz) : 5.1E+03
phasemargin with C3 (deg) : 59  ripple suppr. with C3 (dB) : -19
zetamin without C3 (deg) : 68  Wmin/2K (Hz) : 1.2E+03
zetamax without C3 (deg) : 86  Wmax/2K (Hz) : 1.4E+03
                                         Philips Semiconductors
Optimize ? (Y/N) : Y

```

(a)



(b)



(c)

Fig.68 (a) Loop parameters and (b) calculated Bode plot for a PLL using PC3 with a passive filter. (c) measured Bode plot; phase margin is 57.4° at 1.785 kHz (0 dB)

```

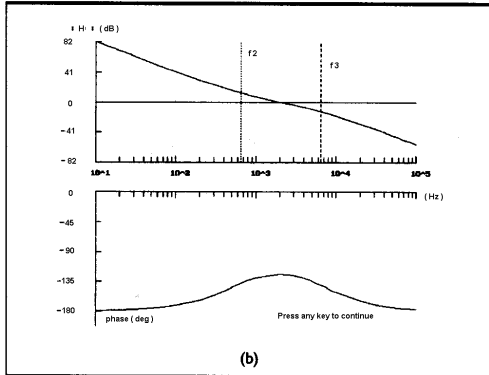
INPUT PARAMETERS
PC : 3      fin (Hz) : 1.000E+05  Spread input freq. (%) : 0.0
Nmax : 30  2FR (Hz) : 2.897E+06  Part-to-part spread (%) : 32.0
Filter : 2  f0 (Hz) : 2.963E+06  Vcc (Volt) : 5.0
N_used : 30

VCO and FILTER PARAMETERS 74HC/7046A
T1 (sec) : 4.0E-04  T2 (sec) : 2.4E-04  T3 (sec) : 2.4E-05
f1 (Hz) : 4.0E+03  f2 (Hz) : 6.5E+02  f3 (Hz) : 6.5E+03
R1 (Ohm) : 1.5E+04  R2 (Ohm) : 9.3E+03  R4 (Ohm) : 5.7E+03
R3 (Ohm) : 1.3E+05  C2 (Far) : 4.3E-08  C3 (Far) : 4.3E-09
C1 (Far) : 1.0E-10

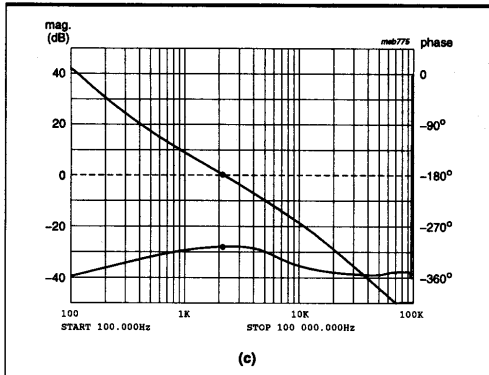
DYNAMIC PARAMETERS
Wn/2x (Hz) : 1.1E+03  pull-in time (sec) : 8.0E-04
W_0dB/2x (Hz) : 2.1E+03  pull-in range (Hz) : 7.0E+03
zeta : 0.72  pull-out range (Hz) : 7.7E+03
overshoot (%) : 20.25  hold range (Hz) : 1.4E+06
KV : 1.9E+04  settling time (<5%) (sec) : 6.5E-04
Winp/M_0dB : 48.6  lock-in range (Hz) : 5.0E+03
phase margin with C3 (deg) : 56  ripple suppr. with C3 (dB) : -22
phase margin without C3 (deg) : 72  without C3 (dB) : 1
zetamin : 0.72  Wnmin/2x (Hz) : 1.1E+03
zetamax : 0.89  Wnmax/2x (Hz) : 1.4E+03
  
```

Optimize ? (Y/N) : Y

(a)



(b)



(c)

Fig.69 (a) Loop parameters and (b) calculated Bode plot for a PLL using PC3 with an active filter. (c) measured Bode plot; phase margin is 56.0° at 2.160 kHz (0 dB)

```

INPUT PARAMETERS
PC : 2      fin (Hz) : 1.000E+05  Spread input freq. (%) : 0.0
Nmax : 30  2FR (Hz) : 2.207E+06  Part-to-part spread (%) : 22.0
Filter : 1  f0 (Hz) : 2.743E+06  Vcc (Volt) : 5.0
N_used : 30

VCO and FILTER PARAMETERS 74HCT 9046A
T1 (sec) : 5.2E-03  T2 (sec) : 3.8E-04  T3 (sec) : 3.9E-05
f1 (Hz) : 3.0E+04  f2 (Hz) : 4.1E+02  f3 (Hz) : 4.0E+03
R1 (Ohm) : 1.9E+04  R3 (Ohm) : 0.0  R4 (Ohm) : 3.8E+02
R2 (Ohm) : 5.6E+04  C2 (Far) : 1.0E-06  C3 (Far) : 1.0E-07
C1 (Far) : 1.0E-10  Rb (Ohm) : 1.0E+05

DYNAMIC PARAMETERS
Wn/2x (Hz) : 7.0E+02  pull-in time (sec) : 4.4E-03
W_0dB/2x (Hz) : 1.3E+03  pull-in range (Hz) : 1.1E+06
zeta : 0.71  pull-out range (Hz) : 9.7E+03
overshoot (%) : 20.61  hold range (Hz) : 1.1E+06
KV : 1.0E+05  settling time (<5%) (sec) : 1.0E-03
Winp/M_0dB : 77.3  lock-in range (Hz) : 6.3E+03
phase margin with C3 (deg) : 56  ripple suppr. with C3 (dB) : -40
phase margin without C3 (deg) : 72  without C3 (dB) : -37
zetamin : 0.71  Wnmin/2x (Hz) : 7.3E+02
zetamax : 0.87  Wnmax/2x (Hz) : 9.0E+02
  
```

Optimize ? (Y/N) : Y

(a)

```

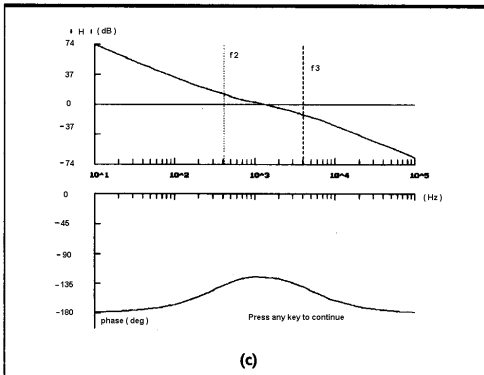
INPUT PARAMETERS
PC : 2      fin (Hz) : 1.000E+05  Spread input freq. (%) : 0.0
Nmax : 30  2FR (Hz) : 2.207E+06  Part-to-part spread (%) : 22.0
Filter : 2  f0 (Hz) : 2.743E+06  Vcc (Volt) : 5.0
N_used : 30

VCO and FILTER PARAMETERS 74HCT 9046A
T1 (sec) : 3.8E-04  T2 (sec) : 3.8E-04  T3 (sec) : 3.9E-05
f1 (Hz) : 4.2E+03  f2 (Hz) : 4.1E+02  f3 (Hz) : 4.0E+03
R1 (Ohm) : 1.9E+04  R3 (Ohm) : 0.0  R4 (Ohm) : 5.6E+03
R2 (Ohm) : 5.6E+04  C2 (Far) : 6.8E-08  C3 (Far) : 7.0E-09
C1 (Far) : 1.0E-10  Rb (Ohm) : 1.0E+05

DYNAMIC PARAMETERS
Wn/2x (Hz) : 7.0E+02  pull-in time (sec) : 3.0E-03
W_0dB/2x (Hz) : 1.3E+03  pull-in range (Hz) : 1.1E+06
zeta : 0.71  pull-out range (Hz) : 9.7E+03
overshoot (%) : 20.61  hold range (Hz) : 1.1E+06
KV : 7.4E+03  settling time (<5%) (sec) : 1.0E-03
Winp/M_0dB : 77.3  lock-in range (Hz) : 6.3E+03
phase margin with C3 (deg) : 56  ripple suppr. with C3 (dB) : -36
phase margin without C3 (deg) : 72  without C3 (dB) : -33
zetamin : 0.71  Wnmin/2x (Hz) : 7.3E+02
zetamax : 0.87  Wnmax/2x (Hz) : 9.0E+02
  
```

Optimize ? (Y/N) : Y

(b)



(c)

Fig.70 (a) Loop parameters for 74HCT9046A PLL using PC2 with a passive filter (b) PC2 with an active filter (c) calculated Bode plot for both cases

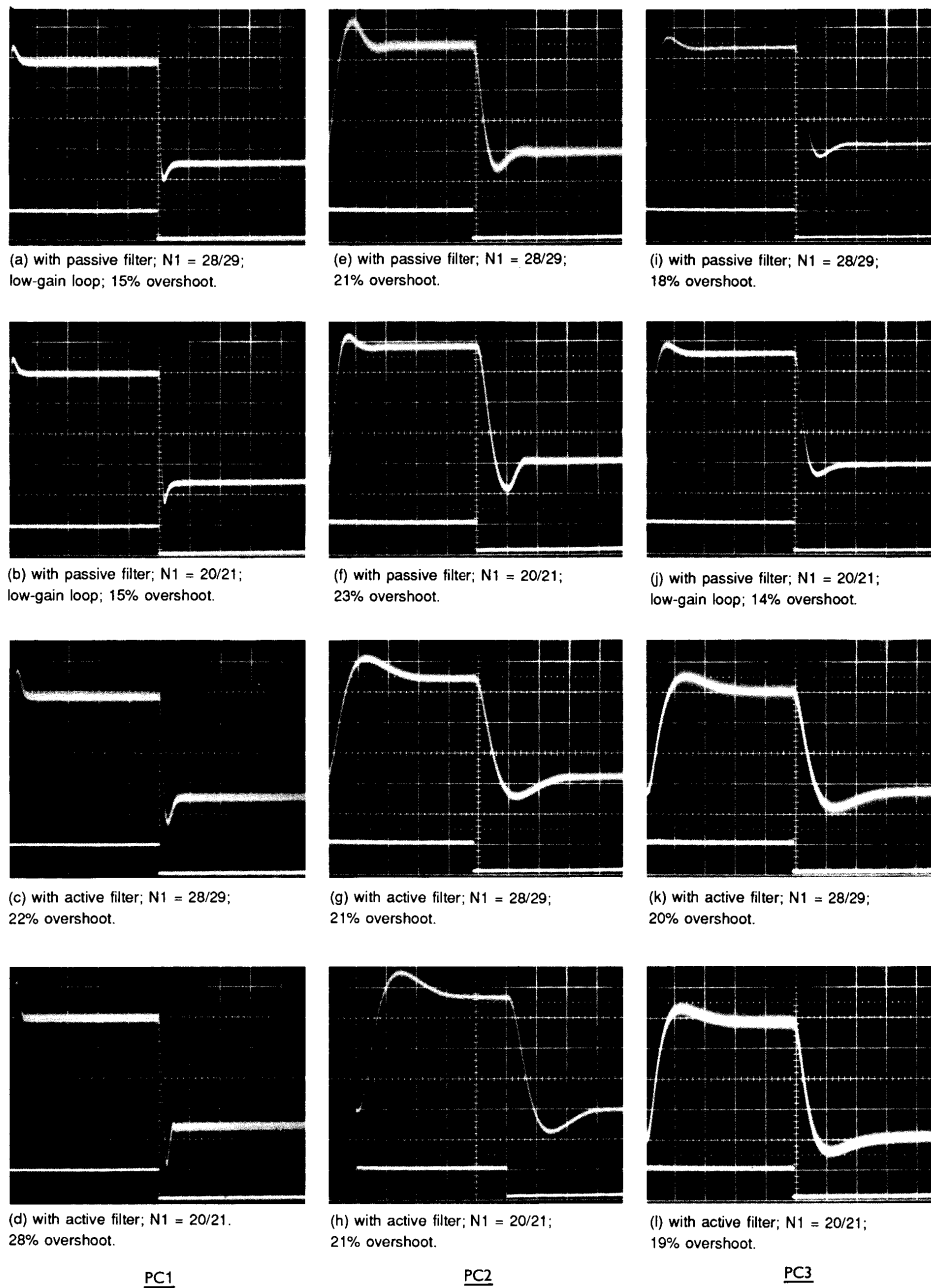
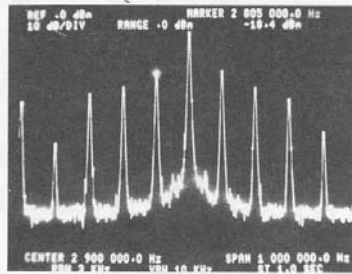
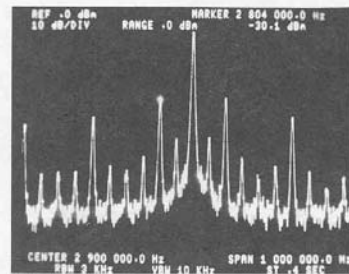


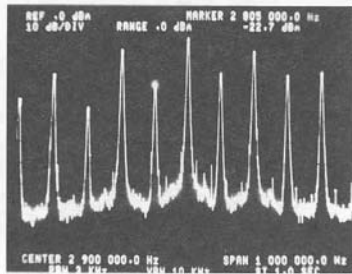
Fig.71 Overshoot and settling time for the frequency synthesizer. Horizontal scale: 0.5 ms/div



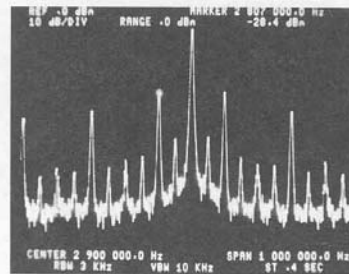
(a) with passive filter; with C3;



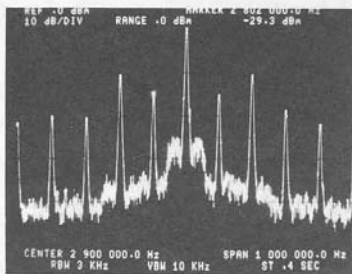
(e) with passive filter; with C3;



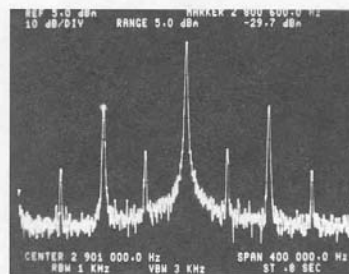
(b) with passive filter; without C3;



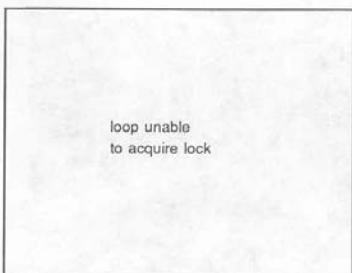
(f) with passive filter; without C3;



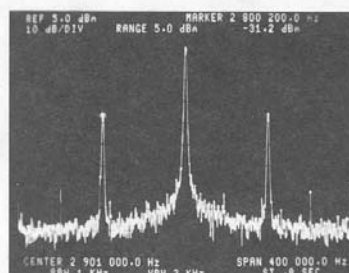
(c) with active filter; with C3;



(g) without  $R_p$ ;



(d) with active filter; without C3.

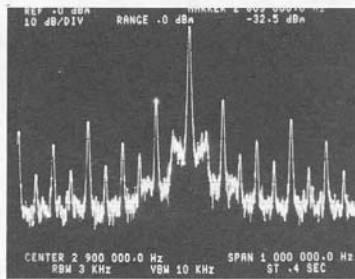


(h) with  $R_p$ ;

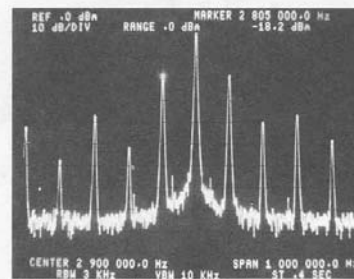
PC1

PC2

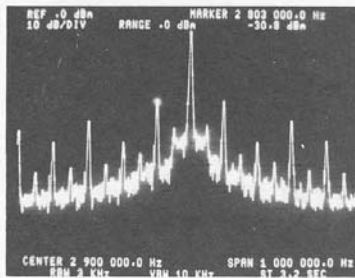
Fig.72 Ripple suppression; vertical scale: 10 dB/div, horizontal scale: 100 kHz/div



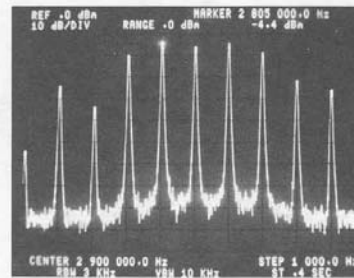
(j) with active filter; with C3;



(k) with passive filter; with C3;

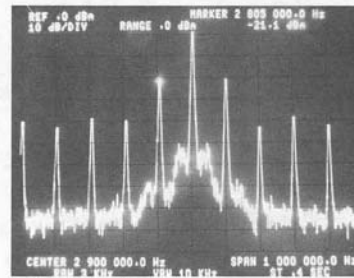


(l) with active filter; without C3.

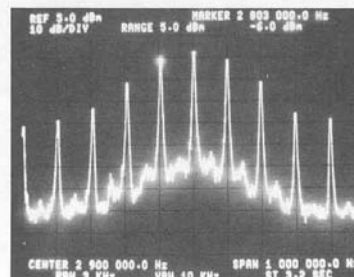


(l) with passive filter; without C3;

PC2 continued



(m) with active filter; with C3;



(n) with active filter; with C3 = 10 nF.  
With C3 < 10 nF, the loop was unable to acquire lock.

PC3

### Video horizontal line synchronizer

Figure 73a is the circuit schematic of a video horizontal line synchronizer designed with the help of the PLL design program. The synchronizer has the following features:

- can be synchronized over at least one octave (double frequency monitor);
- produces no visible phase jitter;
- slew rate clamping to protect the drivers in the horizontal deflection stage from very fast frequency changes;
- equal lock and hold ranges;
- fast settling time after a frequency change.

In this synchronizer, a non-composite sync signal is used to limit the circuitry needed; the circuitry required if a composite signal is used is more complex due to the missing sync pulses during the vertical interval. Such a circuit is given in Fig.73b. A short review of the main circuit functions is given on the next page.

The input signal (horizontal sync) which can range from 15.625 kHz to 31.250 kHz is entered in the design program as an  $f_{in}$  of 23.4375 kHz with an expected deviation of 35%.

Phase comparator PC2 is used because it has the best lock and hold range of the three phase comparators, as well as edge-triggered detection and, here, a noise-free input signal.

An active loop filter was chosen because the input frequency range is so large that with a passive filter, the phase comparator gain would vary too much. In addition, it is easy to insert a slew rate clamp in an active filter. In Fig.73, the clamp is simply the two back-to-back zener diodes and series capacitance of 470 nF. The 360 k $\Omega$  resistor ( $R_p$ ) connected to the output of PC2 reduces phase jitter to an imperceptible level. The filter output is clamped and the component values were selected using Eqs.(45) to (50) and  $V_{low} = 1$  V,  $V_{high} = 25.5$  V (the op-amp supply is 26 V). The output clamping lowers the loop gain and this is entered in the PLL design program by changing the VCO input voltage range from the default value of 2.8 V to  $(24.4/2.8)2.8 = 24.4$  V.

The positive input of the op-amp is biased at  $0.5V_{CC} = 2.5$  V. Note, because the op-amp inverts the output from the phase comparator, the horizontal sync input is connected to the  $COMP_{IN}$  input instead of the  $SIG_{IN}$  input. The tolerance of the external components for the VCO (1% for R1 and R2; 2% for C1) result in a VCO spread of 24%. When an 8% spread is added for temperature changes up to 85 °C, the total spread is 32%. The program calculates the centre frequency  $f_0$  and the VCO operating range  $2f_r$  such that trimming is not required. For smoother response,  $\omega_n$  was lowered to 650 Hz via the optimization facility.

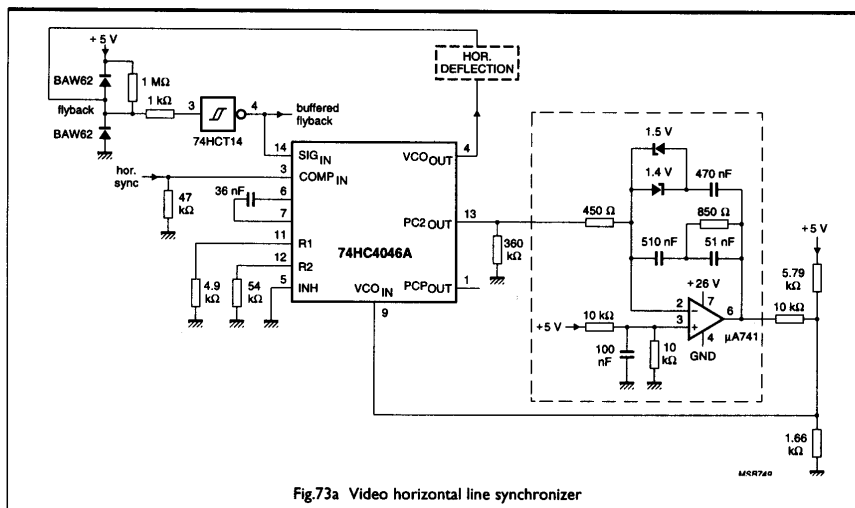


Fig.73a Video horizontal line synchronizer

Figure 73b is the circuit of a video horizontal line synchronizer with a composite horizontal sync signal. During the vertical interval, a few H sync pulses are missing. Then, output PCP<sub>OUT</sub> goes LOW and, after a short detection period of about 400 ns, the output from pin 13 of the HC4002 NOR gate goes HIGH, resetting the BCD counter HC4518 and opening the loop by opening the analog switch at pins 1 and 2 of the HCT4016. The PLL frequency free-wheels for ten flyback periods, after which the loop is closed again and horizontal sync pulses are re-applied. To compensate for the disturbance of the loop during the detect time, the switch at pins 3 and 4 of the HCT4016 is closed by the output from pin 13 of NOR gate HC4002 for the same time interval. This connects the inverted PC<sub>2</sub>OUT from pin 8 of the HCT14 to the amplifier input. After 70 flyback periods, pin 14 of the second section of the HC4518 becomes '1' and the system is enabled for the next vertical interval. This circuit prevents the missing horizontal sync pulses during the vertical interval from influencing the video line synchronization and picture stability.

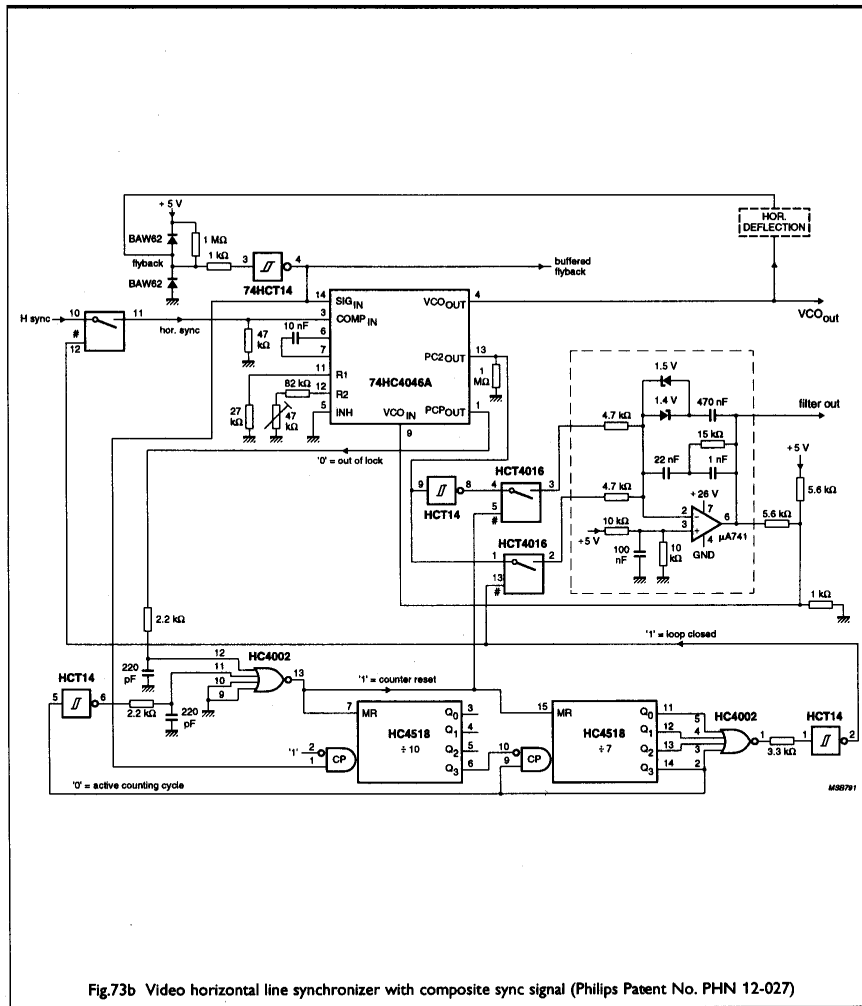




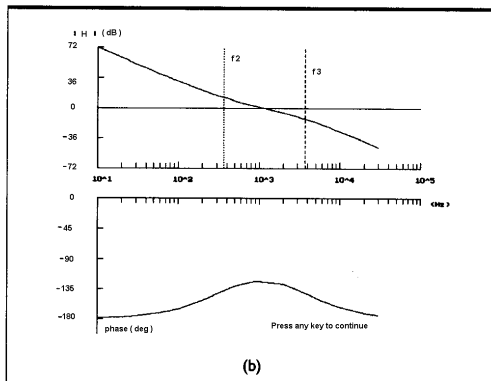
Figure 74(a) shows the results of the calculation program. With a settling time of 0.26 ms and  $\zeta = 0.72$ , no further optimization appears necessary as the Bode plot (Fig.74(b)) and Fig.75 confirms.

INPUT PARAMETERS			
NC	: 2	fin (Hz)	: 2.344E+04
N	: 1	2ER (Hz)	: 1.459E+04
Filter	: 2	f0 (Hz)	: 2.904E+04
		Spread input freq. (%)	: 35.0
		Part-to-part spread (%)	: 32.0
		Vcc (Volt)	: 5.0
VCO and FILTER PARAMETERS 74HC/HCT 4046A/7046A			
T1 (sec)	: 2.3E-04	T2 (sec)	: 4.4E-04
T3 (sec)	: 4.3E-05	T4 (sec)	: 4.3E-05
f1 (Hz)	: 6.8E+03	f2 (Hz)	: 3.7E+02
f3 (Hz)	: 3.7E+03	f4 (Hz)	: 3.7E+03
R1 (Ohm)	: 4.9E+03	R3 (Ohm)	: 4.6E+02
R4 (Ohm)	: 8.5E+02	R5 (Ohm)	: 8.5E+02
R2 (Ohm)	: 5.4E+04	C2 (Far)	: 5.1E-07
C1 (Far)	: 3.6E-08	C3 (Far)	: 5.1E-08
		Rp (Ohm)	: 3.6E+05
DYNAMIC PARAMETERS			
Wn/2 $\pi$ (Hz)	: 6.2E+03	pull-in time (sec)	: 1.2E-03
W <sub>0dB</sub> /2 $\pi$ (Hz)	: 1.2E+03	pull-in range (Hz)	: 1.7E+04
zeta	: 0.72	pull-out range (Hz)	: 8.7E+03
overshoot (%)	: 20.25	hold range (Hz)	: 1.7E+04
Kv	: 3.6E+03	settling time (sec)	: 2.6E-04
Winput/W <sub>0dB</sub>	: 20.3	lock-in range (Hz)	: 5.7E+03
phasemargin with C3 (deg)	: 56	ripple suppr. with C3 (dB)	: -58
without C3 (deg)	: 72	without C3 (dB)	: -58
W-3dB/2 $\pi$ closed loop (Hz)	: 1.3E+03		

Philips Semiconductors

Optimize ? (Y/N): Y

(a)



(b)

Fig.74 (a) Loop parameters and (b) Bode plot generated by the design program for the video horizontal line synchronizer. The measured Bode plot of the real circuit (see Fig.75) is in close agreement with the plot generated by the program

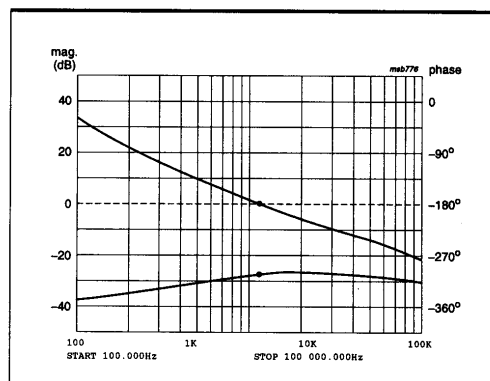


Fig.75 Bode plot measured for the video horizontal line synchronizer built using the design program. The phase margin is 60.5° at 1.163 kHz (0 dB)

### FM demodulator

Figure 76 is a modulation tracking loop, or FM demodulator designed with the help of the design program. The centre frequency is 10.7 MHz which is very close to the maximum specified in the data sheet at  $V_{CC} = 4.5$  V, making it a worst-case situation for the 74HC/HCT4046A for demodulation. Phase comparator PC1 was chosen because it is expected that the input signal will be noisy. However, owing to the limited capture and hold range of this phase comparator, R2 is made adjustable. A passive filter was chosen because the loop delay must be kept to a minimum and the phase difference between the input signal and the VCO frequency may differ from 90°.

For the program, a  $\pm 75$  kHz peak frequency deviation is used and a 1 kHz modulation frequency. Since R2 is adjustable, the VCO part-to-part spread is set to zero. The chosen VCO frequency range was  $2f_R = 3$  MHz.

Figure 77(a) shows the results from running the design program once. The pull-out range obtained was 310 kHz. Capacitor C3 which, at these high frequencies, affects the output transitions of PC1 significantly, was removed. The optimized parameters and the Bode plot are shown in Fig.78.

The demodulated output at the DEM<sub>OUT</sub> pin is connected to a de-emphasis circuit. The distortion is typically 0.5% but depends on the value of R2. The signal-to-noise ratio is about 55 dB. Both values are good for a standard general-purpose PLL circuit and they improve considerably at lower centre frequencies.

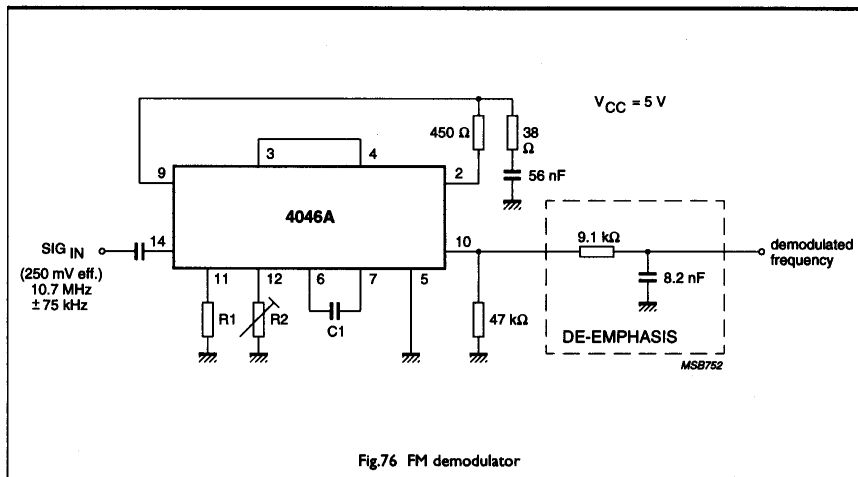


Fig.76 FM demodulator

INPUT PARAMETERS			
PC : 1	f <sub>in</sub> (Hz) : 1.070E+07	Spread input freq. (%) : 0.0	
N : 1	2FR (Hz) : 3.000E+06	Part-to-part spread (%) : 0.0	
Filter : 1	f <sub>0</sub> (Hz) : 1.070E+07	Vcc (Volt) : 5.0	
VCO and FILTER PARAMETERS 74HC/HCT 4046A/7046A			
T1 (sec) : 2.5E-05	T2 (sec) : 2.1E-06	T3 (sec) : 1.9E-07	
f1 (Hz) : 5.9E+03	f2 (Hz) : 7.5E+04	f3 (Hz) : 8.4E+05	
R1 (Ohm) : 1.3E+04	R2 (Ohm) : 9.3E+03	R4 (Ohm) : 7.9E+02	
R3 (Ohm) : 7.6E+03	C2 (Far) : 2.7E-09	C3 (Far) : 2.4E-10	
C1 (Far) : 1.0E-10			
DYNAMIC PARAMETERS			
Wn/2K (Hz) : 1.0E+05	pull-in time (sec) : 5.4E-05		
W <sub>0dB</sub> /2K (Hz) : 1.7E+05	pull-in range (Hz) : 7.7E+05		
seta : 0.70	pull-out range (Hz) : 3.1E+05		
overshoot (%) : 21.03	hold range (Hz) : 1.5E+06		
Kv : 1.1E+07	settling time (sec) : 1.8E-06		
Winput/W <sub>0dB</sub> : 63.7	lock-in range (Hz) : 2.2E+05		
phasemargin with C3 (deg) : 58	ripple suppr. with C3 (dB) : -71		
without C3 (deg) : 67	without C3 (dB) : -44		
W-3dB/2K closed loop (Hz) : 2.0E+05			
peak phase error (deg) : 4.3E-01			

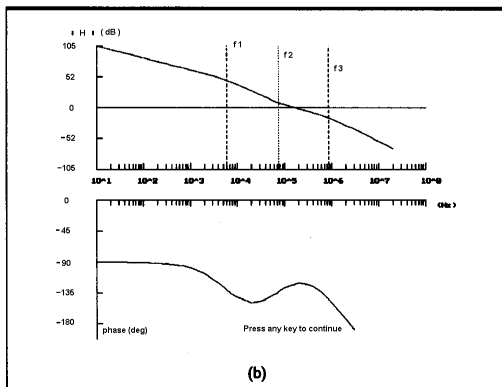
Optimize ? (Y/N) : Y

(a)

INPUT PARAMETERS			
PC : 1	f <sub>in</sub> (Hz) : 1.070E+07	Spread input freq. (%) : 0.0	
N : 1	2FR (Hz) : 3.000E+06	Part-to-part spread (%) : 0.0	
Filter : 1	f <sub>0</sub> (Hz) : 1.070E+07	Vcc (Volt) : 5.0	
VCO and FILTER PARAMETERS 74HC/HCT 4046A/7046A			
T1 (sec) : 2.5E-05	T2 (sec) : 2.1E-06	T3 (sec) : 7.9E-10	
f1 (Hz) : 5.9E+03	f2 (Hz) : 7.5E+04	f3 (Hz) : 2.0E+08	
R1 (Ohm) : 1.3E+04	R2 (Ohm) : 9.3E+03	R4 (Ohm) : 7.9E+02	
R3 (Ohm) : 7.6E+03	C2 (Far) : 2.7E-09	C3 (Far) : 1.0E-12	
C1 (Far) : 1.0E-10			
DYNAMIC PARAMETERS			
Wn/2K (Hz) : 1.0E+05	pull-in time (sec) : 5.4E-05		
W <sub>0dB</sub> /2K (Hz) : 1.7E+05	pull-in range (Hz) : 7.7E+05		
seta : 0.70	pull-out range (Hz) : 3.1E+05		
overshoot (%) : 21.03	hold range (Hz) : 1.5E+06		
Kv : 1.1E+07	settling time (sec) : 1.8E-06		
Winput/W <sub>0dB</sub> : 63.7	lock-in range (Hz) : 2.2E+05		
phasemargin with C3 (deg) : 67	ripple suppr. with C3 (dB) : -44		
without C3 (deg) : 67	without C3 (dB) : -44		
W-3dB/2K closed loop (Hz) : 2.0E+05			
peak phase error (deg) : 4.3E-01			

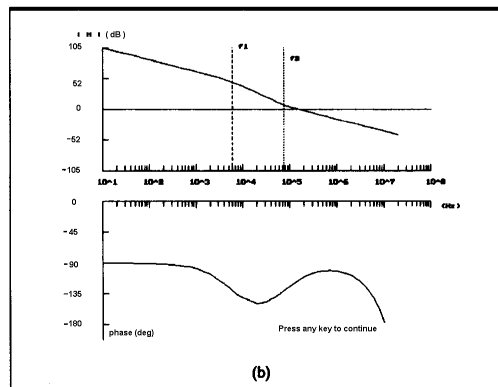
Optimize ? (Y/N) : Y

(a)



(b)

Fig.77 (a) Loop parameters and (b) calculated Bode plot of the FM demodulator after running the program once



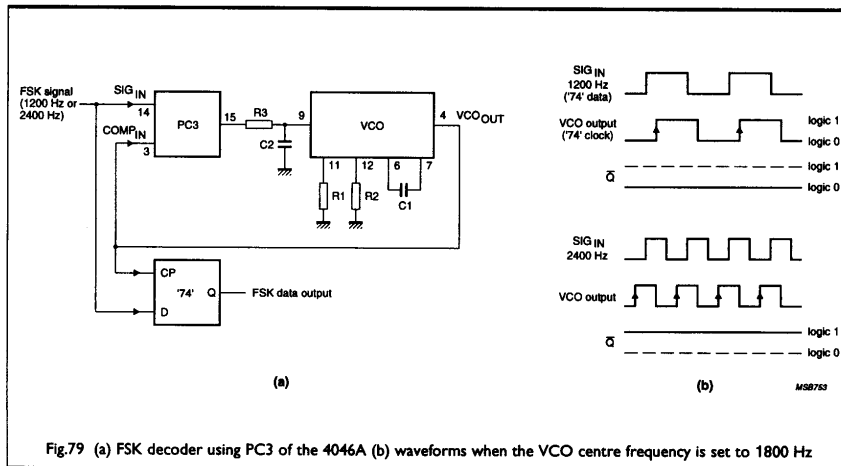
(b)

Fig.78 (a) Loop parameters and (b) Bode plot of the FM demodulator after removing C3

## FSK decoder

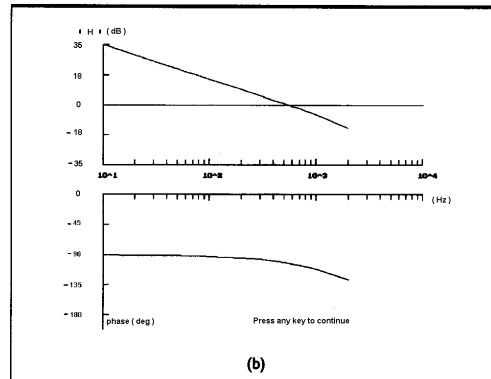
Using the PC3 phase comparator of the 4046A, it's straightforward to build a FSK (Frequency Shift Keying) decoder, see Fig.79(a). If the VCO is trimmed so that its centre frequency is exactly mid-way between the two frequency keys, in this example, at 1800 Hz, then an input signal of 1800 Hz will produce a phase difference of exactly 180°. With the VCO output frequency range set from 800 Hz to 2800 Hz, a signal of 1200 Hz causes the VCO to lower the average voltage of the comparator as shown in Fig.79(b), resulting in a logic LOW output of the HC/HCT74 D-flip-flop. The reverse happens if the input signal is raised to 2400 Hz, producing a logic HIGH.

For a fast settling time as required to receive data at high baud rates, the filter comprises only R3 and C2, because the calculated  $f_2$  and  $f_3$  were both far above the  $\omega_{0\text{ dB}}$  of the open loop and could thus be omitted. Figure 80 shows the results from the design program after inserting values for the filter components with the optimize menu.



INPUT PARAMETERS				
PC	: 3	f <sub>in</sub> (Hz)	: 1.800E+03 Spread input freq. (%) : 0.0	
N	: 1	Z <sub>IN</sub> (Hz)	: 2.000E+03 Part-to-part spread (%) : 0.0	
Filter	: 1	f <sub>0</sub> (Hz)	: 1.800E+03 V <sub>cc</sub> (Volt) : 5.0	
VCO and FILTER PARAMETERS 74HC/HCT 4046A/7046A				
T1 (sec)	: 6.6E-05	T2 (sec)	: 8.5E-06	
f1 (Hz)	: 2.1E+03	f2 (Hz)	: 1.9E+04	
R1 (Ohm)	: 9.5E+04	R3 (Ohm)	: 4.4E+02	
R2 (Ohm)	: 1.5E+06	R4 (Ohm)	: 5.7E+01	
C1 (Far)	: 3.0E-08	C2 (Far)	: 1.5E-07	
C3 (Far)	: 1.5E-08			
DYNAMIC PARAMETERS				
Mn/2k	(Hz)	: 1.1E+03	pull-in time (sec)	: 1.5E-04
M <sub>0dB</sub> /2k	(Hz)	: 5.7E+02	pull-in range (Hz)	: 1.0E+03
zeta		: 1.00	pull-out range (Hz)	: 1.0E+03
overshoot (%)		: 13.56	hold range (Hz)	: 1.0E+03
Kv		: 3.6E+03	settling time (sec)	: 1.3E-04
W <sub>input</sub> /M <sub>0dB</sub>		: 3.2	lock-in range (Hz)	: 1.0E+03
phasemargin with C3 (deg)		: 77	ripple suppr. with C3 (dB)	: -6
without C3 (deg)		: 77	without C3 (dB)	: -6
M <sub>-3dB</sub> /2k closed loop (Hz)		: 2.7E+03		

Optimize ? (Y/N) : Y Philips Semiconductors



### Crystal oscillator

A little known application for the 4046A is as a voltage-controlled crystal oscillator (VCXO), for example, when the part-to-part spread of the VCO is too large for the application but the input frequency is well-defined. Figure 81 shows the circuit.

The crystal is an 'AT'-cut oscillator crystal (such as Philips 4322 143 series in an HC49 encapsulation (see Philips Components Data Handbook PA10) which operates near the anti-resonant or parallel mode. It may be necessary to fine-tune the crystal as indicated in Fig.81. The pulling characteristic of the crystal allows an operating temperature range from  $-40^{\circ}\text{C}$  to  $+85^{\circ}\text{C}$ , plus initial ageing accuracy tolerance factors, while still retaining lock between master and slave VCXOs. For a 6 MHz crystal say with:

- A temperature stability of  $\pm 25$  ppm from  $-40^{\circ}\text{C}$  to  $+85^{\circ}\text{C}$
- Calibration tolerance  $\pm 10$  ppm
- Long-term drift  $\pm 2$  ppm,

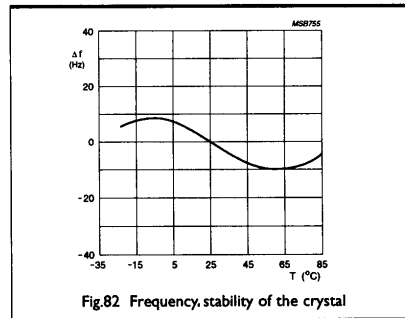
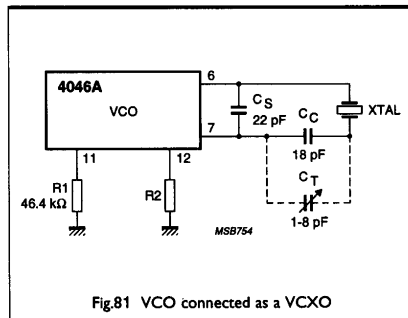
The total (about  $\pm 37$  ppm) means a capture and hold range of at least  $\pm 222$  Hz over which two crystal-stabilized VCOs must track under worst-case conditions. Figure 82 shows the frequency stability of the VCXO as a function of ambient temperature. Table 4 lists some typical measured  $2f_R$  for several crystals. The measurements were made without the trimmer capacitor  $C_T$ . In the case of the 6 MHz crystal, a  $\pm 222$  Hz hold range is well within the  $2f_R$  range of 1400 Hz specified in the example above. At frequencies below 3.1 MHz, the  $2f_R$  becomes too small and the standard crystals will have too low a value for pullability (the listed value of 130 Hz is often already too small). At frequencies above 10 MHz, the VCO is unable to excite the crystal correctly and the VCO behaves as if the crystal was absent. Additional information about the crystal-controlled VCO circuit is given in Ref.4.

**Table 4: Measured  $2f_R$  for several VCXOs.**

crystal freq. (Hz)	R2 (k $\Omega$ )	VCO output frequency (Hz) for an input voltage of:			$2f_R$ (Hz)
		1.1 V	2.5 V	3.9 V	
		3 151 170	19.6	3 151 570	
4 782 720	21.2	4 783 700	4 784 000	4 784 100	400
6 000 000	26.1	5 997 200	5 998 100	5 998 600	1400
8 867 238	26.1	8 843 400	8 858 900	8 862 400	19000
10 000 000	46.4	9 964 500	9 989 400	9 994 200	29700

$V_{CC} = 5$  V;  $T_{amb} = 25^{\circ}\text{C}$ ;  $C_T = 0$  pF.

The frequencies listed are for a typical set-up; actual values will differ slightly.



## APPENDIX A

### Variable gain of PC2 (type a: 74HC(T)4046A/7046A only)

When phase comparator PC2a is used with a passive low-pass filter, its gain (unlike that of PC1 and PC3) depends on the voltage on the filter capacitor. Let's consider PC1 with a passive filter first (Fig.A1), and calculate the transfer function and gain.

To simplify matters, a simple RC filter is used, and from Fig.A1, the average output

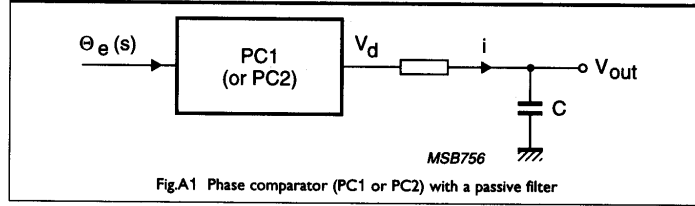


Fig.A1 Phase comparator (PC1 or PC2) with a passive filter

of PC1,  $V_d(s)_{(avg)}$ , is:

$$V_d(s)_{(avg)} = \frac{\theta_e(s)V_{CC}}{\pi} \quad (A1)$$

And:

$$V_{out}(s) = i/sC. \quad (A2)$$

In addition,

$$i = \frac{V_d(s) - V_{out}(s)}{R}$$

$$\begin{aligned} &= \frac{\frac{\theta_e(s)}{\pi} \times V_{CC} - V_{out}(s)}{R} \end{aligned} \quad (A3)$$

$V_{out}(s)$  can be eliminated in Eq.(A3), yielding:

$$V_{out}(s) = \frac{\theta_e(s)V_{CC}}{\pi sCR} \times \frac{s}{s + 1/RC} \quad (A4)$$

For a step input,  $\theta_e(s) = \Delta\theta_e/s$ , and Eq.(A4) becomes:

$$V_{out}(s) = \frac{V_{CC}}{\pi} \times \frac{\Delta\theta_e}{RC} \times \frac{1}{s(s + 1/RC)} \quad (A5)$$

Using the inverse Laplace transform, this is:

$$\frac{V_{out}(t)}{\Delta\theta_e} = \frac{V_{CC}(1 - e^{-t/RC})}{\pi} \quad (A6)$$

where  $V_{CC}/\pi$  is the phase comparator gain which is independent of the voltage on the capacitor.

Now consider the situation with PC2, see Fig.A1 again. If PC2 starts from a 3-state condition, the initial capacitor voltage must be included in the calculations, so now:

$$V_d(s)_{(avg)} = V_{out}(s) + \{V_{CC}/s - V_{out}(s)\}\Delta\theta_e/2\pi \quad (A7)$$

assuming  $\Delta\theta_e > 0$ .

And:

$$V_{out}(s) = V_{C0}/s + i/sC \quad (A8)$$

where  $V_{C0}$  is the initial voltage on the capacitor C.

In addition,

$$\begin{aligned} i &= \{V_d(s) - V_{out}(s)\}/R \\ &= \{V_{CC}/s - V_{out}(s)\}\Delta\theta_e/(2\pi R) \end{aligned} \quad (A9)$$

From Eqs. (A8) and (A9),

$$V_{out}(s) = \{V_{C0}/s + (V_{CC}/s - V_{out}(s))\} \Delta\theta_e / 2\pi s RC \quad (A10)$$

which can be rewritten as:

$$V_{out}(s) = [s\tau / (1 + s\tau)] \times (V_{C0}/s + V_{CC}/s^2\tau) \quad (A11)$$

$$= \frac{V_{C0}}{(s + 1/\tau)} + \frac{V_{CC}}{s\tau(s + 1/\tau)} \quad (A12)$$

where  $\tau = 2\pi RC / \Delta\theta_e$ .

Using the inverse Laplace transform, this is:

$$V_{out}(t) = V_{CC} - (V_{CC} - V_{C0}) \exp(-\Delta\theta_e t / 2\pi RC) \quad (A13)$$

Using the series expansion for  $\exp x$ , and neglecting terms  $x^2/2!$  and higher (true for  $\Delta\theta_e < 2\pi$ ), Eq.(A13) can be rewritten as:

$$V_{out}(t) = V_{C0} + (V_{CC} - V_{C0}) \Delta\theta_e t / 2\pi RC \quad (A14)$$

For small values of  $\Delta\theta_e$ , the AC component of  $V_{out}$  amounts to:

$$\frac{V_{out}(t)}{\Delta\theta_e} = \underbrace{(V_{CC} - V_{C0}) / 2\pi}_{\text{gain of PC2}} \times \underbrace{t / RC}_{\text{transfer characteristic of filter (integrator)}} \quad (A15)$$

If  $V_{C0} = 2.5$  V, the average value of the gain is  $V_{CC}/4\pi$  (the value stated in the data sheet). At  $V_{CC} = 5$  V, and using the VCO input voltage range as the limit for  $V_{C0}$ , the gain of PC2 can vary from  $1.1/2\pi$  to  $3.9/2\pi$ . So, for a synthesizer, for example, built using PC2 and a passive filter, the gain will vary over this range as the division ratio is altered from  $N_{min}$  to  $N_{max}$  since this will alter the VCO input voltage from minimum to maximum.

In the PLL design program, this gain variation is taken into account, when the division ratio is changed (option 0 of the optimize menu). However, an unwanted gain difference still exists for positive or negative phase errors when  $V_{C0} \neq 0.5V_{CC}$ .

If it is anticipated that the full VCO input voltage range will be used (e.g. in synthesizer applications), it is recommended to use an active filter, see Fig.A2, which keeps  $V_{C0}$  constant, resulting in a constant PC2 gain even for large phase errors. In Fig.A2,

$$i = (V_{CC} - 0.5V_{CC}) \times \frac{\theta_e(s)}{2\pi} \times \frac{1}{R} \quad (A16)$$

and

$$V_{out}(s) = -i/sC = \theta_e(s) \{-V_{CC}/4\pi RCs\} \quad (A17)$$

For a step,  $\theta_e(s) = \Delta\theta_e/s$ , and Eq.(A17) becomes:

$$V_{out}(s) = -\Delta\theta_e V_{CC} / 4\pi RC s^2 \quad (A18)$$

Using the inverse Laplace transform, this is:

$$\frac{V_{out}(t)}{\Delta\theta_e} = \underbrace{-V_{CC}/4\pi}_{\text{gain of PC2}} \times \underbrace{t^2 / RC}_{\text{transfer characteristic of filter (integrator)}} \quad (A19)$$

Note that when PC2 is used, a passive filter and an active filter have the same ideal integrator characteristic, see Eqs.(A15) and A(19). This means that even when a passive filter is used with PC2, the loop behaves as though an active filter is present. However, the gain of PC2 when used with a passive filter will vary, as described earlier.

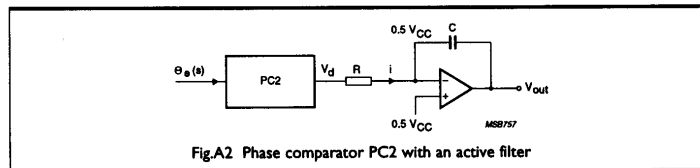


Fig.A2 Phase comparator PC2 with an active filter

## APPENDIX B

### Transient response calculations

Figure B1 shows a general feedback system. The transfer function is:

$$H(s) = \frac{A(s)}{1 + A(s)B(s)} \quad (B1)$$

The error function is:

$$\begin{aligned} H_e(s) &= \theta_e(s)/\theta_i(s) \\ &= \frac{1}{1 + A(s)B(s)} \\ &= 1 - H(s) \end{aligned} \quad (B2)$$

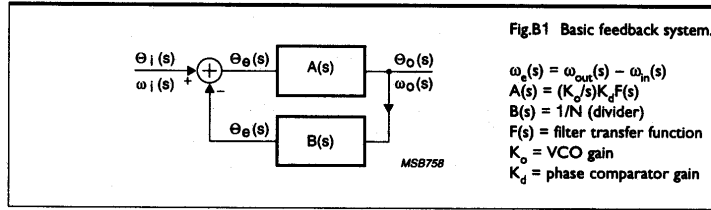


Table B1 lists the transient response when the input is excited by a phase step, a frequency step or a frequency ramp.

**Table B1: Transient response definitions**

	phase step $\theta_i(s) = \Delta\theta_i/s$	frequency step $\omega_i(s) = \Delta\omega_i/s$	frequency ramp $\omega_i(s) = \Delta\omega_i/s^2$
phase response: $\theta_2(s)$	$\frac{\Delta\theta_i H(s)}{s}$	$\theta_i(s)H(s) = \frac{\Delta\omega_i H(s)}{s^2}$	$\frac{\Delta\omega_i H(s)}{s^3}$
phase error: $\theta_e(s)$	$\frac{\Delta\theta_i H_e(s)}{s}$	$\frac{\Delta\omega_i H_e(s)}{s^2}$	$\frac{\Delta\omega_i H_e(s)}{s^3}$
frequency response: $\omega_0(s)$	$s\theta_2(s) = \Delta\theta_i H(s)$	$\frac{\Delta\omega_i H(s)}{s}$	$\frac{\Delta\omega_i H(s)}{s^2}$
frequency error: $\omega_e(s)$	-	$\frac{\Delta\omega_i H_e(s)}{s}$	$\frac{\Delta\omega_i H_e(s)}{s^2}$

### Active filter

First, the transient response of a PLL using an active filter is calculated. In this case,

$$H(s) = \frac{2\zeta\omega_n s + \omega_n^2}{s^2 + 2\zeta\omega_n s + \omega_n^2} \quad (B3)$$

$$H_e(s) = \frac{s^2}{s^2 + 2\zeta\omega_n s + \omega_n^2} \quad (B4)$$

The phase response to a phase step is:

$$\begin{aligned}\theta_2(s) &= \frac{\Delta\theta_i}{s} \times H(s) \\ &= \frac{\Delta\theta_i}{s} \times \frac{2\zeta\omega_n s + \omega_n^2}{s^2 + 2\zeta\omega_n s + \omega_n^2}\end{aligned}\quad (B5)$$

Using the inverse Laplace transform and  $\varphi = \arcsin\zeta$  yields:

$$\theta_2(t) = \Delta\omega_i \left\{ 1 - \frac{1}{\sqrt{1-\zeta^2}} \times \cos[\sqrt{1-\zeta^2}\omega_n t + \varphi] e^{-\zeta\omega_n t} \right\} \quad (B6)$$

and the phase error is:

$$\theta_e(t) = \theta_1(t) - \theta_2(t) = \Delta\theta_i \frac{1}{\sqrt{1-\zeta^2}} \cos[\sqrt{1-\zeta^2}\omega_n t + \varphi] e^{-\zeta\omega_n t} \quad (B7)$$

Equation (B7) describes the curves of Fig.51, which could have been expected because the phase response to a phase step is the same as the frequency response to a frequency step. This can be verified in Table B1, bearing in mind that  $\theta = \omega/s$ .

The phase response to a frequency step (which is the same as the frequency response to a frequency ramp) can be calculated in a similar way.

$$\theta_2(s) = \frac{\Delta\omega_i}{s^2} \times H(s) = \Delta\omega_i \times \left\{ \frac{1}{s^2} - \frac{1}{s^2 + 2\zeta\omega_n s + \omega_n^2} \right\} \quad (B8)$$

Using the inverse Laplace transform yields:

$$\theta_2(t) = \Delta\omega_i \left\{ t - \frac{e^{-\zeta\omega_n t} \sin\sqrt{1-\zeta^2}\omega_n t}{\omega_n \sqrt{1-\zeta^2}} \right\} \quad (B9)$$

And the phase error (with  $\theta_1(t) = \Delta\omega_i t$ ) is:

$$\theta_e(t) = \theta_1(t) - \theta_2(t) = \Delta\omega_i \frac{e^{-\zeta\omega_n t} \sin\sqrt{1-\zeta^2}\omega_n t}{\omega_n \sqrt{1-\zeta^2}} \quad (B10)$$

This function describes the curves of Fig.52.

The phase error due to a frequency ramp is determined as follows.

$$\begin{aligned}\theta_e(s) &= \frac{\Delta\omega_i^3}{s^3} \times H_e(s) \\ &= \frac{\Delta\omega_i}{s^3} \times \frac{s^2}{s^2 + 2\zeta\omega_n s + \omega_n^2}\end{aligned}\quad (B11)$$

$$= \frac{\Delta\omega_i}{\omega_n^2} \times \left\{ \frac{1}{s} - \frac{s + \omega_n \zeta + \omega_n \zeta}{s^2 + 2\zeta\omega_n s + \omega_n^2} \right\} \quad (B12)$$

Using the inverse Laplace transform yields:

$$\theta_e(t) = \frac{\Delta\omega_i}{\omega_n^2} \times \left\{ 1 - e^{-\zeta\omega_n t} \left[ \cos\sqrt{1-\zeta^2}\omega_n t + \zeta \frac{\sin\sqrt{1-\zeta^2}\omega_n t}{\sqrt{1-\zeta^2}} \right] \right\} \quad (B13)$$

With  $\varphi = \arcsin\zeta$ :

$$\theta_e(t) = \frac{\Delta\omega_i}{\omega_n^2} \times \left\{ \frac{[1 - e^{-\zeta\omega_n t}] \cos[\sqrt{1-\zeta^2}\omega_n t - \varphi]}{\sqrt{1-\zeta^2}} \right\} \quad (B14)$$

This function describes the curves of Fig.50.



### Passive filter

For a passive filter, the transfer function is:

$$H(s) = \frac{\omega_n^2(s\tau_2 + 1)}{s^2 + 2\zeta\omega_n s + \omega_n^2} \quad (\text{B15})$$

with  $\tau_1 = R3C$  (C is the filter capacitor)

$$\tau_2 = R4C.$$

The phase response to a phase step (or the frequency response to a frequency step) is:

$$\theta_2(s) = \Delta\theta_i \left\{ \frac{1}{s} - \frac{s + 2\zeta\omega_n - \omega_n^2\tau_2}{s^2 + 2\zeta\omega_n s + \omega_n^2} \right\} \quad (\text{B16})$$

Using the inverse Laplace transform yields:

$$\theta_2(t) = \Delta\theta_i \left\{ 1 - e^{-\zeta\omega_n t} \left[ \cos\sqrt{(1-\zeta^2)}\omega_n t + \frac{\zeta\sin\sqrt{(1-\zeta^2)}\omega_n t}{(1-\zeta^2)} - \frac{\omega_n\tau_2\sin\sqrt{(1-\zeta^2)}\omega_n t}{\sqrt{(1-\zeta^2)}} \right] \right\} \quad (\text{B17})$$

And the phase error is:

$$\theta_e(t) = \Delta\theta_i \frac{e^{-\zeta\omega_n t}}{\sqrt{(1-\zeta^2)}} \left\{ \cos[\sqrt{(1-\zeta^2)}\omega_n t - \varphi] - \omega_n\tau_2\sin[\sqrt{(1-\zeta^2)}\omega_n t] \right\} \quad (\text{B18})$$

With  $\tau_2 = 0$ , this is the function of Fig.50.

Another approach is to substitute  $2\zeta\omega_n - \omega_n^2\tau_2 = 1/(\tau_1 + \tau_2)$  in Eq.(B16), and transforming to the time domain yields:

$$\theta_2(t) = \Delta\theta_i \left\{ 1 - \frac{e^{-\zeta\omega_n t}}{\sqrt{(1-\zeta^2)}} \left[ \cos\sqrt{(1-\zeta^2)}\omega_n t + \varphi + \omega_n/K_dK_o \sin\sqrt{(1-\zeta^2)}\omega_n t \right] \right\} \quad (\text{B19})$$

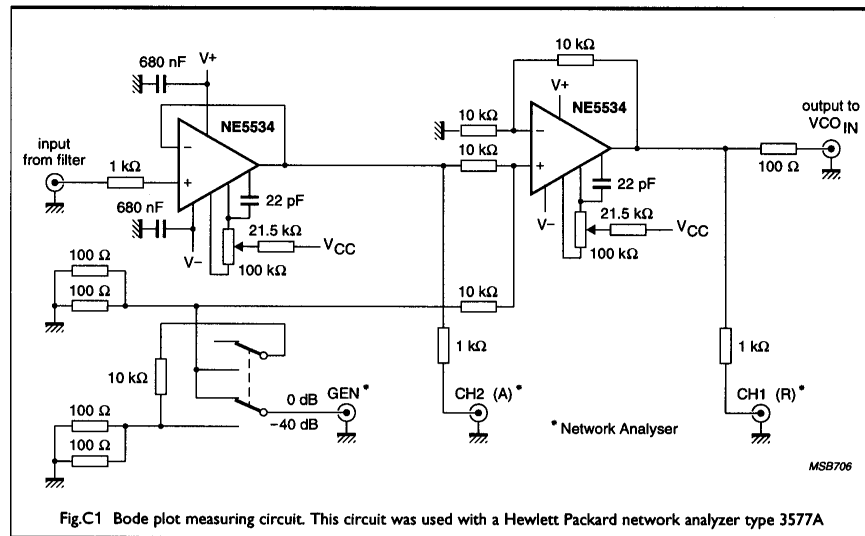
and the phase error is:

$$\theta_e(t) = \Delta\theta_i \frac{e^{-\zeta\omega_n t}}{\sqrt{(1-\zeta^2)}} \left\{ \cos[\sqrt{(1-\zeta^2)}\omega_n t + \varphi] + \omega_n/K_dK_o \sin[\sqrt{(1-\zeta^2)}\omega_n t] \right\} \quad (\text{B20})$$

For a high-gain loop,  $K_dK_o \gg \omega_n$ , and Eq.(B20) describes Fig.51. Depending on the gain of the loop and the passive filter used, there is a gradual change from Fig.50 to Fig.51. When PC2 is used, the gain is extremely high and Fig.51 is always valid.

## APPENDIX C

### Bode plot measuring circuit



## APPENDIX D

### Symbols

$\pm\Delta\omega_{HI}$	hold range (see Fig.2)
$\pm\Delta\omega_{LIH}$	lock-in range (see Fig.2)
$\pm\Delta\omega_{PI}$	pull-in range (see Fig.2)
$\pm\Delta\omega_{PO}$	pull-out range (see Fig.2)
$2f_R$	VCO output frequency range (see Fig.2)
$B_i$	noise bandwidth of the input signal
$B_L$	noise bandwidth of a loop
$f_0$	VCO centre frequency
$f_{min}$	the minimum frequency of the VCO
$f_{max}$	the maximum frequency of the VCO
$f_{off}$	VCO offset frequency
$f_{in}, \omega_{in}$	frequency of the input signal
$\phi_{in}$	phase of the input signal
$f_{out}, \omega_{out}$	frequency of the output signal
$\phi_{out}$	phase of the output signal
$H(s)$	closed-loop transfer function
$H_e(s)$	closed-loop error function
$K_d$	phase comparator conversion gain
$K_o$	VCO conversion gain
$K_v$	total loop conversion gain ( $K_o K_d / N$ )
$N$	division ratio of a +N counter
$s$	Laplace operator
$T_{AV}$	average time before losing lock due to phase noise
$T_p$	pull-in time
$T_S$	settling time
$T_{S(5\%)}$	settling time (output within 5% of the applied step)
$\omega_n$	natural frequency
$\omega_{3dB}$	the 3 dB bandwidth of the closed-loop gain
$\zeta$	damping factor

### REFERENCES

1. Automatic Feedback Control System Synthesis, Chap.4, McGraw-Hill, New York, 1955.
2. Gardner, F., Phaselock techniques, Wiley, New York, 1979.
3. Best, R., Phase-locked loops, McGraw-Hill, New York, 1984.
4. Clock generator with crystal-controlled phase-locked loop (NE564); AN182 in Philips Semiconductors Data Handbook IC11, 'General-purpose Linear ICs', 1995.

**Note:**

The full type number of the HCMOS products mentioned in this publication is 74HC/HCTxxxx. Both the HC and HCT versions are specified for a temperature range of -40 °C to +125 °C. For brevity, where it isn't required to distinguish between HC and HCT versions, the prefixes 74HC and 74HCT are omitted. The 9046A type is only available as an HCT version.